Role for PP1γ2 in spermatogenesis and sperm morphogenesis

A dissertation submitted to
Kent State University in partial
fulfillment of the requirements for the
degree of Doctor of Philosophy

By

Rumela Chakrabarti

March, 2007

Dissertation written by
Rumela Chakrabarti

B.S., Fergusson College, Pune University, Pune, India, 1999
M.S., Pune University, Pune, India, 2001
Ph.D., Kent State University, Kent, Ohio, USA, 2007

Approved by

Srinivasan Vijayaraghavan, PhD. (Chair, Doctoral Dissertation Committee)
Gail Fraizer, PhD. (Members, Doctoral Dissertation Committee)
Douglas Kline, PhD.
Ken Rosenthal, PhD.
Gary Meszaros, PhD.

Accepted by

Robert Dorman, PhD. (Chair, School of Biomedical Sciences)
John R. D. Stalvey, PhD. (Dean, College of Arts and Sciences)

TABLE OF CONTENTS

LIST OF FIGURES

LIST OF TABLES

ACKNOWLEDGMENTS

I would like to express my gratitude to my advisor, Dr. Srinivasan Vijayaraghavan, for his support and guidance. I would like to thank him for training and teaching me how to be a biologist. He helped me achieve my goals in reproductive physiology research.

I would also like to thank my committee members, Dr. Douglas Kline, Dr. Gail Fraizer, Dr. Ken Rosenthal and Dr. Gary Meszaros.

I would specially thank Mike Model for his help in the confocal microscopy and Haruna Shibata (Chiba University, Japan) for her help in the Laser Capture Microdissection. I also convey my deepest gratitude to Zaohua Huang, Kimberly Myers, John Ferrara, Pawan Puri, Ben Ingersoll, Vinay Pasupuleti, Praveena Thiagarajan, Shandilya Ramdas, David Soler, Valerie Gilbert, and Nilam Sinha for their continuous help in the experiments and discussions. I would also like to thank my friend -Somik Chatterjee.

Finally, I would like to deeply thank my parents and husband, Rita Chakrabarti (mother), Rathindranath Chakrabarti (father) and Gourab Majumder (husband). They strongly supported me in every aspect of life. I could not have done this without their constant support and encouragement.

Introduction

1. Spermatogenesis

Starting from a self-renewing stem cell pool, male germ cells develop in the seminiferous tubules of the testes throughout life from puberty to old age. Testes, besides containing germ cells, also contain somatic cells like sertoli cells, interstitial cells, mast cells and macrophages (Johnson and Everitt, 2000). Male germ cell differentiation is a highly regulated, complex process that takes place within the seminiferous tubules. The complete process of germ cell development is called *spermatogenesis* (Genuth 1998, Sharpe 1994). The products of spermatogenesis are the mature male gametes, namely the spermatozoa or sperm. Spermatogenesis can be subdivided into 3 main phases: (i) spermatogonial proliferation, (ii) meiosis of spermatocytes and (iii) spermiogenesis, a morphological process converting haploid spermatids to spermatozoa (Leblond and Clermont, 1952) followed by spermiation, release of mature testicular sperm in the lumen in testis (Fig. 1).

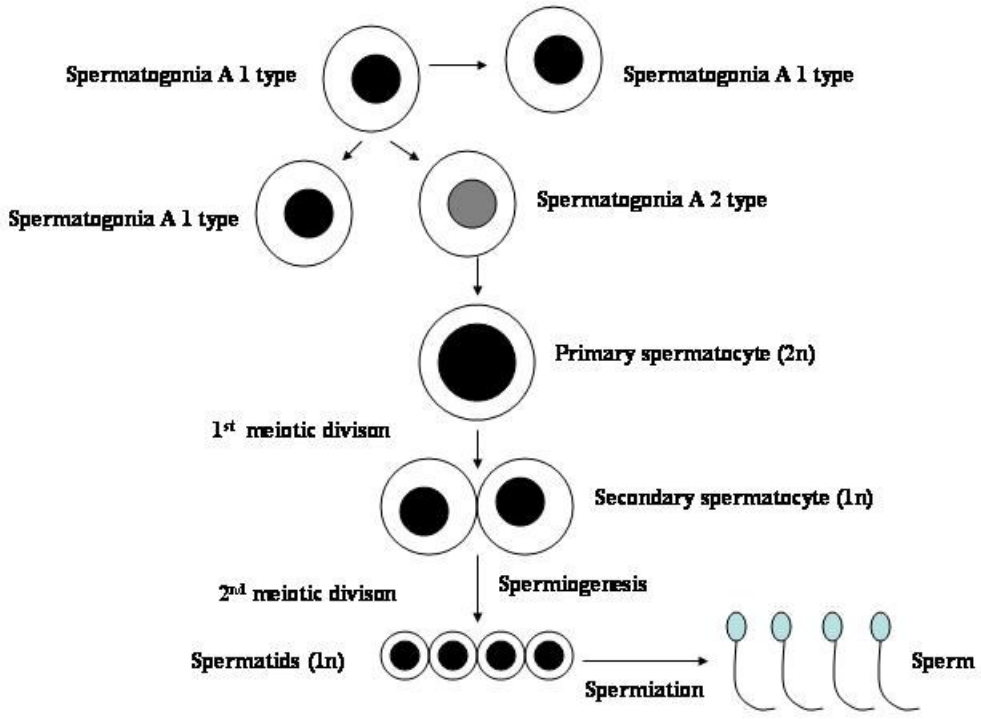

Figure 1. Overview of spermatogenesis

In a cross section of the seminiferous tubule (Fig. 2), the spermatogenic stem cells, other premeiotic germ cells and somatic sertoli cells are situated on the basal lamina of the seminiferous tubule. The next layer is formed by spermatocytes while haploid spermatids and elongated spermatids are situated in the adluminal compartment.

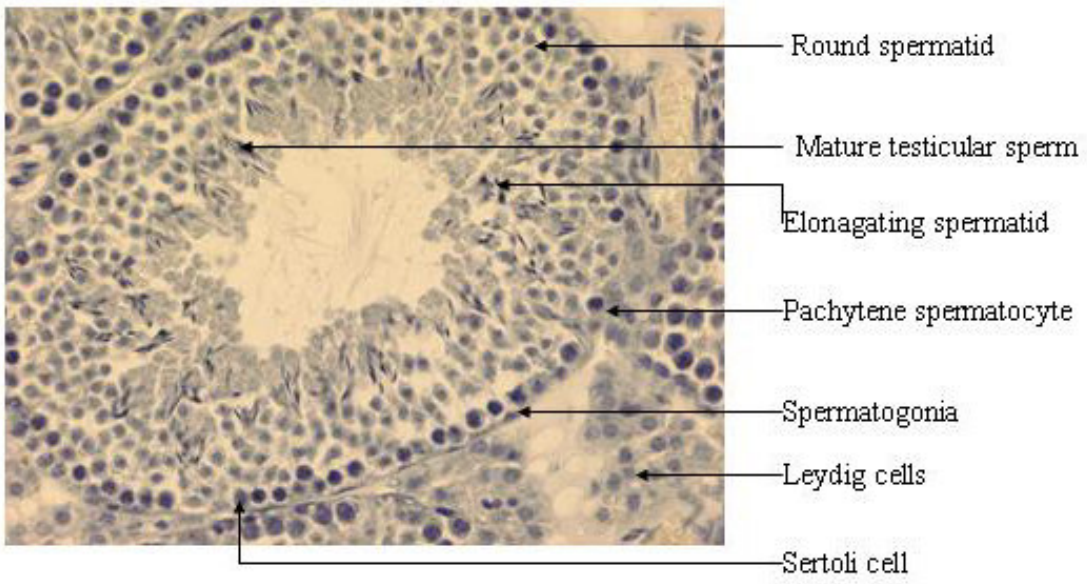

Figure 2. Cross section of mouse testis showing all the different cell types in seminiferous tubule

During spermatogenesis male germ cells undergo a complex differentiation where morphological alterations lead to the formation of differentiated sperm. The A1 spermatogonia are found adjacent to the outer basement membrane of the seminiferous tubule. At sexual maturity, these spermatogonia begin dividing mitotically to produce more type A1 spermatogonia as well as a second, paler type of cell, the type A2 spermatogonia. Thus, each type A1 spermatogonium is a stem cell capable of regenerating itself as well as of producing a new cell type. The A2 spermatogonia divide

to produce A3 spermatogonia, which then beget type A4 spermatogonia, which beget intermediate spermatogonia. These intermediate spermatogonia divide to form the type B spermatogonia which then divide mitotically to generate the primary spermatocytes- the cells that enter meiosis (Johnson and Everitt, 2000). During divisions from type A spermaogonia to spermatids, cells move further away from the basement membrane of the seminiferous tubule closer to the lumen. Thus, each type of cell can be found in the particular layer of the tubule. A characteristic feature of spermatogenesis is that, after mitotic and meiotic divisions, dividing germ cells fail to complete cytokinesis resulting in formation of cytoplasmic bridges that interconnect a large number of cells (Burgos and Fawcett, 1955; Fawcett *et al.*, 1959) (Fig. 1). Kinetic analyses reveal that hundreds or even thousands of cells theoretically may be connected by bridges at completion of spermatogenesis (Dym and Fawcett, 1971). Primary (preleptotene) spermatocytes, when entering meiosis, give rise to leptotene and zygotene spermatocytes. These cells differentiate into pachytene and diplotene spermatocytes followed by meiotic divisions and formation of haploid step 1 spermatids (spermiogenesis starts after formation of these cells). Haploid spermatids are morphologically classified into 16 types in mouse (Russell *et al.*, 1990). Spermatids are haploid, round, unflagellated cells that differentiate morphologically to form mature spermatozoa in a subprocess called *spermiogenesis*. Key events during spermiogenesis are: formation of the acrosome over the nucleus and concurrent rotation of the nucleus so that the acrosomal cap faces the basal membrane of the tubule; formation of the flagellum from the centriole on the opposite side of the nucleus; nuclear condensation; ejection of cytoplasmic droplet; formation of mitochondria in a ring around the flagellum (Bedford JM, Hoskins DD, 1990).

At completion of spermiogenesis, mature spermatozoa are released into seminiferous tubule lumen by a subprocess called *spermiation*. Spermiation is a complex process (Beardsley and Donnell, 2003) that involves 1) removal of excess spermatid cytoplasm from around the flagella to form the streamlined spermatozoan; 2) extension of spermatids into the tubule lumen; 3) retraction of the sertoli cell cytoplasm from around the spermatid head; and 4) disengagement of spermatids from Sertoli cells into the tubule lumen.

Based on morphological criteria of spermatids and other germ cells, spermatogenesis can be broadly subdivided into different cell associations, also called stages as shown in Figure 3.

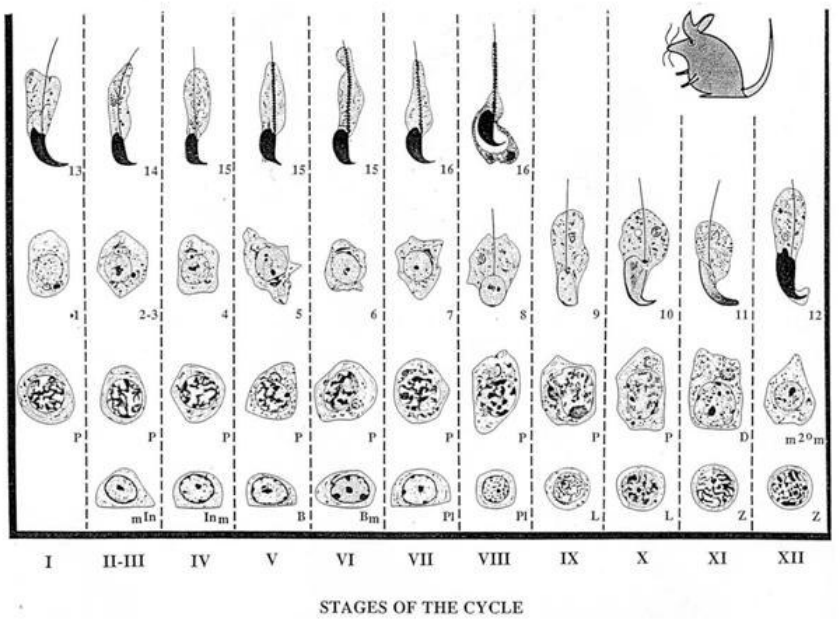

Figure 3. Different stages of mice seminiferous epithelial cycle. Total 12 stages are present in mouse with 16 different spermatids. It may be noted that pachytene spermatocytes are present in almost all stages.

The cycle and wave of the seminiferous epithelium

Inside seminiferous tubules, male germ cells at various stages of differentiation form defined cell associations which follow each other in sequential order. These defined cell associations inside the seminiferous tubules can be classified into twelve (in mouse; Oakberg, 1956) or fourteen (in rats; Leblond and Clermont, 1952) different stages of seminiferous epithelial cycle. Each stage contains male germ cells of defined phases of differentiation and can be accurately identified by morphological features of the acrosome and the nucleus of developing spermatids (Johnson and Everitt, 2000). The duration of the cycle is constant: stage I development to stage XIV is 12.9 days in Sprague Dawley rats and 8.6 days in mice (stage I to stage XII). Different segments of the seminiferous epithelial wave absorb light in a different way making it possible to identify stages in freshly isolated seminiferous tubules under a transillumination stereomicroscope (Kotaja *et al.*, 2004). Increased light absorption is associated with nucleoprotein changes and progressive chromatin condensation of haploid germ cells. Stages II-VI can be identified through dark spots that are spermatid bundles associated with Sertoli cells. At stages VII-VIII, a dark absorption zone at the lumen of seminiferous tubule is seen. Formation of a pale absorption zone at IX-X is observed after spermiation when mature testicular sperm are released in the lumen.

Gene and protein expression during spermatogenesis

Comprehensive understanding of spermatogenesis requires identification and functional characterization of unique genes, since this developmental process is regulated

by a precisely programmed cell and stage-specific gene expression. The genes that are transcribed specifically during spermatogenesis are often those whose products are necessary for sperm structure, sperm motility or binding to the egg. Regulation of gene expression in male germ cells occurs at three levels: intrinsic, interactive, and extrinsic (Eddy, 2002). A highly conserved genetic program "intrinsic" to germ cells determines sequence of events that underlies germ cell development. Sertoli cells are crucial for the "interactive" process as well as for providing essential support for germ cell proliferation and progression through the phases of development. The interactive level of regulation is dependent on "extrinsic" influences, primarily testosterone and follicle-stimulating hormone (FSH). During meiosis and other processes unique to germ cells, the intrinsic program determines which genes are utilized and when they are expressed. In the postmeiotic phase, it coordinates expression of genes whose products are responsible for constructing the spermatozoa. Spermatogenesis occurs in overlapping waves, with cohorts of germ cells developing in synchrony. The intrinsic program operating within a particular germ cell requires information from and provides information to neighboring cells to achieve this coordination.

A highly, specialized transcriptional mechanism ensures stringent stage-specific gene expression in germ cells (Hecht, 1990). The alterations of gene expression during sperm development are dramatic. The cytology of spermatogenesis is very well established. Cells at every particular stage have a specific structure and may be easily discriminated from each other. Strict correlation is found amongst the cell type and expression pattern. For example, c-kit is expressed in spermatogonia (Wolfes, Kogawa *et al.* 1989; Sorrentino, Giorgi *et al.* 1991; McCarrey, Berg *et al.* 1992), HSP70.2 in

spermatocytes (Eddy, 2002). Most dramatic changes happen during differentiation of round spermatids to mature sperm cells. Almost all proteins and structures become substituted by new proteins and structures characteristic for sperm. Protein degradation and synthesis machineries are very active in round spermatids. For example, histones become ubiquitinated and degraded in round spermatids (Baarends, Hoogerbrugge *et al.* 1999) and protamines and transition proteins are synthesised to substitute the histones and thereby compact the chromatin (Kistler, Sassone *et al.* 1994).

2. Sperm Biology

a. Sperm structure

The spermatozoon is a highly differentiated cell to carry out its special function. It displays a basic organization which is different from other cells. The highly differentiated and streamlined spermatozoon is composed of a head containing the acrosome, a condensed nucleus, and a flagellum consisting of a middle piece, a principal piece and an end piece, as shown in following figure (Fig. 4).

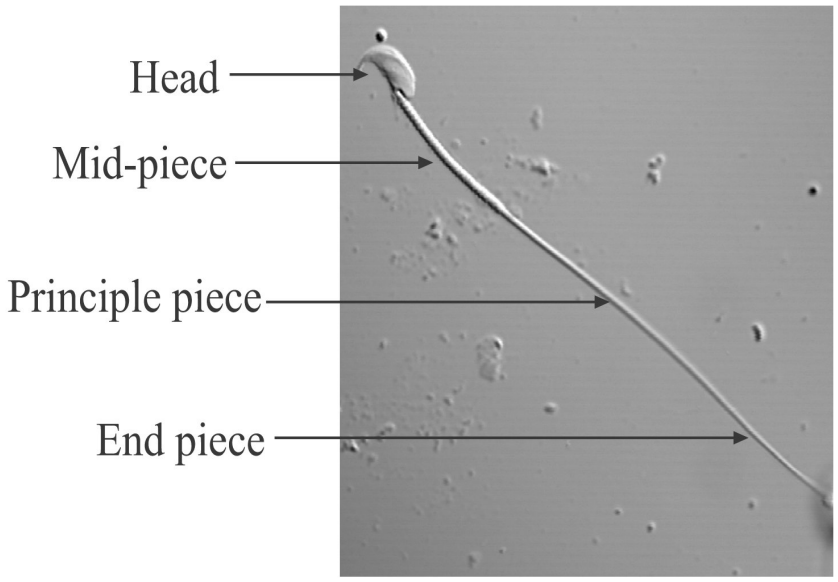

Figure 4. Mouse sperm image indicating head, mid-piece, principle piece and end piece.

The entire cell is, of course, enveloped by a plasma membrane. However, this membrane is differentiated over the head and tail, respectively, in its surface proteins and in certain other characteristics. For example, the membrane overlying the anterior head region is capable of undergoing controlled physiological breakdown immediately prior to penetration of the egg's zona pellucida, at the same time remaining intact over the posterior part of the head and over the tail.

i. The Nucleus

The nucleus is contained within the head, which, for most mammals, has a flattened or oval shape. In rodents, however, sperm head is hook shaped. The bulk of the sperm head is formed by the nucleus, which extends throughout the length of the head. The nucleus is highly condensed in mature sperm, and under electron microscope its

chromatin appears dense and homogeneous. Its major components are DNA and an associated basic protein rich in arginine and cysteine. Chemical bonds established between the free sulfhydryl groups (-SH) of cysteine form disulfide (S-S) links which are responsible in part for the highly stable nature of the nucleus in mature sperm.

ii. The Acrosome

Another structure in the mature sperm head that plays a critical role in fertilization is the acrosome. The acrosome is a large lysosomal-like structure that forms around the anterior portion of the nucleus. It is bounded by a membrane that is considered to have an *inner acrosomal membrane* that faces the nucleus, while an *outer acrosomal membrane* which is in close contact with the plasma membrane. This is a membrane-limited bag which follows the contour of the anterior two-thirds of the nuclear surface and which is filled with homogeneous material of low electron density. This material is enzymic and contains hyaluronidase, as well as a trypsin-like enzyme and also other proteases. It is believed that the acrosomal enzymes have a digestive role in enabling the sperm to penetrate between the granulosa cells that surround the freshly ovulated egg (Eddy, 2006). These enzymes may also be involved in the stage of sperm penetration through the zona pellucida, the outer coat of the egg. The posterior portion of the acrosome is the equatorial segment, which remains intact during the acrosome reaction and is the site of initial contact between sperm and egg at fertilization. Besides the equatorial segment, the post acrosomal part of the sperm head is occupied by diffuse material lying between the plasma membrane and nuclear membrane. This material also has been shown to be

enzymatically active; it extends anteriorly and can be seen to occupy the narrow space between the acrosome and the nuclear surface. Its function is not clear.

iii. The Basal Plate

Posteriorly, the nucleus rests upon a basal plate. The basal plate is adherent to the nuclear envelope, defining the implantation fossa and forming the site of attachment of the flagellum to the sperm head.

iv. The Tail

During spermiogenesis, the haploid sperm cell develops a tail or flagellum, and all of its mitochondria become aligned in a helix around the first part of the tail, forming the mid-piece. The tail contains the motor apparatus of sperm. The tail is again divided into mid-piece, principle piece and end piece. It consists of two central microtubules surrounded by 9 microtubule doublets (This structure is called the axoneme). The complex structure of the mammalian sperm flagellum has been well described at a morphological level. In addition to the axoneme, which is present throughout the length of the flagellum and generates its motor force, there are a number of cytoskeletal accessory structures in discrete regions (Fawcett, 1975; Clermont *et al.*, 1990). The mid-piece, the most proximal portion of the flagellum, contains 9 outer dense fibers (ODFs) and a mitochondrial sheath.

The outer dense fibres (ODF) are sperm tail-specific cytoskeletal structures (Fawcett *et al.*, 1975). They consist of nine fibers which surround the axoneme on its outer side accompanying the tubuli doublets in the middle and principal piece of the

sperm tail (Fig. 5A). At the anterior end, the ODF make close contact with the paracentriolar connecting piece and extend posteriorly for varying lengths into the principal piece. Outer dense fibers were speculated to be contractile because of their close association with axoneme. Other studies suggested that the tensile strength of sperm of several mammalian species correlates with the size of outer dense fibers (Baltz *et al.*, 1990). It was also suggested that it provides mechanical support to sperm during their passage through epididymis or ejaculation where harsh shear forces are encountered (Baltz *et al.*, 1990). Absence of outer dense fibers alters flagellar flexibility and results in modified flagellar beat, causing sterility (Browder *et al.*, 1991). The fact that these structures are found only in the sperm tails of mammals makes it tempting to speculate that this structure may have a mammalian specific function.

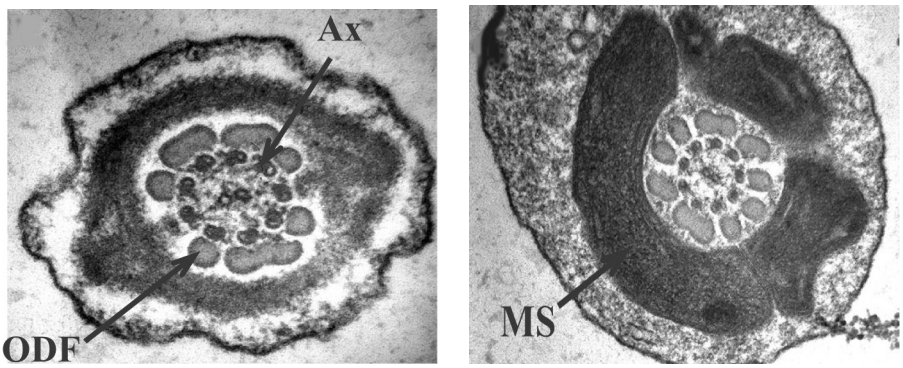

A **B**

Figure 5. A: Electron micrograph of mouse principle piece cross section showing normal structural organization of ODF: outer dense fibers and AX: axoneme (typical 9+9+2 arrangement) **B:** Electron micrograph of mouse mid-piece cross section showing normal arrangement of mitochondria tightly coiled around the outer dense fibers.

The mitochondria are helically wrapped around the outer dense fibers in the middle piece of the sperm tail (Fig. 5B). In mice, mitochondria are usually arranged in two parallel lines around the flagellum (Eddy, 2006). The principal piece is distal to the mid-piece and is the longest subdivision of the flagellum. Although the mitochondrial sheath is no longer present in this region, the fibrous sheath (FS) encases both the ODFs and the axoneme. The fibrous sheath essentially defines the principal piece of the flagellum, which begins at the termination of the mid-piece sheath and extends for most of the remaining flagellar length. The fibrous sheath is composed of two cytoskeletal elements: two longitudinal columns and numerous transverse ribs. These structures, which surround the dense fibers, are composed of a central medulla and a thin limiting cortex (Fawcett, 1970, 1975). The fibrous sheath has been described as an insoluble keratin- like structure with extensive disulphide linkages (Bedford and Calvin, 1974;

O'Brien and Bellve, 1980) and as a modified form of the intermediate filament proteins in morphological, biochemical, physical and immunological features (Eddy *et al.*, 1992; Jassim *et al.*, 1992). The two longitudinal columns of the FS replace ODFs 3 and 8 and are connected to each other by numerous transverse ribs. The classical view is that fibrous sheath helps in the bending of the flagellum. However recent studies identified additional roles for fibrous sheath. It is believed to serve as a scaffold for components involved in signal transduction, energy production and other functions (Eddy *et al.*, 2004). The end piece is the short, terminal section of the flagellum containing only the axoneme, surrounded by the plasma membrane.

b. Epididymal sperm maturation and motility

Spermatozoa leave the testis neither fully motile nor able to recognize or fertilize an egg. They must traverse a long duct, the epididymis, to acquire these abilities. These transformations of spermatozoa are called *epididymal sperm maturation*. For a number of years, the epididymis was considered a holding tube for the spermatozoa; the epididymis was thought not to influence the process of sperm maturation, but was a place where spermatozoa aged. However, it is now clear that the epididymis is actively involved in the sperm maturation process, not only providing an appropriate environment but also providing many of the molecules needed by the spermatozoa to allow them to fertilize an egg. The maturation of spermatozoa and the acquisition of motility and fertilizing ability do not occur as a function of the passage of time, but rather as a consequence of exposure to the luminal environment of the epididymis (Orgebin-Crist, 1967). The composition of

the luminal fluid that bathes spermatozoa as they transit through the epididymis is highly complex and changes progressively along the tissue (Turner, 1991). The secretory and absorptive activities of the epididymal epithelium mediate the changes in the luminal fluid and thus determine the microenvironment in which spermatozoa are able to become fully mature.

The epididymal epithelium is composed of four major epithelial cell types and can be divided anatomically into four segments: the initial segment, caput, corpus, and cauda epididymidis. It is now established that discrete functions take place in the various segments. On a physiological level, this is evidenced by studies of sperm populations taken from discrete regions of the adult epididymis in which developing spermatozoa exhibit segment-related acquisition of motility and fertilizing ability (Kathryn *et al.*, 2001). Sperm are immotile and infertile in caput but caudal sperm possesses forward motility and the ability to fertilize an egg. Extensive modifications associated with sperm maturation are: spermatozoal motility parameters change from immotile or vibratory to direct forward movements, membranes are remodeled; protein composition and location of specific proteins change, glycoproteins are acquired or altered, phospholipids are removed or used, and the lipid composition of the membrane changes (Robaire and Hermo 1988; Jones *et al.*, 1998). Also in the epididymis, chromatin condensation and stabilization of the spermatozoon occurs, and the acrosome acquires its final shape (Mortimer, 1994). When ejaculation occurs, spermatozoa are transported to vas deferens from caudal epididymis (Bedford and Hoskins, 1990; Genuth, 1998).

c. Hyperactivation and Capacitation

Mammalian spermatozoa cannot fertilize oocytes immediately upon ejaculation nor upon retrieval from the epididymis. A series of metabolic and physiological changes must occur before they acquire the ability to penetrate the *zona pellucida* and bind to the oocyte. These changes occur during transit through the female reproductive tract (Austin, 1951; Chang, 1951), and are collectively termed 'capacitation'. The changes which occur during capacitation include (see Yanagimachi, 1981; Farooqui, 1983): (i) removal of molecules adsorbed onto or incorporated into the sperm plasma membrane during epididymal transit; (ii) reduction in the net negative charge of the sperm surface, e.g. by removal of sialic acid residues (Langlais and Roberts, 1985); (iii) increased rate of respiration, as measured by increased oxygen uptake and increased glycolytic activity (Hamner and Williams, 1963; Mounib and Chang, 1964); (iv) efflux of cholesterol (Davis *et al.*, 1980; Davis, 1982), which increases the membrane fluidity. Serum albumin mediates cholesterol loss *in vitro* (Go and Wolf, 1985); (v) redistribution of intramembranous particles, leaving sterol-depleted areas over the acrosomal region (guinea pig spermatozoa: Langlais and Roberts, 1985); (vi) changes in lectin binding sites; and in chlortetracycline binding patterns (this is due to changes in Ca^{2+} distribution); (vii) changes in osmotic properties of the sperm plasma membrane and in membrane permeability; and (viii) accumulation of Ca^{2+}. Capacitation results in hyperactivated motility and the ability of the spermatozoon to undergo the acrosome reaction (Bedford, 1983). Since hyperactivation is caused by changes in the flagellar beat pattern,

capacitation probably involves alterations in the physical and chemical properties of the tail plasma membrane as well as the head plasma membrane (Yanagimachi, 1988). Hyperactivation is a flagellar phenomenon, even though it is often measured by changes in the movement of the sperm head. It is generally accepted that hyperactivation is a calcium-dependent phenomenon, with evidence accumulated from a number of species, including human (Yanagimachi, 1988, 1994; Cooper, 1982).

d. Regulation of sperm motility

Factors involved in signal cascades lead to changes and or activation in the conformation, phosphorylations and / or localization of proteins in the pathway. Similarly several factors are involved in triggering and maintaining sperm motility. Key factors involved in the initiation of progressive motility and induction of hyperactivated motility in sperm are activating factors such as calcium ions (Ca^{2+}), bicarbonate (HCO^{3-}) and cyclic adenosine monophosphate (cAMP). Other possible mechanism that had been suggested for the initiation of motility is that it occurs as a result of release from the influence of an inhibitor of motility. Sperm motility quiescence factors were reported in bovine and rat epididymal fluid (Carr and Acott, 1984; Turner, 1982).

Calcium has important roles in multiple aspects of sperm function including motility. Recent studies with knock out mice have demonstrated at least four components that participate in the regulation of calcium levels: Catsper1, Catsper2, voltage dependent calcium channel (VDCC) and PMCA4. Catsper 1 and 2 mutant mice are infertile and fail to develop hyperactivated motility (Ren *et al.*, 2001; Quill *et al.*, 2003). Gene knockout

studies with VDCC and PMCA4 also suggested their roles in sperm function. VDCC mutant sperm show defective sperm motility (Sakata *et al.*, 2002). Reports on PMCA4 mutant sperm indicated a role in progressive velocity, track speed and intracellular calcium levels in comparison with wild type sperm. (Schuh *et al.*, 2004). cAMP is a key second messenger in the regulation of sperm motility. Increase in cAMP levels lead to increase in sperm motility (Vijayaraghavan *et al.* review, 2007). cAMP in sperm presumably through the activation of cAMP dependent PKA which phosphorylates serine and threonine residues on neighboring proteins triggers a cascade of protein phosphorylation events primarily in flagellum. Recent studies with genetic approaches confirmed the role of cAMP and PKA in sperm function. Targeted disruption of sperm adenyl cyclase and the catalytic subunit of PKA result in infertility in male mice due to lack of sperm motility (Nolan *et al.*, 2004; Esposito *et al.*, 2004).

e. The role of kinases and phosphatases in sperm function

The steady-state phosphorylation status of a protein is determined by the relative activity, of the protein kinases and phosphatases acting on that protein. Increases in sperm protein phosphorylation have been implicated in the initiation of progressive motility, hyperactivated motility, capacitation, the acrosome reaction, and fertilization. Most sperm proteins which become phosphorylated between release from the epididymis and fertilization are in the flagellum and potentially involved in motility (Bracho *et al.*, 1998). Research in sperm protein phosphorylation, until recently, was largely focused on protein kinases, protein kinase A (PKA) in particular (San Agustin & Witman, 1994;

Breitbart, 2003). It is well known that motility stimulation can be affected by cAMP-mediated PKA activation (Hoskins *et al.*, 1975; Hoskins *et al.*, 1978; Lindemann, 1978). A role for PKA necessarily implies a function for a protein phosphatase since protein phosphorylation is a result of the net activities of protein kinases and phosphatases. Protein phosphatases can significantly modify and restrict PKA action. Inclusion of protein phosphatases in the reactivation media prevents motility initiation (Takahashi *et al.*, 1985; Murofushi *et al.*, 1986). It is likely that a protein phosphatase might be involved in the regulation of flagellar motility. The inhibition of phosphatase activity results in the stimulation of motility (Vijayaraghavan, 1996), strongly suggests that phosphates have an important role in regulation of this and other processes in sperm. While phosphatases are important components of signalling and regulatory pathways in other cell types, little is known about phosphatases in spermatogenesis and sperm.

Eukaryotic protein phosphatases are classified into two distinct gene families: PPP and PTP. PPP are the phosphoprotein phosphatases and belong to serine threonine phosphatases while PTP are phosphotyrosine phosphatases (Barfod et al, 1998). Protein phosphatase 1 (PP1) belongs to a family of protein phosphatases, PPP, which include PP1, PP2A, PP2B (calcineurin) among others. The enzyme PP1, which exists in multiple isoforms in diverse organisms, from yeast to mammals, is a highly conserved protein. In mammals there are four catalytic subunit isoforms of PP1, encoded by three genes: PP1α, PP1β, PP1γ1, and PP1γ2 (Wera & Hemmings, 1995; Cohen, 2002; Ceulemans & Bollen, 2004). There is a high degree of conservation of these isoforms in diverse species.

PP1γ2 is predominantly expressed in testes while the other isoforms, PP1α, β and γ1, are widely expressed in mammalian tissues. The functional importance of PP1

isoforms remains unclear. Though the number of protein kinases, are far more than protein phosphatases, however the targeting or regulatory units for phosphatases are greater in number leading to diverse function of phosphatases at cellular level. It has been thus rightly speculated that phosphatases may associate with distinct regulatory subunits and thereby serve unique physiological functions but so far there has been little evidence to support this idea (Lesage, 2004). PP1 activity is regulated by many hormones and growth factors (Sheonilikar, 1998, review). As the levels of PP1 catalytic subunit do not change in response to physiological stimuli, hormonal regulation is thought to occur primarily through endogenous inhibitors and in some cases, through regulatory subunits (Sheonilikar, 1998, review). The largest number of phosphatase inhibitors thus far identified target PP1. These include Inhibitor-1 (I-1), Inhibitor-2 (I-2), dopmine- and cAMP-regulated phosphoprotein of Mr 32,000 (DARPP-32), nuclear inhibitor of PP1 (NIPP-1), C-kinase activated phosphatase inhibitor (CPI17), and ribosomal inhibitor of PP1 (RIPP-1). In addition, a large number of PP1-binding proteins have been shown to inhibit the phosphorylase a phosphatase activity of PP1 in vitro (eg. nek) (Cohen, 2000). The precise role of these latter proteins in controlling PP1 activity in intact cells remains unknown, but some of these PP1-binding proteins may also turn out to be phosphatase inhibitors. Regardless, PP1 inhibitors are among the best understood phosphatase regulators and have set many of the prevailing beleifs for phosphatase regulation.

f. Role of PP1γ2 in spermatozoa

Enzyme activity and Western blot analyses showed that PP1γ2 is a predominant serine/threonine protein phosphatase in spermatozoa (Smith *et al.*, 1996; Vijayaraghavan *et al.*, 1996; Chakrabarti *et al.*, 2007). The activity of a protein phosphatase (that is highly expressed in testes and spermatozoa, PP1γ2) has been found to be inversely related to motility (Vijayaraghavan *et al.*, 1996; Smith *et al.*,. 1996; 1999). Inhibition of PP1 with calyculin A (CA) or okadaic acid (OA) causes motility initiation in caput spermatozoa and stimulation of motility in caudal spermatozoa (Vijayaraghavan *et al.*, 1996; Smith *et al.*, 1999). These inhibitors have also been found to promote hyperactivation (Si, 1999) and acrosome reaction (Si and Okuno, 1999). The stimulatory effect of these agents bypasses the requirements for high cAMP and pH levels that were thought to be essential to the initiation of sperm motility. PP1γ2 activity is higher in caput than in caudal spermatozoa (Smith *et al.*, 1999). Studies on fowl spermatozoa found that CA and OA stimulated rooster sperm motility (Ashizawa *et al.*, 1994; Ashizawa *et al.*, 1995). The enzyme PP1γ2 is present in spermatozoa of a wide range of mammalian species including humans and non-human primates (Vijayaraghavan, S. 1996, Smith *et al.*, 1999). Taken together these data suggest a key role for the protein phosphatase-PP1γ2 in flagellar motility in general.

g. The role of PP1γ2 in sperm function and spermatogenesis

The enzymes PP1γ1 and PP1γ2 are alternatively spliced variants generated from a single gene (Kitagawa *et al.*, 1990; Varmuza *et al.*, 1999). They are identical in all

respects except that PP1γ2 has a unique 21-amino-acid carboxy terminus extension. While PP1α, PP1β, and PP1γ1 are ubiquitous, PP1γ2 is predominantly expressed in testis and is the only isoform of PP1 detected in spermatozoa (Smith *et al.*, 1996; Vijayaraghavan *et al.*, 1996; Ceulemans & Bollen, 2004). Targeted disruption of *Ppp1cc*, resulting in the loss of PP1γ1 and PP1γ2 causes infertility in male mice due to impaired spermiogenesis and leading to the absence of epididymal spermatozoa (Varmuza *et al.*, 1999, 2003). This indicates that one or both of the isoforms are involved in sperm development and possibly spermiation (the release of mature sperm from the seminiferous epithelium into the lumen). It is not known if spermatogenesis requires both- PP1γ isoforms or only PP1γ2. The main objective of this dissertation is to understand the roles of different PP1 isoforms in postnatal testes and sperm development and to determine the role of PP1γ2 in sperm morphogenesis and post meiotic protein expression during spermatogenesis using *Ppp1cc*-null mice model. Data presented in this dissertation are published in Vijayaraghavan *et al.*, Gamete biology: Emerging frontiers in fertility and contraceptive development, 2007 and Chakrabarti *et al.*, Biology of Reproduction, 2007.

The three aims of this dissertation are:

1. Determine spatio-temporal distribution of PP1 isoforms in developing and mature testes to understand their roles in spermatogenesis

2. Examination of *Ppp1cc*-null mice in greater detail to understand morphological and histo-chemical defects in testes and sperm in comparison with wild type mice

3. Determine role for PP1γ2 in sperm morphogenesis

Methods

Expression of recombinant proteins and purification

The rat PP1γ1 or PP1γ2 cDNA (Dr. Edgar F da Cruz e silva, Portugal) was within a pTACTAC vector containing a trp-lac fusion promoter that preceded the PP1 DNA. *E-coli* (bl21), harboring the cDNA were grown in one liter of LB medium containing 1 mM $MnCl_2$ and ampicillin (0.1 mg/ml) at 37° C with shaking at 250 rpm. After 10 h incubation at 26° C an OD $_{600nm}$ of ~0.6), 0.3 mM isopropyl-β-D-thiogalactopyranoside (IPTG) was added to induce the expression of PP1γ1 or PP1γ2. Cells were incubated for up to an additional 13 h and then centrifuged at 4000g for 30 min. The pellet was resuspended in 6 ml of 10 mM Tris-HCl buffer (pH 8.0), 30 Mm imidazole, 300 mM NaCl, 10% glycerol containing 1mM $MnCl_2$, 0.2mM PMSF, 4mM benzamidine, 15mM 2-mercaptoethanol, 0.1 mM EGTA, pepstatin A(10 μg/ml), leupeptin (10 μg/ml) and chymostatin (10 μg/ml) (buffer C). Cells were lysed using a homogenizer. Cell debris was removed by centrifugation at 35,000g for 15 min, and the supernatant was clarified by centrifugation at 35,000g for 45 min. The resulting supernatant was loaded on a Ni-NTA-agarose column (volume, 3 ml) at a rate of 1 ml/min; the column washed with buffer C, and His6-PP1γ1 or His6-PPγ2 were eluted with an increasing linear gradient of imidazole (30-500 mM) in buffer C (total gradient volume, 10 ml). The fractions were collected and analyzed by SDS-PAGE and phosphatase assay for active PP1γ1 or PP1γ2

fractions. Fractions containing active His6-PP1γ1 or PP1γ2 were pooled and stored in small aliquots at -80° C containing glycerol.

Protein phosphatase activity assay

Preparation of ^{32}P radio-labeled phosphorylase *a* and its use as a substrate for measurement of PP1 activity has been previously reported (Vijayaraghavan *et al.*, 1996). The substrate and recombinant proteins were incubated (in a total volume of 40 µl) at 30° C with 1 mM Mn^{2+} and with or without PP1-specific inhibitors for 10 min. At the end of this incubation, the reaction was terminated with 180 µl 20% trichloro acetic acid (TCA) after which the tubes were centrifuged for 5 min at 16,000 x g at 4°C. The supernatants were analyzed for $^{32}PO4$ released from phosphorylase *a*. This assay is specific for the protein phosphatases PP1 and PP2A.

Cloning of PP1γ2 in myc and non myc vector

The full length cDNA for PP1γ2 were introduced in n-myc-pcDNA4.1 (Dr. T. Weimbs, Cleveland Clinic Foundation) and pcDNA3.1+ (gift from Dr. G. Fraizer, Kent State University) using BamH1 and XhoI respectively yielding expression vectors for PP1γ2 (+/- myc tag). These subclones would be used in cell culture to study sub-cellular localization of PP1γ2 in somatic cells.

Cell culture, transfection, Western blot and immunocytochemistry of cultured cells

HEK 293 cells (human embryonic kidney cell line) were maintained in culture in Dulbecco's modified Eagle's minimum essential medium, supplemented with 10 % fetal calf serum, 2 mM L-glutamine, 50 μU/ml penicillin, 50 μg/ml streptomycin and 1 % non-essential amino acids. In preparation for experiments and 24 h prior to experimentation, cells were seeded at a density of 0.5 million cells per 35 mm dish. Experiments were conducted using lipofectamine as the transfection reagent. Lipofectamine (6 μg) was mixed with 100 μl of serum-free medium and incubated at room temperature for 5 min prior to adding to 100 μl of serum-free medium containing cDNA (2 μg). After mixing this solution containing transfection reagent and cDNA was incubated for 20 min at room temperature and then added to the cells. The cells were incubated for 6 h at 37° C. After incubation with the transfection reagent and cDNA, media with serum (to give 10 %) was added to cells and cells were grown for 48 h.

For Western blot analysis or activity assays, cells were washed with PBS for 5 min, twice and harvested in passive lysis buffer (Promega) or RIPA lysis buffer (Upstate Biotechnology, IL). Following centrifugation, (16,000g for 10 min), the supernatants were used for Western blot analysis or activity assay. For immunocytochemistry (ICC), 40 h after transfection, the HEK293 cells were washed twice with PBS and fixed for 10 min in 20 % methanol. Cell permeabilization was performed by 10 min incubation in PBS supplemented with 0.5 % Triton X-100. The permeabilized cells were washed three times in PBS for 5 min each, blocked with PBS supplemented with 5% BSA and 5 % goat serum and incubated for 1 h in a blocking solution. The slides were then incubated

with primary antibody for 1 h at room temperature or overnight at 4° C, washed 3 times with PBS for 5 min each, and incubated with a secondary antibody which is conjugated to Indocarbocyanine(Cy3), (Jackson Laboratories, West Grove, PA) for 1 h at room temperature. The slides were washed 5 times with PBS and examined by fluorescence microscopy.

Preparation of mouse testes, caudal and caput extracts

Testes from wild-type and *Ppp1cc*-null mice were homogenized in RIPA lysis buffer (Upstate Biotechnology, IL), containing 10 mM benzamidine-HCl, 1 mM PMSF, 0.01 mM TPCK, and 5 mM β-mercaptoethanol using 1 ml buffer for 0.1 g tissue. The homogenates were centrifuged at 16,000 x g at 4^{o}C for 10 min. The supernatants are referred to as testis extract. Testis extracts were supplemented with 10% (v/v) glycerol and stored at –20^{o}C until further use. Caudal epididymal spermatozoa were isolated from mouse epididymides and washed twice with Whittingham's media (99.3 mM NaCl, 2.7 mM KCl, 1.8 mM $CaCl_2 \cdot 2H_2O$, 0.5 mM $MgCl_2 \cdot 6H_2O$, 0.36 mM NaH_2PO_4, 25 mM $NaHCO_3$, 25 mM sodium lactate, 0.50 mM sodium pyruvate, 5.55 mM glucose, 100 U/ml penicillin-G potassium salt, 50 mg/ml streptomycin sulfate). Spermatozoa were collected by centrifugation and the pelleted spermatozoa were suspended in RIPA lysis buffer containing 10 mM benzamidine-HCl, 1 mM PMSF, 0.01 mM TPCK, and 5 mM β-mercaptoethanol. The sperm suspension was sonicated with three 5-sec bursts of a Biosonic sonicator (Bronwell Scientific, Rochester, NY) at maximum setting. The sperm sonicate was centrifuged at 16,000 x g at 4^{o}C for 10 min. The 16,000 x g supernatants

were supplemented with 10% (v/v) glycerol and stored at –20^{o}C until further use. This preparation is referred to as soluble sperm extracts in this article.

SDS PAGE and Western blot analysis

Extracts for Western blot analysis were prepared by boiling with SDS sample buffer for 5 min. Testis and sperm proteins were separated by 12% SDS-PAGE based on the protocol of Laemmli (Laemmli, 1970). Proteins were then electrophoretically transferred to Immobilon-P-PVDF membrane (Millipore Corp., Bedford, MA). Nonspecific protein binding sites on the membrane were blocked with 5% nonfat dry milk in Tris-buffered saline (TBS: 25 mM Tris-HCl, pH 7.4, 150 mM NaCl). The blots were then incubated with primary antibodies at 4^{o}C overnight except SP17 and FSII which were incubated for 1 h at room temperature. After the wash, the blots were incubated with an appropriate horseradish peroxidase-conjugated secondary antibody (1:2000) for 1 h at room temperature. Blots were washed with TTBS 2 X 15 min each and 4 X 5 min each. The blots were then developed with ECL.

Genotype and PCR

The genotypes of all offspring of mutant mice were analyzed by polymerase chain reaction (PCR). For amplification of the wild-type and the mutant allele, the DNA was extracted from mouse ear punch. Genotyping has been performed by PCR analysis of ear DNA, using one common primer from intron IV (5’ CTCAGGCCAATGCTGTCTGC 3’), a neo-specific primer for the mutant allele (5’ GGTGGATGTGGAATGTGTGCG 3’),

and a wild-type allele-specific primer from the deleted portion of intron VI (5' ACTCATAGCCATCTTCAACCA 3'). These primers amplify an 500-bp fragment from the wild-type allele and an 250-bp fragment from the mutant allele The PCR conditions were as follows: 94°C/1 min, 55°C/1 min, 72°C/1 min 30 sec for 30 cycles performed in 25-µl volumes containing 10 mM Tris–HCl, 1.5 mM MgCl2, 50 mM KCl, 0.2 mM each dATP, dCTP, dGTP, and dTTP, 25 pmol each primer, 2.5 U *Taq* polymerase , and 2-5 ul genomic DNA. 12-15 µl of each PCR was loaded on a 1.5% agarose gel and visualized under ultraviolet light.

Hematoxylin staining of tissue sections and immunohistochemistry

Testes of both wild-type and *Ppp1cc*-null mice were fixed in 4% paraformaldehyde in PBS at 4°C for 40 h. The testes were then transferred to 75% ethanol and dehydrated, permeabilized, and embedded in paraffin using a Shandon Tissue Processor (Thermo Electron Corporation, Waltham, MA). Multiple 8 µm thick sections of the whole testis were attached to poly-L-lysine-coated slides, deparaffinized, and rehydrated using standard procedure. Slides were stained with Harris's Haematoxylin for 2 min. Sections were briefly washed in running tap water for 2 min. Slides were then dipped in acid rinse solution (1 ml glacial acetic acid+ 49 ml of d water) followed by a brief wash with bluing solution for 1 min (1g sodium bicarbonate in 1liter of water). Slides were then washed in tap water for 1 min and dehydrated with increasing concentration of alcohols. The coverslips were mounted with DPX and dried overnight.

For immunohistochemistry, multiple 8 µm thick sections of the whole testis were attached to poly-L-lysine-coated slides, deparaffinized, and rehydrated using standard procedures. Antigen retrieval was performed using 1X Antigen Retrieval Citra Solution (BioGenex, San Ramon, CA). Sections immersed in Citra solution were microwaved for three separate, three-minute periods on high setting with a cooling period of one minute between each heating cycle. Sections were washed briefly in distilled water and then washed three times for 10 minutes with phosphate buffered saline (PBS). Sections were incubated for 1 h at room temperature in a blocking solution containing 10% normal goat serum in PBS at room temperature. The slides were then incubated with primary antibodies for 2 h at room temperature or overnight at 4°C, washed three times with PBS, and incubated with corresponding secondary antibody (1:250) conjugated to indocarbocyanine (Cy3; Jackson Laboratories, West Grove, PA) for 1 h at room temperature. The slides were washed five times with PBS and mounted with Vectashield mounting media and examined using a FluoView 500 Confocal Fluorescence Microscope (Olympus, Melville, NY). Control slides were processed in the same manner except that the primary antibody was omitted.

Quantitative analysis of testicular sperm

Testes of both wild-type and *Ppp1cc*-null mice were fixed in 4% paraformaldehyde in PBS at 4°C for 40 h. The testes were then transferred to 75% ethanol and dehydrated in increasing grades of alcohol, permeabilized, and embedded in paraffin using a Shandon Tissue Processor (Thermo Electron Corporation, Waltham,

MA). Multiple 8 μm thick sections of the whole testis were attached to poly-L-lysine-coated slides, deparaffinized, and rehydrated using standard procedures. Sections were stained with Hematoxylin stain. A quantitative analysis of the testicular spermatozoa population in wild *vs*. null testes was performed to estimate the loss of the testicular sperm cells in null testes in the absence of PP1γ gene.

ICC of epididymal sperm

Caudal and caput epididymal spermatozoa were isolated from mouse epididymides and washed twice with Whittingham's media (99.3 mM NaCl, 2.7 mM KCl, 1.8 mM $CaCl_2 \cdot 2H_2O$, 0.5 mM $MgCl_2 \cdot 6H_2O$, 0.36 mM NaH_2PO_4, 25 mM $NaHCO_3$, 25 mM sodium lactate, 0.50 mM sodium pyruvate, 5.55 mM glucose, 100 U/ml penicillin-G potassium salt, 50 mg/ml streptomycin sulfate). Sperm were then resuspended in PBS. The cells were fixed in 4% formaldehyde in PBS at 4 C for 1/2 h. The sperm solution was then treated with 0.2% Triton X-100. The fixed sperm was attached to poly-L-lysine coated slides. The slides were washed once with TTBS, 3 times with TTBS supplemented with 5% BSA, and incubated for 1 h in a blocking solution containing 5% BSA and 5% normal goat serum in TTBS at room temperature. The slides were then incubated with primary antibody (anti-PP1γ2 antibody) for 1 h at room temperature or overnight at 4 C, washed 3 times with TTBS, and incubated with a secondary antibody which is conjugated to Indocarbocyanine (Cy3), (Jackson Laboratories, West Grove, PA) for 1 h at room temperature. The slides were washed 5 times with TTBS and examined by fluorescence microscopy.

Testicular sperm isolation and indirect immunofluorescence with MitoTracker Green

Testicular sperm were isolated using the protocol described by Kotaja *et al.,* 2004. Testis from both wild-type and null mice were decapsulated (removing the membrane covering the tissue) in PBS. Seminiferous tubules were untangled manually using fine forceps and small pieces of the tubule were stretched and observed by transillumination. Dark regions containing testicular sperm with condensed nuclei were then teased open and sperm suspensions were observed using DIC optics of confocal microscopy. For staining with MitoTracker Green (Invitrogen), sperm suspensions were incubated with 200 µl of MitoTracker Green (0.25 mM) for 10 min and then examined using a FluoView 500 Confocal Fluorescence Microscope (Olympus, Melville, NY).

Scanning Electron Microscopy

Seminiferous tubules were dissected in HEPES buffer along with 100 mM sucrose to release the testicular sperm cells along with other germ cells which were immediately fixed in 1.25 % Glutaraledyde and 1% paraformaldehyde in Mgcl2 and Cacl2, 0.1 M sucrose and .15 M hepes, pH 7.4 for 1-2 h on ice. The fixed sperm was attached to poly-L-lysine coated coverslips and washed 3 times in HEPES buffer with sucrose for 5 min each and dehydrated with increasing concentration of alcohols. Dehydration step was followed by critical point drying for 45 min and gold coated for 4 min. Slides were observed using JEOL JEM5400 SEM.

Transmission Electron Microscopy

Tissue preparation for light and electron microscopy involved a modification of the technique described in Orth and Christensen, 1977. Briefly, 20-week old mice were anesthetized with Avertin (1.25% tribromethanol injected IP at 25-30 μl/g of body weight), and then perfused through the descending aorta with 2.5% glutaraldehyde in 0.1M sodium cacodylate. Following fixation, the testes were removed, minced and immersed in the same fixative for 15 min at 4°C. After washing in 0.1M sodium cacodylate buffer, the tissue blocks were post-fixed in 1.33% OsO_4 for 90 min at 4°C, then dehydrated through a graded series of ethanols, infiltrated with and subsequently embedded in Epon/Araldite.

For light microscopy of EM fixed tissue, 1 μm thick sections were cut and dried onto slides, followed by staining in 1% toluidine blue in 1% sodium borate. Sections were viewed and photographed with a Leitz Orthoplan 2. For electron microscopy, ultrathin sections, 85 nm thick, were cut and placed onto grids, followed by staining for 5 min in 10% uranyl acetate in methanol and then in Reynold's Lead Citrate for 2 min. Sections were viewed and photographed with a Philips 400 TEM.

RNA extraction of tissues and cDNA preparation

Total RNA was isolated from whole tissues (testes, lung, caudal epididymis, brain, heart, liver, spleen and kidney) using TRIzol reagent (Invitrogen, Carlsbad, CA). Total

RNA (1 µg) was pretreated with DNA wipe out (Qiagen) and reverse transcribed using Qiagen kit in the presence of random primers (Qiagen) using standarad protocol of the manufacturer.

RNA analysis of individual germ cells using Laser Capture Micro-dissection

Mouse testes tissue was immediately embedded in optimal cutting compound (OCT) medium after dissection and subsequently in isopentane and liquid nitrogen. Using a cryostat, tissue sections were cut to 8 µm thickness and placed on RNAse-free microscope slides. Tissues were stained with Mayer's hematoxylin reagent. The pure population of spermatogonia, primary spermatocytes (pachytene), round spermatids and elongating spermatids were microdissected using the LCM (LM200, Arcturus Engineering, Mountain View, CA, USA) system according to the manufacturer's instructions. Individual germ cells were isolated after identifying their correct stage. Stages were identified on the basis of nuclear stain of different germ cell as mentioned in the introduction in Fig. 3. Approximately a set of 2,000 cells of each type were micro-dissected. Total RNAs were extracted from the LCM-captured cells using RNA pico pure Kit (Arcturus, CA). The RNAs from spermatogonia, primary spermatocyte, round spermatid cells and elongated spermatids were used as templates to reverse transcribe the first-strand cDNA using the Qiagen cDNA Synthesis Kit according to the manufacturer's protocol. Then the cDNA was amplified by RT- PCR. A sample of 2 µl of the first-strand cDNA mixture was transferred to a tube containing 18 µl of PCR reaction system: 11 µl deonized water, 2µl PCR buffer, 2.5 µl dNTP mix, 2 ul of Mgcl2, 0.2 µl PCR primer and

0.2 ul of AmpliTaq polymerase. The PCR products were separated by electrophoresis on a 2 % agarose/EtBr gel in 1×TAE buffer.

Table 1. List of all the primers used for this study

Sds22	5'-CTCGTCGACGCCAATATGGCGGCAGAGC-3' 5'-CTCGCGGCCGCAGGGCTCAGAACCTGACGTA-3'
SP-10	5'-CTGGGTCTTTATCTGCTTGGA-3' 5'-GAGAGGTTCATTCCGACAGC-3'
PP1γ exon4	5'-GCTGTGGAAAACGTTCACAG-3'
PP1γ1exon8	5'-CTCATCGATGCGTGCCATACAGTCCA-3'
PP1γ2exon8	5'-AACCATTCTCAGCACATGGC-3'
AKAP4	5'-CAATAAGCGTTGTTGTGATCCTAGA-3' 5'-AGGGCCAGGAGTTTCAGAAT-3'
ODF2	5'-TCATGGCCTTGAAGGATACCA-3' 5'-TGCAGTGCTGTTCCCTCA-3'
PP1α	5'-TCAAGCCCGCTGATAAGAAT-3' 5'-CAAGAGACCAGATGGGTTGC-3'
PP1β	5'-TTGAAACCATCTGAAAAGAAAGC-3' 5'-CTGTAATGAGGGGTAAGTTTTCTT-3'
b- actin	5'-AGAGGGAAATCGTGCGTGAC-3' 5'-CAATAGTGATGACCT GGC CGT-3'
Cyclophilin	5'-CTTTGCAGACGCCGCTGTCTCTTTTCGCCG-3' 5'-GCATTTGCCATGGACAAGATGCCAGGA-3'

Results

A. Antibody specificity

1. Purification and characterization of recombinant PP1γ1 and PP1γ2

To determine antibody specificity, we made recombinant His-PP1γ2 and His-PP1γ1. Recombinant His-PP1γ2 and His-PP1γ1 from cDNA inserts in pTACTAC plasmids were prepared in E. coli. His-PP1γ2 and His-PP1γ1 pTACTAC plasmids were a generous gift from Dr. Edgar F da Cruz e silva (Signal Transduction Laboratory, Center for Cell Biology, University of Aveiro, Aveiro, Portugal). His-PP1γ1 or PP1γ2 purification fractions were analyzed by probing a Western blot with anti-his, PP1γ1 or PP1γ2 antibodies as well as using phosphatase assays to determine the fractions containing the active recombinant proteins. As shown in Figure 6A, the majority of PP1γ2 were eluted from the nickel column in the 300mM fractions of imidazole. Purity of his-PP1γ2 was confirmed by staining the companion gel with commassie blue stain (Fig. 6D). Fractions were reconfirmed using anti-his antibody (Fig. 6B). Similarly, PP1γ1 was purified from 300 mM imidazole fractions (Fig. 6C). Dialysis to generate fusion protein suitable for binding assays was performed on those elution fractions which showed activity using phosphatase assay; the remaining fractions were discarded. To determine if the recombinant PP1γ2 or PP1γ1 behaves like the native PP1 forms, the biochemical activities of the proteins were confirmed using inhibitor like I2, OA and CA (Fig. 7A and 7B).

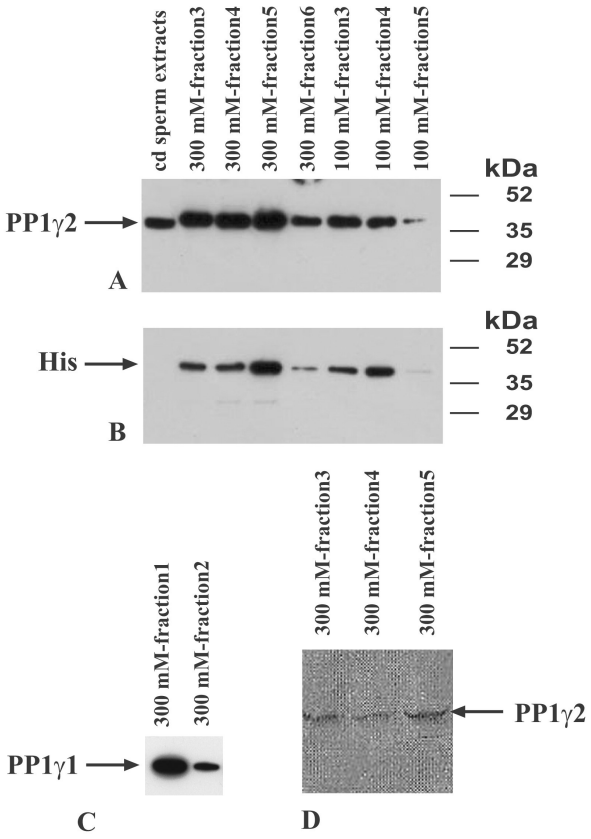

Figure 6. Purification of His-PP1γ2 and His-PP1γ1. A: Western blot of his-PP1γ2 purification elution fractions 3–6 of 300 mM immidazole and 100 mM immidazole in lanes 2-8 from left to right. Caudal (cd) sperm extracts were used as positive control. **B:** Companion blot was probed with anti-his antibody. **C:** Western blot of his-PP1γ1 purification elution fractions of 300 mM. **D:** Gel stained with commasie blue stain to

show purity of His-PP1γ2 protein at three different fractions of 300 mM immidazole eluate.

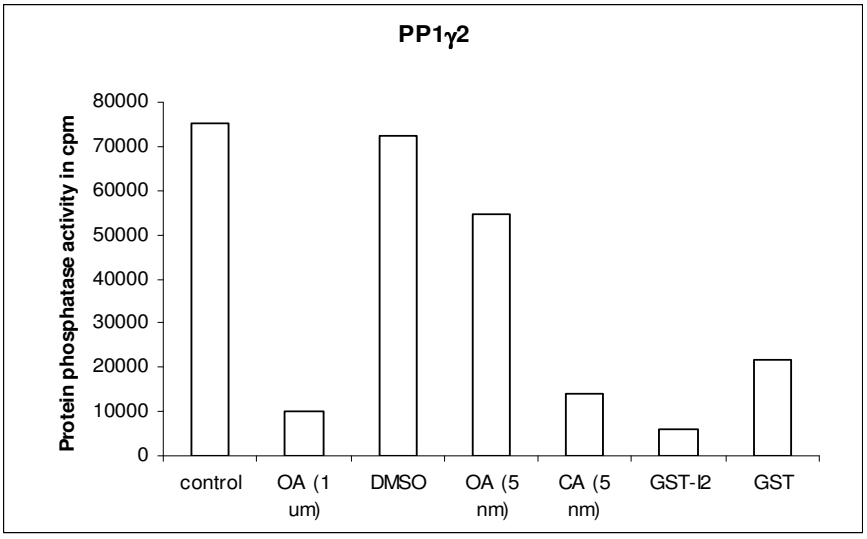

A

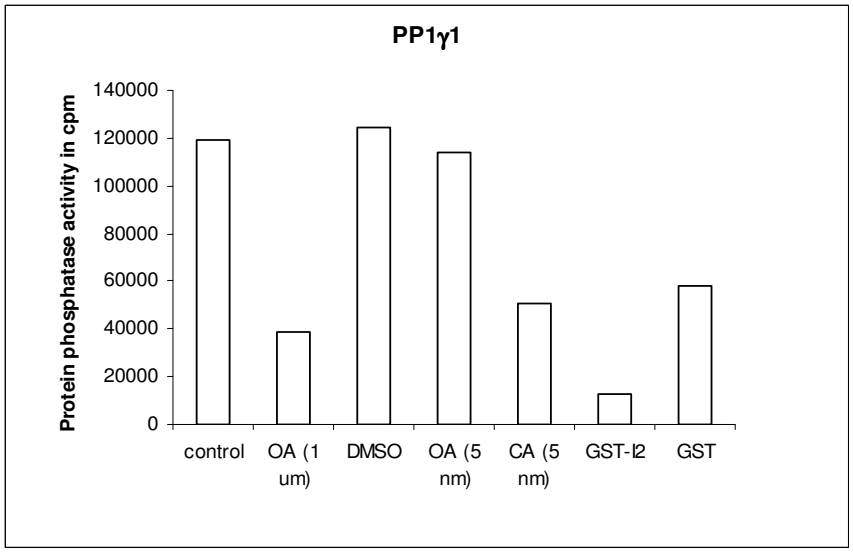

B

Figure 7. A and B: Characterization of protein phosphatase activity present in recombinant PP1γ2 and PP1γ1 prepared as described in *Materials and Methods*. Phosphorylase phosphatase activity was measured in the presence of the indicated doses

of OA, CA, GST-I2 and GST (DMSO was used as control as inhibitors were made in DMSO).

The amino acid sequences of PP1 isoforms are 98% similar (Kitagawa *et al.*, 1990) as shown by Fig. 8. The amino acid sequences for the three isoforms of PP1 allowed us to select specific peptides to be used to produce isoform specific antibodies. The C-terminal regions of PP1α, PP1γ2, and PP1γ1 were chosen since they exhibited the greatest divergence (Wang, 2005; Sasaki, 1995). Figure 9A shows the alignment of their deduced C-termini and highlights the peptides chosen for antibody production. Western blot analysis using recombinant proteins (PP1γ1 and PP1γ2) showed that each antibody reacted specifically and strongly against the isoform to which it was raised and showed essentially no cross-reactivity to the other isoforms (Fig. 9B). Specificity of PP1α antibody is well established (Smith *et al.*, 1996).

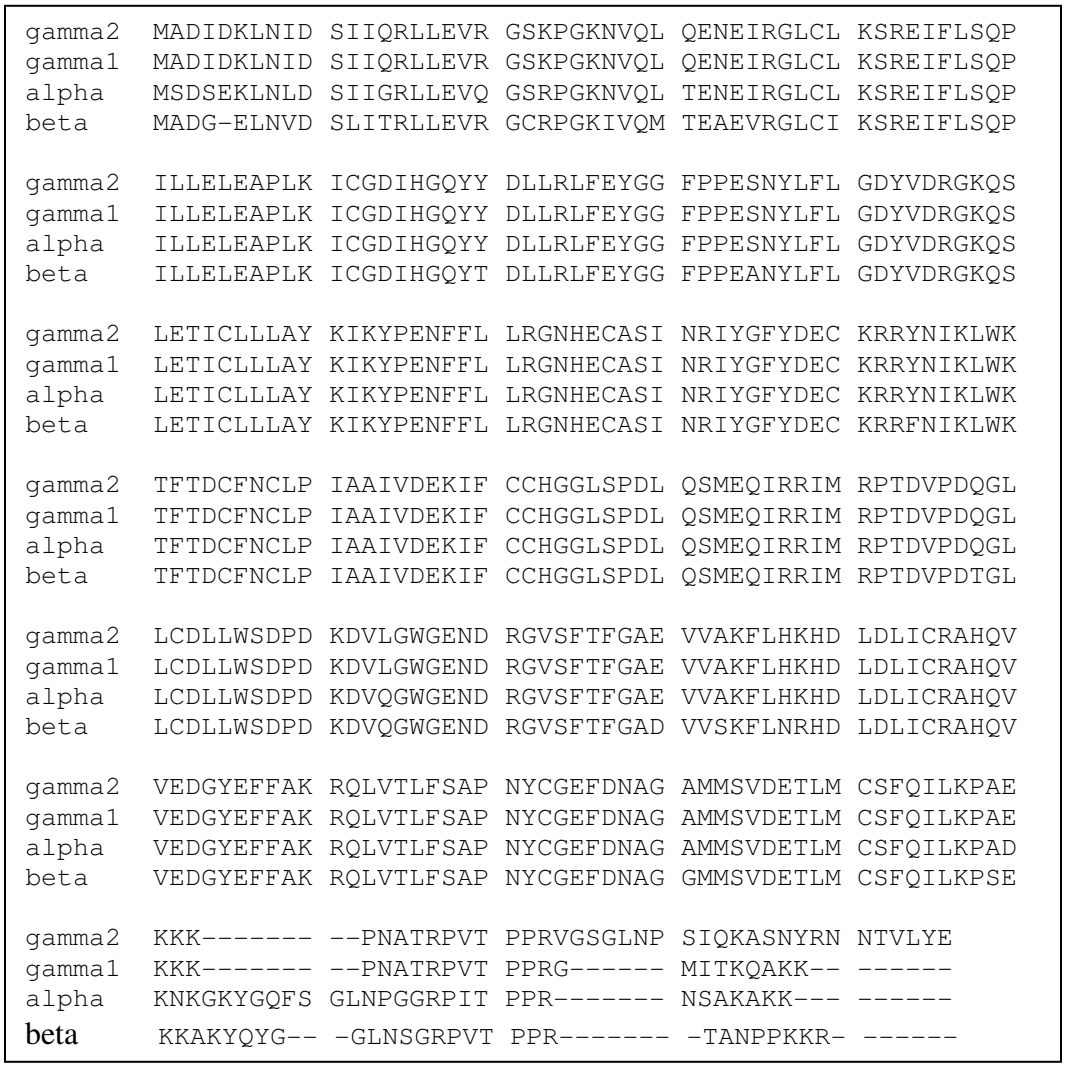

Figure 8. Amino acid sequences of PP1 isoforms showing 98 % similarity. Major divergence are observed in the C-terminus of the sequence.

PP1α TPPR---N --S--AKAKK---------
PP1γ1 TPPR---GMIT--KQAKK---------
PP1γ2 TPPR**VGSGLNPSIQKASNYRNNTVLYE**

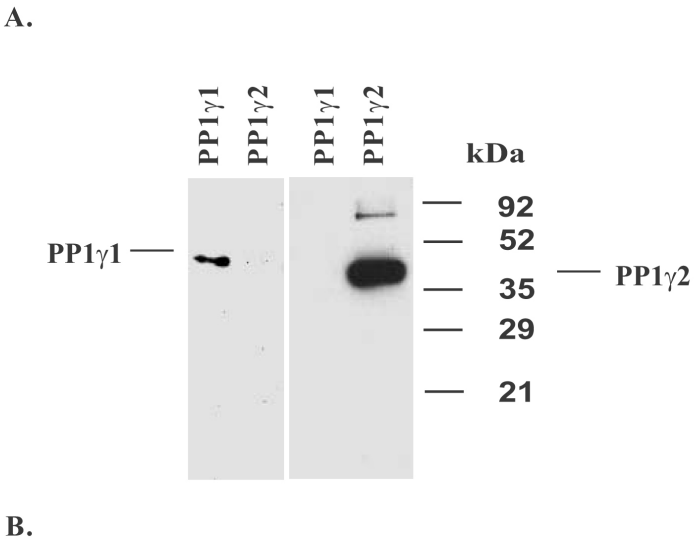

Figure 9. A: Isoforms of PP1 are most divergent at their C termini. Single letter code sequences of amino acids of PP1α, PP1γ1 and PP1γ2 at their divergent COOH termini are shown. The peptide sequences used for generation of the isoform specific antibodies are underlined. **B:** Characterization of PP1 isoform antibodies. Purified, recombinant PP1γ1 or PP1γ2 were immunoblotted with respective antibodies indicated at the left and right respectively.

B. Spatiotemporal Distribution of PP1 isoforms suggest an independent role for each isoform in spermatogenesis

A detailed analysis of distribution and developmental changes in the expression of PP1 isoforms, - PP1α, PP1γ1 and PP1γ2 in mouse testis has never been reported. Such detailed information on PP1 isoform distribution was available for brain (Strack *et al.*, 1999; da Cruz e Silva *et al.*, 1995). In our study, isoform-specific antibodies raised against PP1γ1, PP1γ2 and PP1α were employed to determine the distribution of these proteins in wild-type testicular cells and spermatozoa from mice.

1. Expression of PP1γ2 is testis predominant while PP1γ1 is ubiquitous

To shed light on the relative expression levels of PP1γ2 in testis and other somatic tissues, we performed Western blot analysis of different tissues (testes, liver, lung, uterus, spleen, brain) besides testis extracts (Fig. 10A). We loaded 50 μg of protein/ lane. Caudal epididymal sperm extracts (20 μg) were loaded as positive control. PP1γ2 was detected in testes and caudal sperm extracts. Brain extracts showed much reduced expression of PP1γ2 which is in accordance with previous report (Strack *et al.*, 1999). This indicates that PP1γ2 is indeed a predominant protein in testis. In comparison, when a companion blot was probed with PP1γ1 antibody, its expression was detected in all somatic tissues besides testis extracts (Fig. 10B).

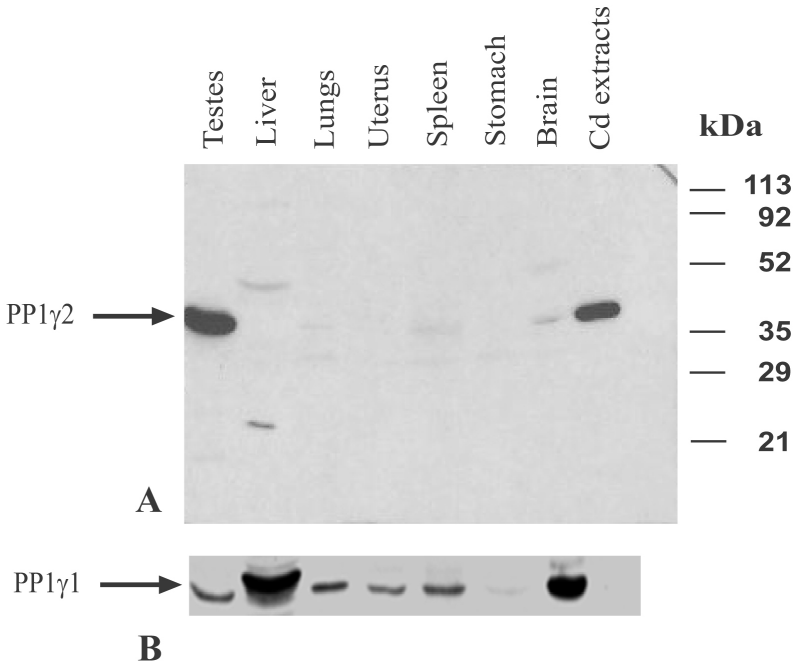

Figure 10. (A and B) Detection of immunoreactive PP1γ2 and PP1γ1 proteins in mouse tissues. Protein extracts from testes, liver, lung uterus, spleen, stomach, brain and epididymal caudal sperm extracts were separated by SDS/PAGE, transferred on to nitrocellulose membrane, and probed with PP1γ2 antibody **(A)** and PP1γ1 antibody **(B)**. 50 µg of protein was loaded per lane with the exception of caudal sperm extracts where 20 µg was used. PP1γ2 expression was predominant in testes extracts *vs*. expression of PP1γ1 which is ubiquitous. **A:** Brain extracts showed faint expression of PP1γ2 in comparison with testes.

2. Comparison of expression pattern of PP1 isoforms in testes and sperm

Western blot analyses were then performed to determine whether all three isoforms of PP1 (PP1γ1 (37 kDa), PP1γ2 (39 kDa) and PP1α (36 kDa)) are present in mouse testis and sperm. All three PP1 isoforms were observed in testis extracts (Fig. 11); however, PP1γ2 (39kDa) was the only PP1 isoform detected in sperm extracts (Fig. 11). These observations with mouse testes and sperm extracts are similar to those found with bovine, human, and rhesus monkey (Vijayaraghavan *et al.*, 1996).

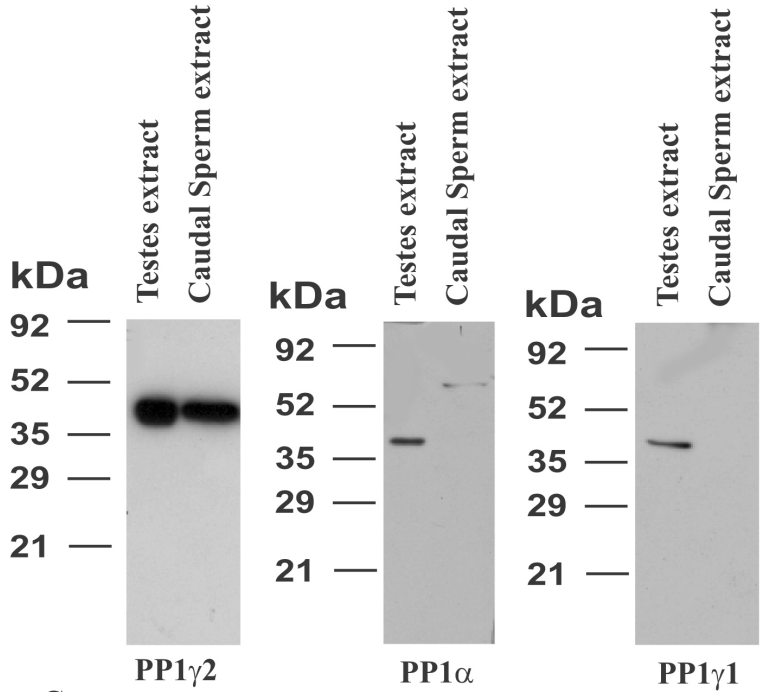

Figure 11. PP1γ2 is the only PP1 isoform in caudal sperm. Western blot analysis of mouse testis and sperm extracts was performed as described in *Materials and Methods*. Blots were probed with PP1γ2 (39 kDa), PP1α (36 kDa) and PP1γ1 (37 kDa) antibodies. Testis extracts (20 μg) contain all three isoforms of PP1; however caudal sperm extracts (20 μg) contain only PP1γ2.

3. Postnatal expression of PP1γ1, PP1γ2 and PP1α during developmental stages of mouse testes

Next, we determined expression of PP1 isoforms in testis from mice of increasing postnatal ages (Fig. 12). Western blot analysis was performed on extracts prepared from testis of 8 day, 14 day, 18 day, and 1-2 month old mice in each experiment. These ages were selected as they mark the approximate times at which distinct germ cell populations are produced in testis (Bellve, 1979). Postnatally from day 1 to day 8, spermatogonia are the predominant cells in seminiferous tubules in the testis. From day 8 to day 10 there is differentiation and onset of meiosis resulting in the formation of spermatocytes. Secondary spermatocytes are formed by day 14 and spermatid formation occurs at approximately day 18. Expression of the different PP1 isoforms in testis was strikingly age-dependent. Immunoreactive PP1γ2 increased with age, while expression of PP1γ1 and PP1α appeared to decrease with age (Fig. 12).

The observation that PP1γ2 protein expression increases postnatally during testes development in mice is supported by Reverse-Transcriptase PCR analysis (Fig. 13). The expression of RNA for PP1γ2 increased postnatally in contrast with PP1γ1 and PP1α. However, message for PP1α and PP1β appears to remain similar throughout development. During mouse testicular development, spermatocytes and haploid germ cells appears around day 14-21. Therefore this result indicates that the expression of PP1γ2 correlates with the onset of meiosis and formation of post meiotic germ cells.

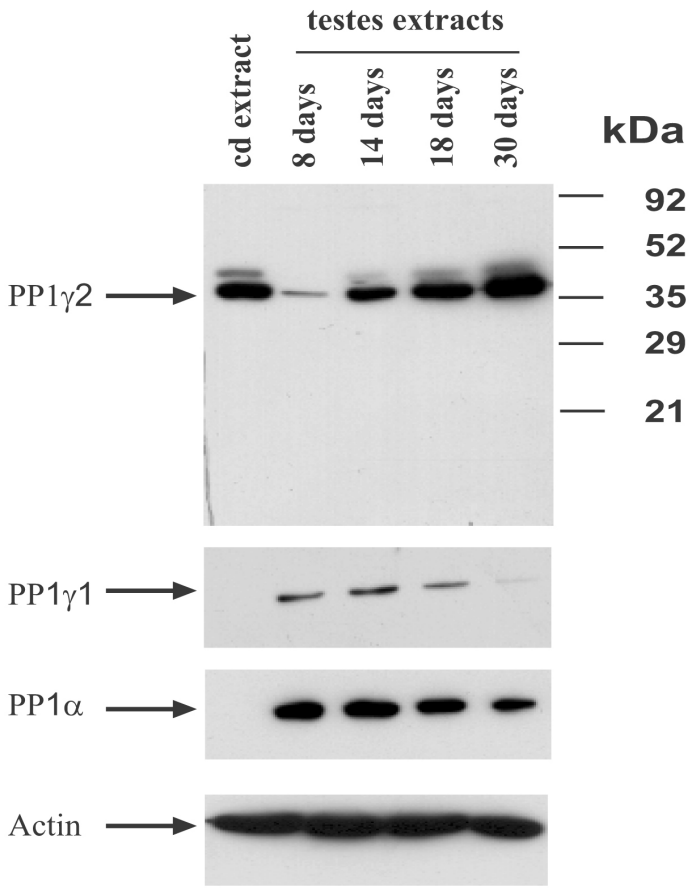

Figure 12. Expression of PP1 isoforms in postnatal testis extracts. In each experiment, equal concentrations of testis extracts (20 μg) from each age group were analyzed. Extracts were subjected to Western blot analysis with the indicated antibodies and visualized using Enhanced chemiluminescence (ECL). Postnatal expression of PP1γ2 increases with age. Expression of PP1γ1 and PP1α decreases with age. Equal amounts of caudal sperm extracts (cd) were used as control. Companion blot with testis extracts were developed to actin antibody to demonstrate repeatable equal loading.

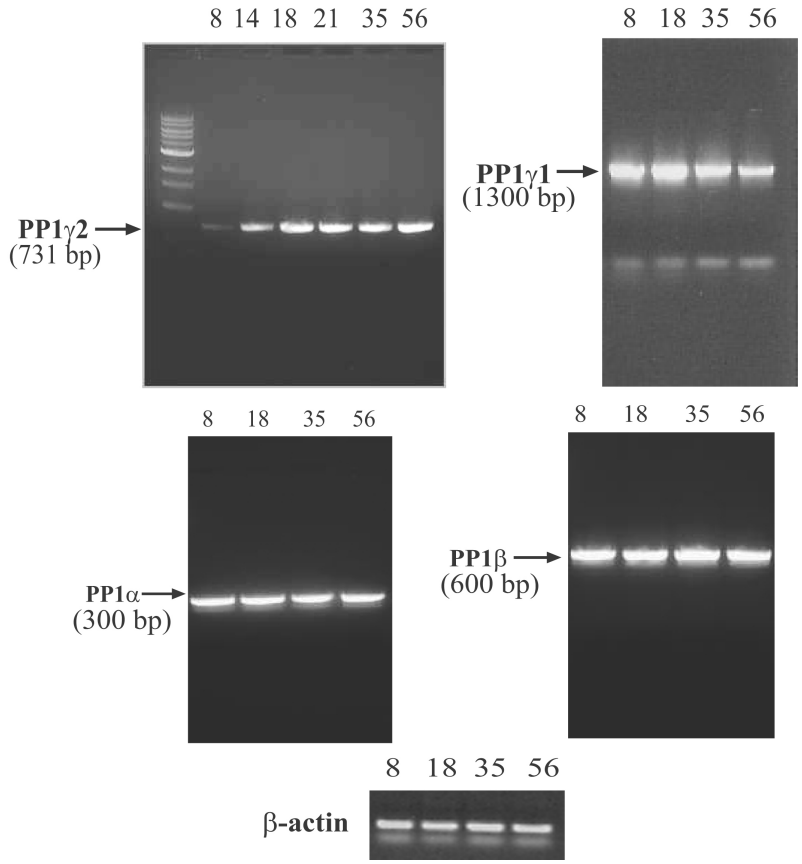

Figure 13. Expression of PP1γ1, PP1γ2, PP1α and PP1β mRNA in developing mouse testes. Testes were removed from mouse ranging in age from day 8 to 56. RNA was prepared and converted to cDNA and analyzed by PCR as described in the *Materials and Methods*. Postnatal expression of PP1γ2 mRNA increases with age. Expression of PP1γ1 decreases with age during postnatal development of testes. Expression of PP1α and PP1β remains same throughout development. Equal amount of RNA was loaded in all the experiments as indicated by β-actin.

4. PP1γ2, PP1γ1 and PP1α protein expression during male germ cell differentiation

We next determined the sub-cellular localization of PP1 isoforms in testes. To determine the expression pattern of PP1γ2 during male germ cell differentiation, paraffin embedded adult mouse testes were cross-sectioned to a thickness of 8 μm (which were mounted on a glass slide). Formaldehyde-fixed testis sections after rehydration were incubated with PP1γ1, PP1γ2 and PP1α antibodies followed by incubation with Cy3-labeled secondary antibodies. Fluorescence patterns showed a distinct expression blueprint of the different PP1 isoforms in testis sections. PP1γ2 immunofluorescence was predominant in the cytoplasm of secondary spermatocytes and round spermatids, elongated spermatids and spermatozoa at all stages of adult mouse testis (Fig. 14B and D). Fluorescence was weak in spermatogonia, pachytene spermatocytes, and peritubular cells. Interstitial cells showed no immunoreactive PP1γ2. No signal was detected when preimmune sera were used (Fig. 14E).

Immunofluorescence for PP1γ1 was distinctly different from that observed for PP1γ2. Intense fluorescence was observed in interstitial cells (Fig. 15B and D) and weak fluorescence was observed at all stages of spermatogenesis in adult mouse testis in both the cytoplasm and nuclei of all cells. No signal was detected when secondary antibody alone was used (Fig. 15E).

With PP1α antibody, intense fluorescence was observed in the cytoplasm of interstitial cells, peritubular cells, spermatogonia and pachytene spermatocytes in adult mice testis (Fig. 16B and D). No signal was detected when secondary antibody was used alone (Fig. 16E).

In a parallel approach, we looked at the differential distribution of PP1γ2 in HEK293 cells. The intracellular distribution pattern of the PP1γ2 protein was examined by transfection of HEK293 cells with and without a myc-tagged PP1γ2 construct. Preparation of the myc-PP1γ2 construct and transfection was performed as described in the *Materials and Methods*. Figure 17B shows an image of a HEK293 cell expressing the myc-tagged PP1γ2 protein. The red colour represents fluorescence from expressed PP1γ2 protein. PP1γ2 protein was predominantly expressed in the cytoplasm of HEK293 transfectants however an occasional distribution of PP1γ2 in the nucleus was observed which possibly could be related to different stages of cell cycle. (Fig. 17B). To confirm that the localization is not altered due to the myc tag, another construct with no myc tag was used to confirm the previous results of predominant cytoplasmic localization of PP1γ2 (data not shown). Our data suggests a unique distribution of PP1γ2 gene even at cellular level in comparison with the other isoforms of PP1 which show nuclear or nucleolar localization (Andreassen *et al.*, 1998).

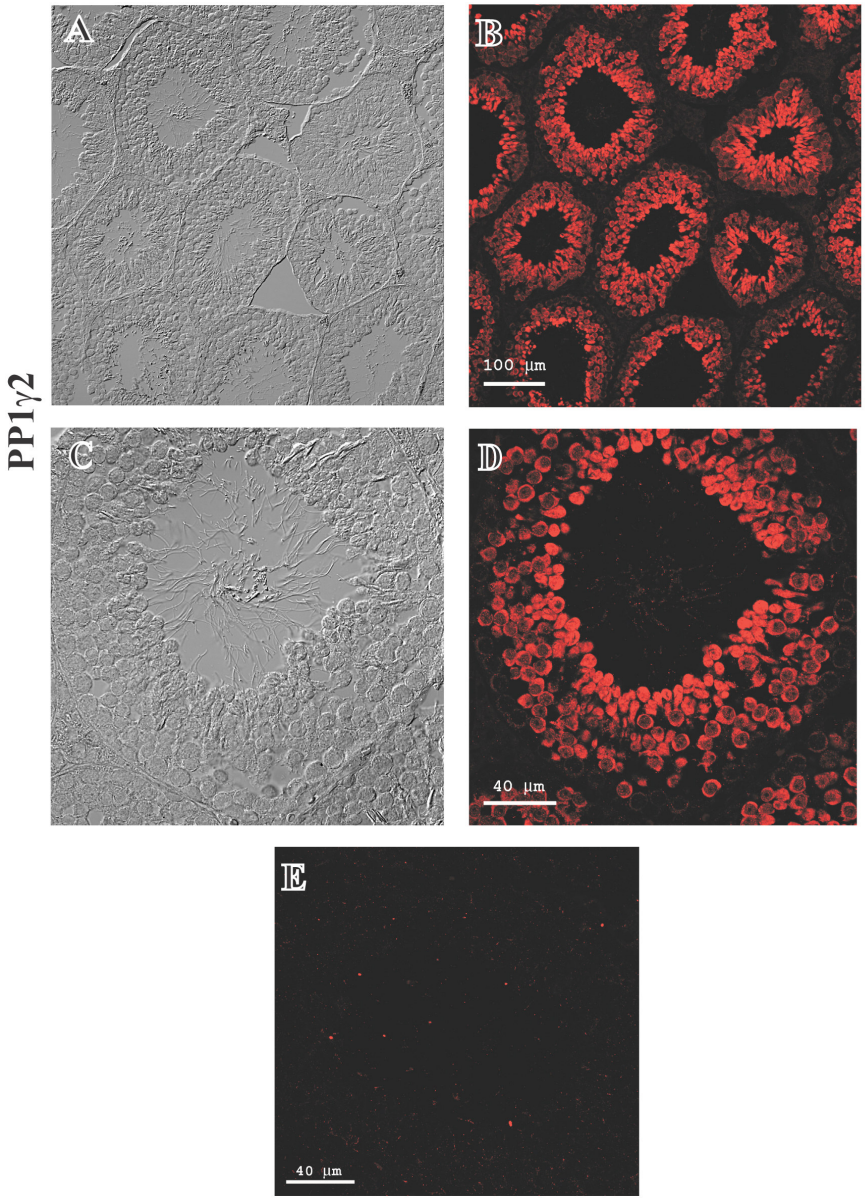

Figure 14. Distinct cellular and sub-cellular distribution of PP1γ2 in wild-type mouse testes sections. B, D: PP1γ2 is prominently expressed in the cytoplasm of germ cells ranging from secondary spermatocytes and round spermatids to elongating spermatids and spermatozoa. **A and C:** The corresponding brightfield images using DIC optics of confocal microscope. Bar=100 µm (**A and B**), 40 µm (**C, D and E**). **E:** No signal was seen when preimmune sera was used.

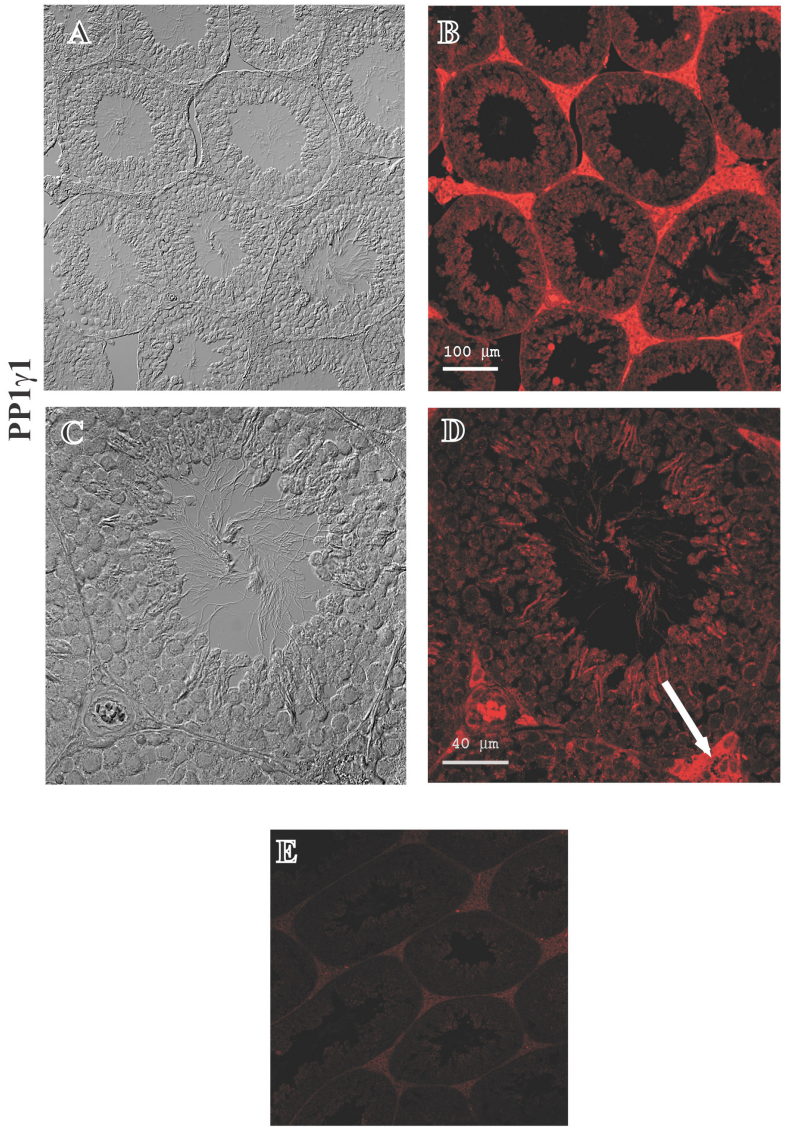

Figure 15. Distinct cellular and sub-cellular distribution of PP1γ1 in wild-type mouse testes sections. B, D: PP1γ1 expression is observed predominantly in the interstitial cells of Leydig. Weak expression of PP1γ1 was observed in all germ cells ranging from spermatogonia to spermatids. Arrow indicates expression of PP1γ1 in interstitial cells **(D)**. **A, C:** The corresponding brightfield images using DIC optics of confocal microscope. Bar=100 µm (**A, B and E**), 40 µm (**C and D**). **E:** No signal was seen when secondary antibody was used alone.

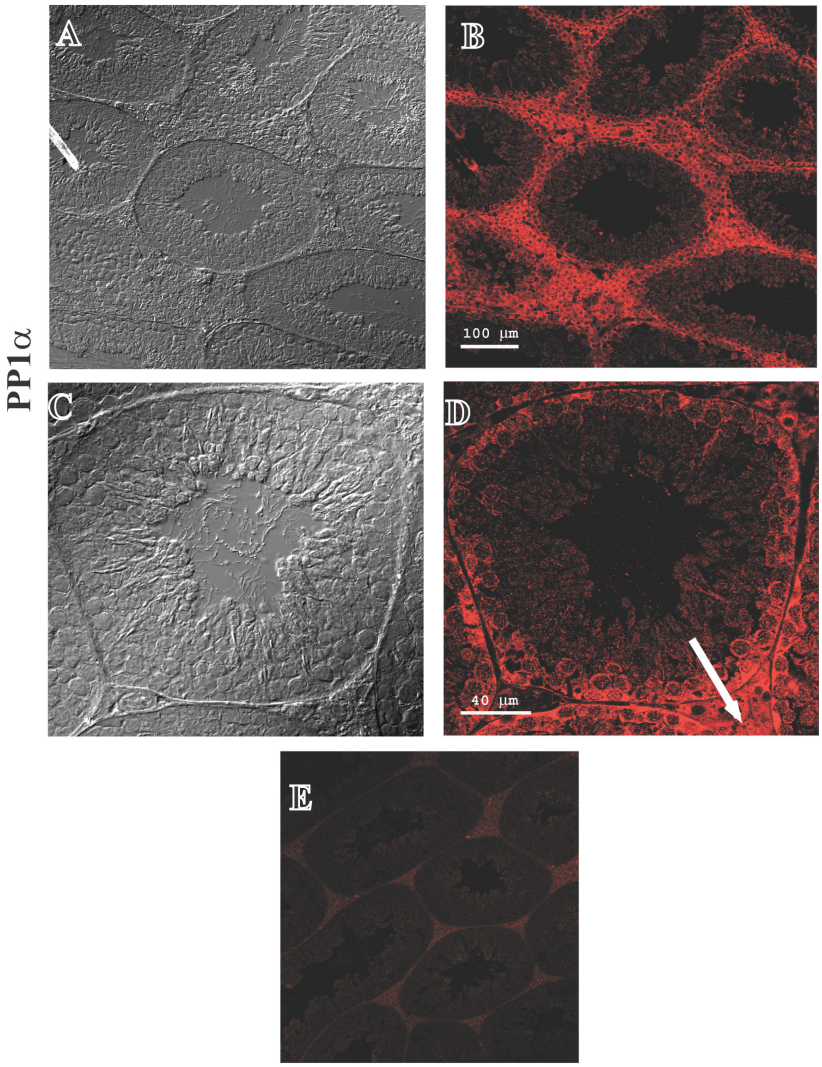

Figure 16. Distinct cellular and sub-cellular distribution of PP1α in wild-type mouse testes sections. B, D: PP1α showed strong expression in interstitial cells, spermatogonia, peritubular cells and pachytene spermatocytes. Arrow indicates expression of PP1α in interstitial cells **(D)**. **A and C:** The corresponding brightfield images using DIC optics of confocal microscope. Bar=100 µm (**A, B and E**), 40 µm (**C and D**). **E:** No signal was seen when secondary antibody was used alone.

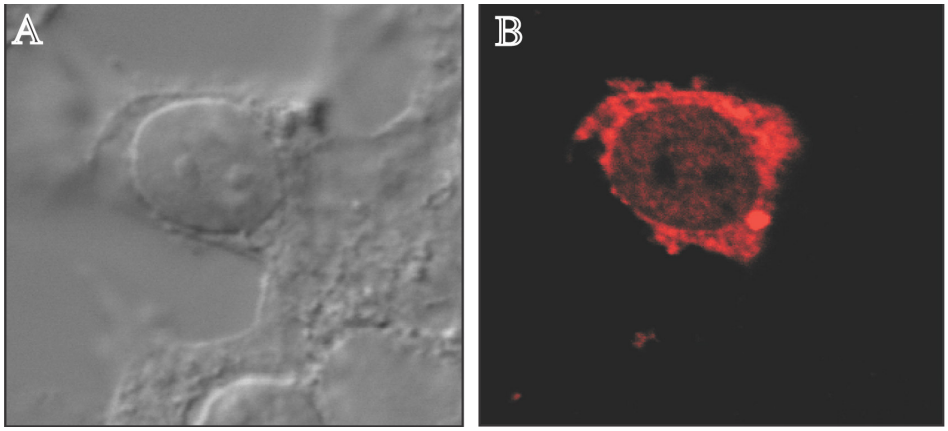

Figure17. Differential distribution of PP1γ2 in HEK293 cells B: PP1γ2 is predominantly expressed in the cytoplasm. **A** is a brightfield image of **B**. Primary antibody was detected with Cy3-conjugated secondary antibodies.

5. Expression of PP1γ1 decreases when cells transfected with PP1γ2

We next attempted to determine if expression of PP1γ2 has any effect on expression of PP1γ1 in HEK293 cells. Interestingly, we observed a decrease in expression of PP1γ1 in PP1γ2 expressing HEK293 cells. HEK293 cells were transfected with two μg of DNA (constructs containing PP1γ2 with and without myc tag). Figure 18A shows expression of PP1γ2 in HEK293 cells with PP1γ2 antibody. Expression of PP1γ1 appears to decrease in PP1γ2-transfected cell with either of the constructs (Fig.18B).

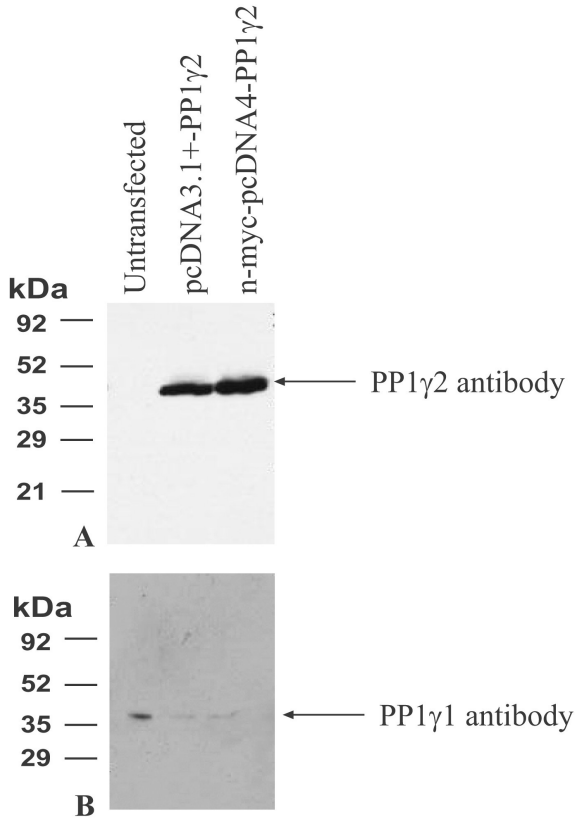

Figure 18. HEK293 cells expressing full length PP1γ2 protein. A: Cell lysates prepared in Passive Lysis Buffer (Promega) after 48 h of transfection (30µg total protein) from HEK293 probed on a Western blot with anti-PP1γ2 antibodies. **B:** Similar lysates probed with anti-PP1γ1 antibodies shows decrease in expression of PP1γ1 with either of the PP1γ2 constructs.

6. Expression of PP1γ1 and PP1γ2 in individual germ cells by Laser Capture Microscopy suggest specific role of PP1γ2 in post-meiotic germ cells

The technology of laser capture microdissection (LCM) was a significant advance in the methods of cell separation (Simone *et al.*, 1998; Bonner *et al.*, 1997; Emmert-Buck *et al.*, 1997). This technique originated at the NIH, and commercially developed through a Collaborative Research and Development Agreement partnership with Arcturus Engineering Inc.(CA). It's a reliable, rapid method for isolating specific and a pure population of cells or even a single cell from a complex tissue. LCM provides an opportunity to isolate germ cells in specific stages of differention, allowing identification of specific expressed genes. In this study, we used laser capture microdissection (LCM) and Reverse transcriptase-polymerase chain reaction to examine the pattern of expression of mRNA for PP1γ1 and PP1γ2 in germ cells in testis of adult mice such as spermatogonia (g), pachytene spermatocytes (p), spermatids (r) and elongating spermatids (e). The enriched individual germ cells captured from sections of mouse testis using LCM were determined by PCR using primers for c-kit, hsp-70-2, and sds22 (c-kit and hsp-70-2 primers were a generous gift from Haruna Shibata, Chiba University, Japan). RNA was extracted from each population of cells using RNA pico pure kit of Arcturus (Mount view, CA). cDNA was made using the RT-transcription kit of Qiagen (Quantitect Reverse Transcription kit, Qiagen, CA) with random hexamers. The integrity of the RNA was checked by PCR with β-actin primers. Enrichment of spermatogonia was checked using c-kit primers which is predominantly expressed in spermatogonia and

spermatocytes (Fig. 19A) (Wolfes, Kogawa *et al.* 1989; Sorrentino, Giorgi *et al.* 1991; McCarrey, Berg *et al.* 1992). HSP-70-2 primers were used to assess the purity of pachytene spermatcytes as it is known to be to be predominantly expressed in pachytene spermatocytes and spermatids (Fig. 19A) (Eddy, 2002). sds22 primers were used to check the purity of the round spermatids as sds22 mRNA is reported to be predominantly expressed in spermatids (http://mrg.genetics.washington.edu/search.html) (Fig. 19A) .

PP1γ1 and PP1γ2 primers (as indicated in the *Materials and Methods*) were used to perform PCR to detect their respective transcripts. PP1γ1 mRNA was only detected in spermatogonia and pachytene spermatocytes (Fig. 19B). In contrast, PP1γ2 mRNA was present in spermatogonia, pachytene spermatocytes, round spermatids and elongating spermatids indicating that it is the only isoform of PP1γ present in post meiotic germ cells (Fig. 19B).

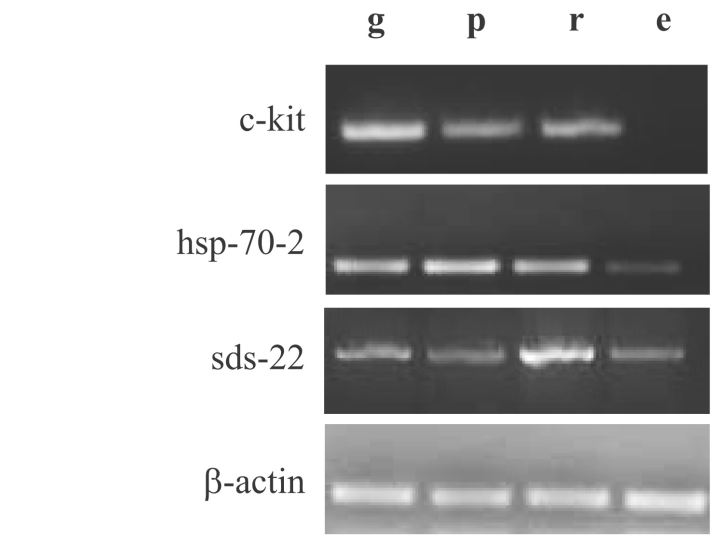

A.

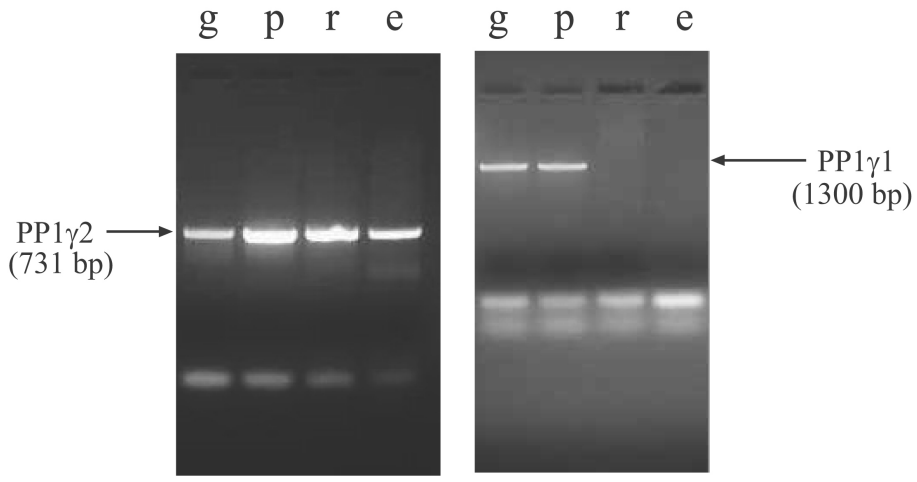

B.

Figure 19. Expression of PP1γ1 and PP1γ2 in individual germ cells using LCM

A: Enriched individual cell type populations of spermatogonia (g), pachytene spermatocytes (p), round spermatids (r) and elongating spermatids (e) by RT-PCR amplification with primers specific for the ckit, hsp-70-2 and sds22 as outlined under *Materials and Methods*. **B:** Total RNA prepared from LCM isolated cells was used as

templates. The 741-bp PP1γ2 and 1300-bp PP1γ1 mRNA products are shown separated on ethidium bromide-2% agarose gel. The mRNA-encoding PP1γ2 but not PP1γ1 are expressed in all types of germ cells such as g, p, r and e. However, PP1γ1 is exclusively expressed in spermatogonia and spermatocytes and absent in the next two layers of germ cells. β-actin was used as control.

In summary, findings of studies in this aim are:

1. PP1γ2 is predominantly present in testis.

2. Testes contain all three isoforms of PP1 (PP1γ1, PP1γ2 and PP1α), however, PP1γ2 is the only isoform in sperm.

3. Postnatal mRNA and protein expression of PP1γ2 increases while PP1γ1 and PP1α mRNA and protein remains constant or decrease during testes development.

4. PP1γ2 shows a distinct cellular and sub-cellular distribution in germ cells and somatic cells in comparison with PP1γ1 and PP1α. Protein expression of PP1γ2 is detected exclusively in post-meiotic germ cells in contrast with the other two isoforms of PP1 which are present in leydig cells, spermatogonia, primary spermatocytes and peritubular cells.

5. mRNA expression of PP1γ2 is detected in developing spermatogonia (even though expression of protein is first observed in secondary spermatocytes) in contrast to mRNA for PP1γ1 which is present only in spermatogonia and pachytene spermatocytes.

C. Morphological and histo-chemical analysis of *Ppp1cc*-null mice testes and epididymis

1. Generation of *Ppp1cc*-null mice

Heterozygotes for the *Ppp1cc*-null gene were obtained from Dr. Susan Varmuza (Varmuza *et al.*, 1999). F1 animals, which transmitted the PP1γ deleted allele (i.e heterozygous at PP1γ allele) were intercrossed to obtain F2 animals. The breeding strategy was undertaken such that the lines were established in a CD1 genetic background. It is noteworthy to mention that heterozygous animals appeared normal and were fertile. The average litter size derived from their matings was comparable to that of wild type matings. Homozygous males were infertile but females were fertile (Varmuza *et al.*, 1999).

2. Genotyping and Analysis of PP1 (PP1γ1, PP1γ1, PP1α) expression in *Ppp1cc*-null mice

Genotyping was performed by PCR analysis from DNA isolated from an ear clip. One common primer from intron IV (5' CTCAGGCCAATGCTGTCTGC 3'), a neo-specific primer for the mutant allele (5' GGTGGATGTGGAATGTGTGCG 3'), and a wild-type allele-specific primer from the deleted portion of intron VI (5' ACTCATAGCCATCTTCAACCA 3') were used. These primers amplify 500-bp fragment from the wild-type allele and 250-bp fragment from the mutant allele (Fig. 20A).

Total testicular protein was extracted from wild type, heterozygous and homozygous mice using RIPA lysis buffer with proteolytic inhibitors (RIPA+). Western blot analysis was performed with PP1γ1, PP1γ2 and PP1α antibodies. The companion blot was probed with actin antibody to demonstrate equal loading. Expression of PP1γ1 and PP1γ2 were observed in wild type and heterozygous mice but not in homozygous mice (Fig. 20 B).

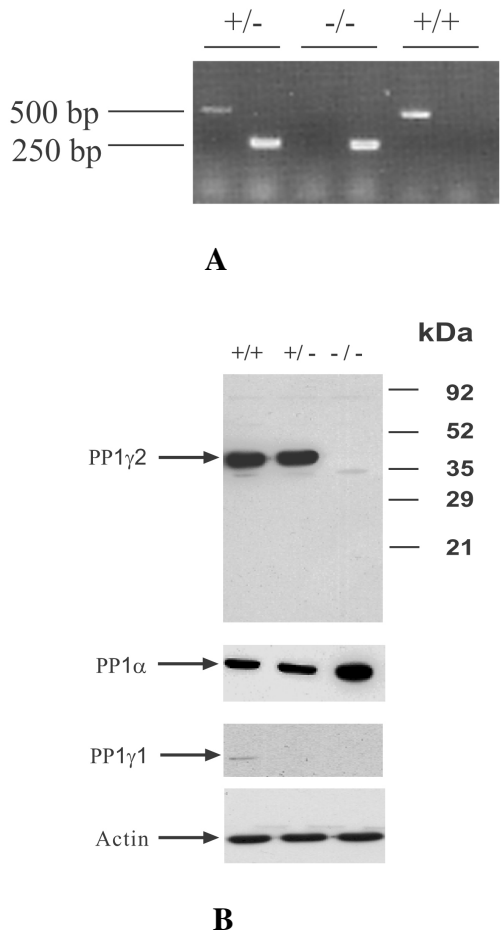

Figure 20. A: Results of typical PCR-based genotyping of +/+ (wild type), +/- (heterozygote), and -/- (*Ppp1cc*-null) mice using primers as described above. The 500-bp wild-type band and the 250-bp mutant band are indicated in the figure. **B: Expression of PP1 isoforms in testis extracts of wild-type (+/+), heterozygotes (+/-) and *Ppp1cc*-null mice (-/-).** In each experiment, equal amounts of testis extracts (20 μg) were assessed. Extracts were analyzed using western blot with respective isoform specific antibodies and visualized using chemiluminescence. Expression of PP1γ1 and PP1γ2 were absent as expected in the mice lacking the *Ppp1cc* gene. Expression of PP1α appears to increase in the testis extracts of mice lacking the *Ppp1cc* gene. Companion

blot with testis extracts were subjected to actin antibody to demonstrate repeatable equal loading.

3. Morphological analysis of *Ppp1cc*-null testes and epididymis in comparison with wild type and heterozygote mice

a. Testes weight in wild, heterozygote and null mice

Testes of PP1γ knock-out appeared smaller in size than wild type mice. Therefore testes from three mice (3-4 months) were weighed for each wild, heterozygote and null mice and the mean weight was taken. The result shows a reduced testis weight in null mice in comparison with the wild and heterozygous mice (Fig. 21).

b. Reduced number of spermatozoa in testis of *Ppp1cc*-null mice and absence of epididymal sperm in null mice

We next found that differentiation of post-meiotic spermatids into spermatozoa is inhibited in *Ppp1cc*-null mice. In agreement with a previous report (Varmuza *et al.*, 1999, 2003), the number of elongating spermatids in each seminiferous tubule was reduced in *Ppp1cc*-null (Fig. 22B) compared to wild-type testes (Fig. 22A). The defect in spermatogenesis was highly variable between seminiferous tubule cross sections, ranging from a mild loss of round and elongating/condensing spermatids to a nearly complete loss of haploid germ cells. Thus, numbers of round spermatids were comparable in some seminiferous tubules in both wild-type and null testes. Surprisingly, epididymides of

Ppp1cc-null males were virtually devoid of spermatozoa (Fig. 22D) even though *Ppp1cc*-null testes contained spermatozoa, albeit at lower numbers (Fig. 22C) than wild-type (Fig. 22A). Epididymides from *Ppp1cc*-null males contained immature germ cells, including round spermatids and occasionally pachytene spermatocytes (Fig. 22D).

Further examination of seminiferous tubules from *Ppp1cc*-null testes showed multiple defects which include a) vacuoles (Fig. 23C), b) sloughing of germ cells into the lumen, c) mislocated germ cells (Fig. 23B and C), d) sertoli cell defects (Fig. 23B) and possible spermiation defects (Fig. 23C) as previously described (Varmuza *et al.*, 1999). Diploidy or multinucleated spermatids were also observed (Fig. 23C).

We used standard light and transmission electron microscopy (TEM) of fixed sections to confirm and expand upon the observations made by confocal microscopy of *Ppp1cc*-null testes. Light micrographs of testis sections from *Ppp1cc*-null mice showed severely reduced number of elongated spermatids near the lumen. Tubule lumens in these testes also tended to be small or absent, possibly as a result of the failure of spermatid maturation and spermiation (Fig. 24A and B).

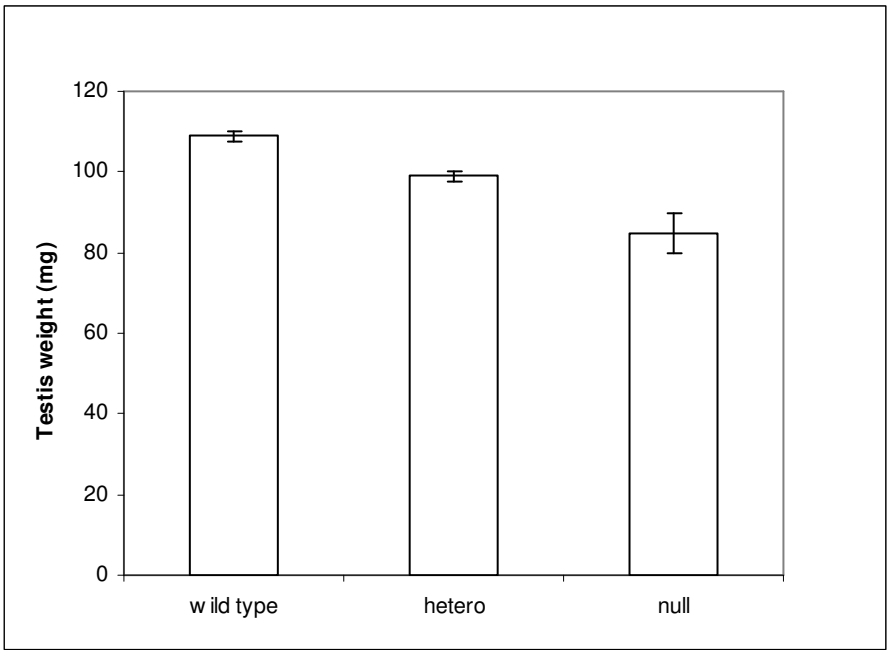

Figure 21. Testis weights of +/+, +/-, and -/- males. Thin bars represent SEM. Three animals (n=3) of similar ages (3-4 months) per group was analyzed.

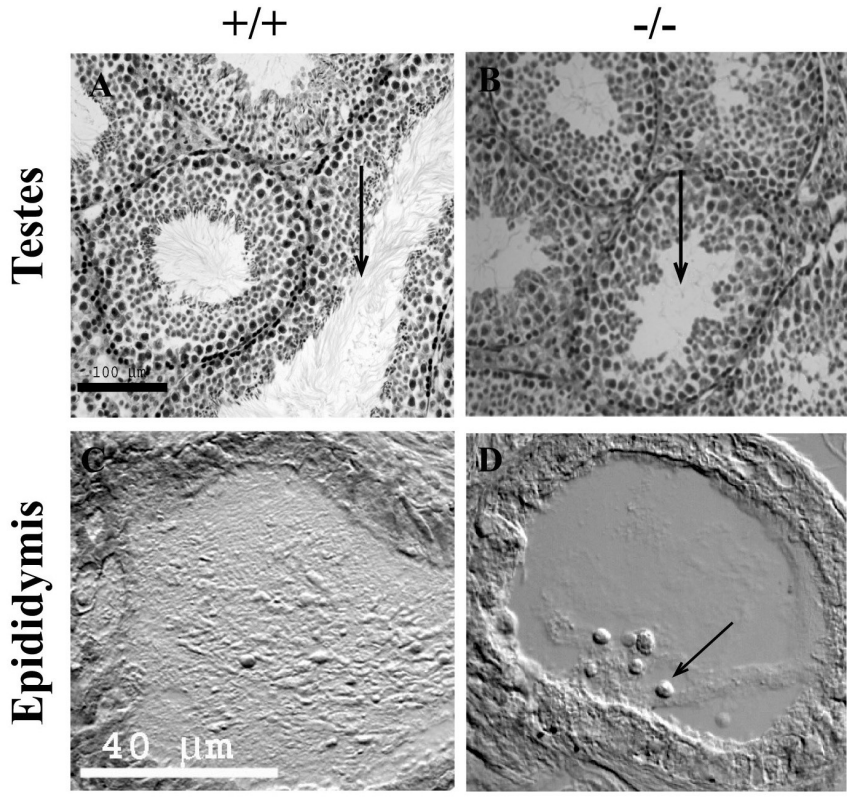

Figure 22. Testis and epididymis morphology of wild-type and *Ppp1cc*-null mice. Histological analysis of **A:** wild-type and **B:** *Ppp1cc*-null testes. Note the reduced numbers of testicular sperm in null mice in comparison with the wild-type testis sections (arrows). Histology of wild-type **C:** and *Ppp1cc*-null **D:** epididymides. *Ppp1cc*-null epididymis contains no sperm; only immature germ cells (arrow) are present. These images are representation of observation on multiple sections and different testes preparations. Bar=100 µm (**A, B**), 40 µm (**C, D**)

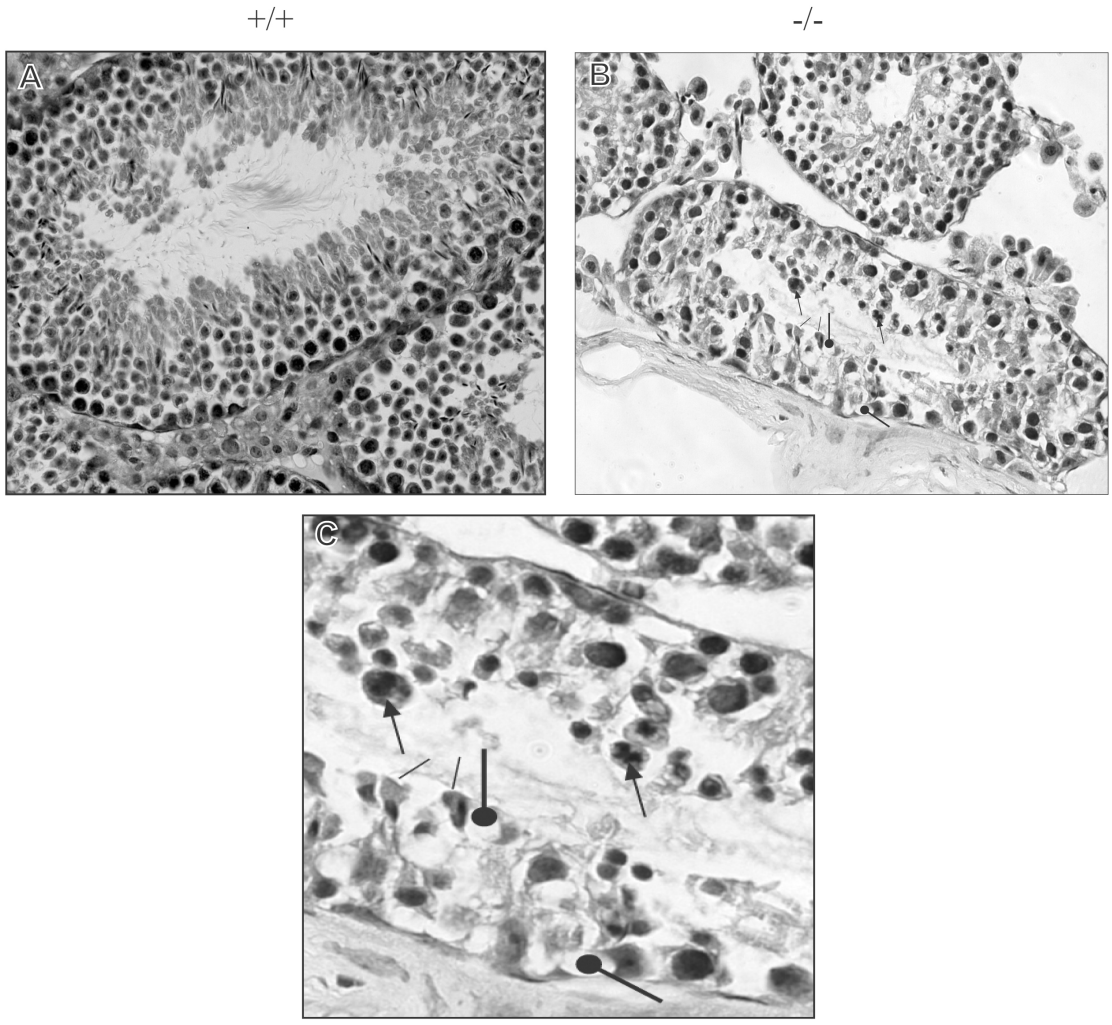

Figure 23. Morphological defects in *Ppp1cc*-null testes. Brightfield images of testes from wild type **(A)** and null mice (**B**). **(B)** *Ppp1cc*-null mice have abnormalities in spermatogenesis. In wild type mice **(A),** the seminiferous tubules are of normal diameter and have a normal complement of the various germ cell types, including elongated spermatids. In the *Ppp1cc*-null mice **(B)**, the seminiferous tubules are smaller in diameter and more variable in appearance. **C:** Seminiferous tubules in *Ppp1cc* knockout vary in their germ cell content, often lacking groups of germ cells. Diploidy is often observed in spermatids as indicated by arrows. Vacuoles are often observed in the tubule as shown by bullet headed arrows.

Occasional spermiation defects are observed in elongating spermatids which are indicated by black lines.

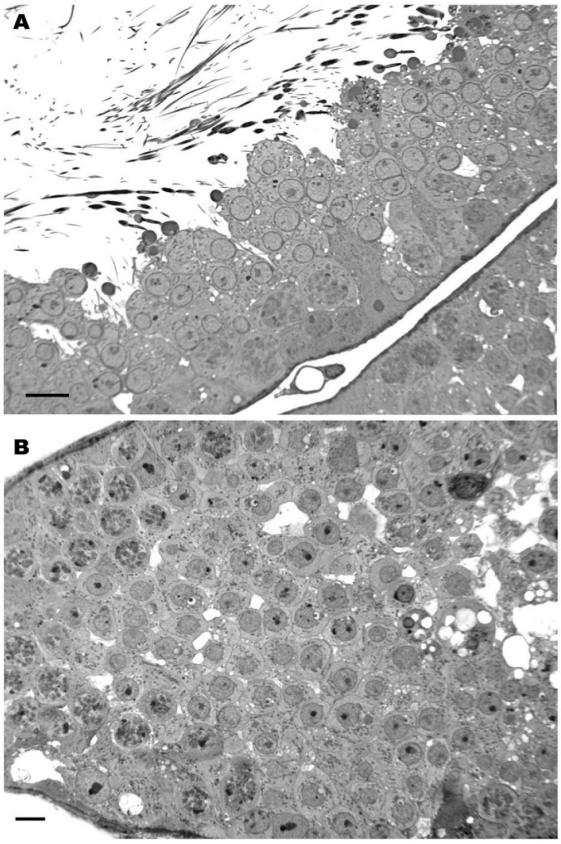

Figure 24. Light micrographs of testes fixed for electron microscopy from *Ppp1cc* A: +/- and B: -/- littermates. In testes of -/- males, the architecture of the seminiferous epithelium is generally normal except for an almost total absence of mature elongated spermatids near the lumen. Instead, vacuolated structures indicating degeneration of maturing germ cells are commonly seen in this location (right side in **B**). Tubule lumens in these testes also tend to be small or absent, likely to be a result of the failure of spermiogenesis maturation and spermiation. Bars = 10 μm.

d. Motility assay, ICC and IHC for wild type and heterozygote animals

We next investigated sperm from heterozygote animals for motility and presence of immunoreactive PP1γ2. Numbers of caudal and caput epididymal sperm are comparable to those in wild type (data not shown). Caudal sperm from heterozygotes show comparable motility pattern (eg. forward progressive motility, beat frequency) to wild type sperm as indicated by the CASA analysis (data not shown). Immunocytochemistry with PP1γ2 demonstrated staining in the whole tail and part of the posterior head in the heterozygote caudal and caput sperm (Fig. 25A and B) which is comparable to the wild type (Fig. 25C). Testes sections from heterozygote animals showed comparable staining with PP1γ1 and PP1γ2 antibodies respectively (Fig. 26A and B).

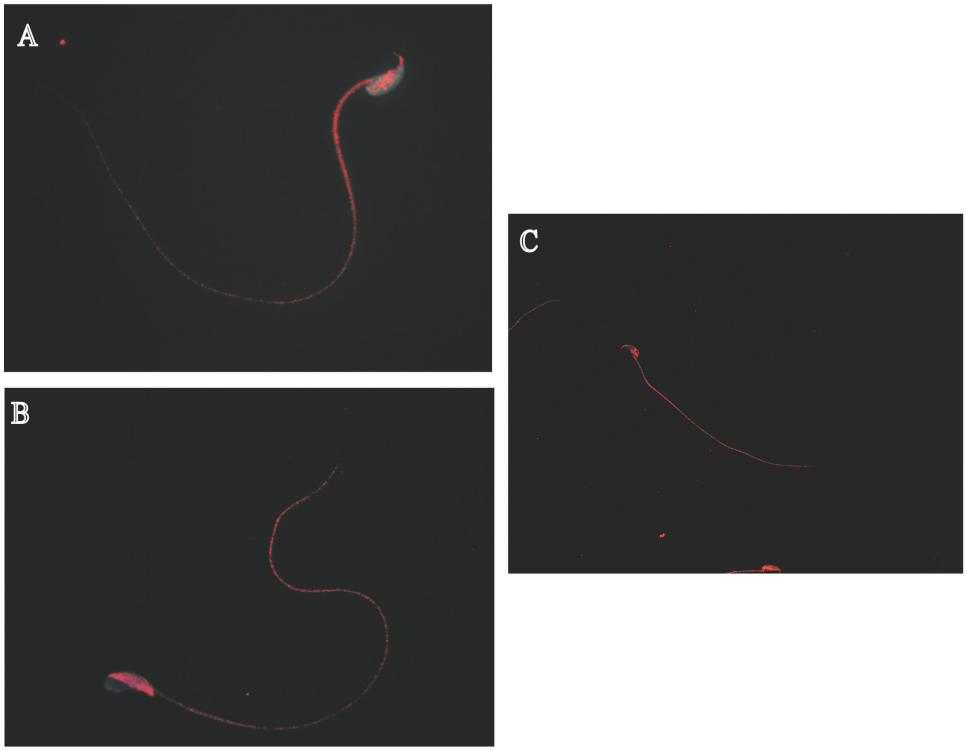

Figure 25. Sub-cellular localization of PP1γ2 in caudal and caput sperm from *Ppp1cc* heterozygote mouse. A: Heterozygote caudal sperm. **B:** Heterozygote caput sperm. Blue represents DAPI staining to indicate the nucleus and the red is for PP1γ2 staining due to cy3-conjugated secondary antibody. **C:** Wild type caudal sperm with PP1γ2 antibody.

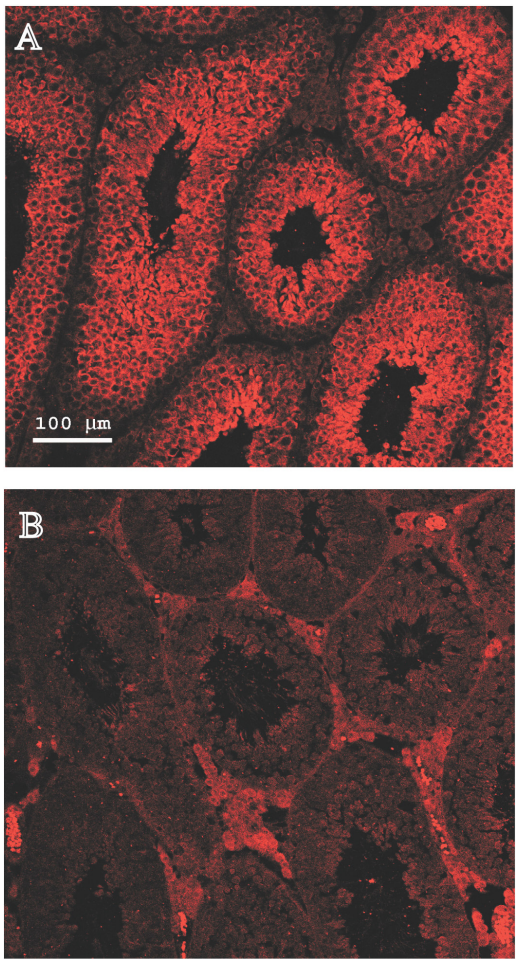

Figure 26. Cellular localization of PP1γ2 and PP1γ1 in *Ppp1cc* heterozygote testes sections. A: Expression of PP1γ2 was observed predominantly in secondary spermatocytes, round and elongating spermatids. Weak expression was observed in spermatogonia and pachytene spermatocytes. Interstitial cells showed no staining with PP1γ2 antibody. **B:** Expression of PP1γ1 was observed predominantly in interstitial cells. Weak expression was observed in spermatogonia, pachytene spermatocytes, secondary spermatocytes, round and elongating spermatids. Bar: 100 µm (A-B).

e. Quantitative analysis of testicular sperm in wild and null testes sections indicates a 70-80 % reduction in testicular sperm in null mice

We used formaldehyde-fixed, paraffin-embedded and Hematoxylin-stained testis sections to determine the quantitative values for testicular sperm in both wild and null mice. Using the steps mentioned in the *Materials and Methods*, seminiferous tubules from *Ppp1cc*-null testes showed ~80% reduction in sperm number compared to the wild type as showed in the figure below (Fig. 27). However in some of the tubules, comparable amounts of testicular sperm were observed in both wild and null testes sections.

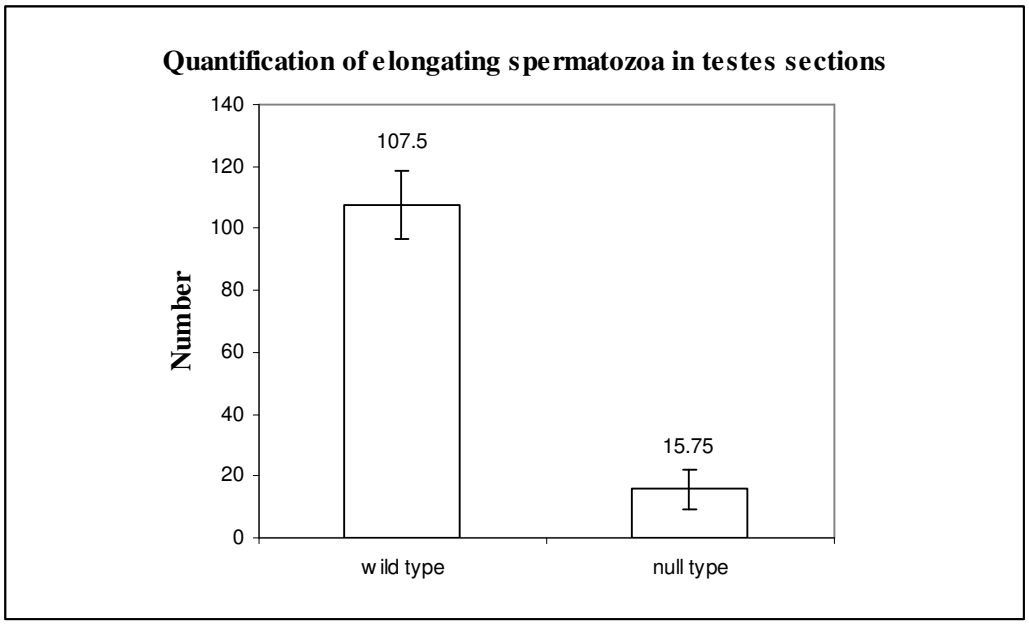

Figure 27. Testicular sperm numbers in testes sections of wild type and *Ppp1cc*-null mice. Thin bars represent SEM. Thirty tubules (n=30) from testes of mice of similar ages (3-4 months) per group was analyzed. Numbers on the top of the bars indicate the mean value of elongating spermatids and mature testicular sperm per testis section analyzed.

4. Isolation and characterization of testicular spermatozoa of null testes in comparison with wild type.

a. Abnormal mitochondrial organization, outer dense fiber complex and fibrous sheath formation in testicular spermatozoa of *Ppp1cc*-null mice

Since the epididymides of *Ppp1cc*-null mice were devoid of spermatozoa, testicular spermatozoa were used. There were sufficient mutant spermatozoa from testis of *Ppp1cc*-null mice to make this observation. Testicular sperm were collected using methods described by Kotaja *et al.* (Kotaja *et al.*, 2004). Spermatozoa were examined using confocal microscopy with differential interference contrast (DIC) optics. Instead of the wild-type hook-shaped sperm head structure (Fig. 28A), mutant sperm showed a range of head shapes from round to oblong (Fig. 28B, C, F). Surprisingly, we also observed disorganized mitochondria in the mid-pieces of mutant sperm. In wild-type sperm, the mitochondrial sheath is helical and tightly wrapped around the mid-piece (Fig. 28D). In sperm from *Ppp1cc*-null mice, the mitochondrial sheath was much more loosely arranged (Fig. 28F), while in some instances, the mitochondria were absent (Fig. 28I). This observation was confirmed by staining *Ppp1cc* -null testicular sperm with MitoTracker Green which show either loosely arranged mitochondria in the mid-piece region (Fig. 28G) or complete absence of mitochondrial sheath (Fig. 28H).

We also used scanning (SEM) and transmission electron microscopy (TEM) of fixed testicular sperm and testes sections respectively to confirm and expand upon the observations made by confocal microscopy of *Ppp1cc*-null testes. SEM images confirmed our previous

confocal data indicating defect in mid-piece and head shape of mutant sperm (Fig. 29A and B). Four distinct abnormalities were observed by TEM of testicular sperm, (Fig. 30A-E). First, some abnormal head shapes were observed, possibly due to degenerating condensing spermatids (data not shown). More prominently, mitochondrial sheaths in the mid-pieces of elongating spermatids and testicular spermatozoa appeared disorganized and did not form the tightly packed helical structures observed in wild-type sperm. Third and the most prominently observed defect, outer dense fibers were disorganized with a highly increased number of florets throughout the flagella of mutant sperm. Fourth, a subtle abnormality in the development of the fibrous sheath was observed, specifically in the formation of distinct, triangular-shaped longitudinal columns and inward projections that replace the ODFs associated with axonemal microtubule doublets 3 and 8 in wild-type sperm.

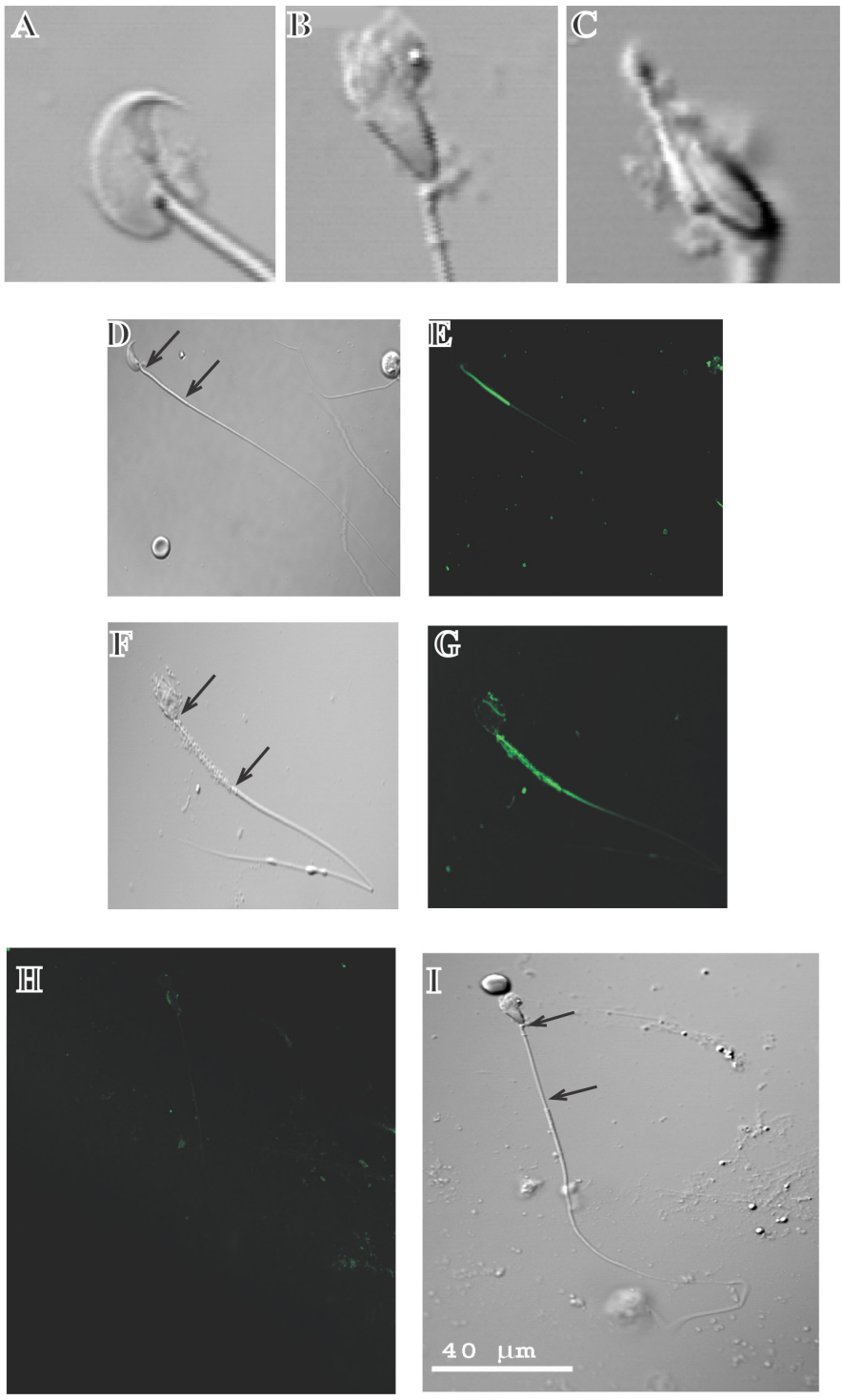

Figure 28. Aberrant morphology of testicular spermatozoa of *Ppp1cc*-null mouse shown with DIC optics and fluorescence mitochondrial staining. A: Normal hook shape head of

testicular spermatozoa of wild type mouse. **B, C, F:** *Ppp1cc*-null sperm display a variety of severely malformed heads and mid-pieces. All null spermatozoa show some degree of head malformation, ranging from the mildest observed phenotype (**B, C**) to the most severe phenotypes (**F**). Tail abnormalities include **F:** mid-pieces that have disorganized mitochondrial sheaths or **I:** mid-pieces that are thinner than the principal pieces due to the absence of mitochondrial sheaths. **D:** Tightly wrapped mitochondrial sheath of wild-type sperm. Arrows delineate the mitochondrial sheath. **E and G:** Mitochondrial sheath stained with MitoTracker Green in wild type and *Ppp1cc*-null mouse respectively. **H:** Shows absence of staining with MitoTracker Green in null testicular sperm due to absence of mitochondrial sheath. Bar=40 μm (**A-I**)

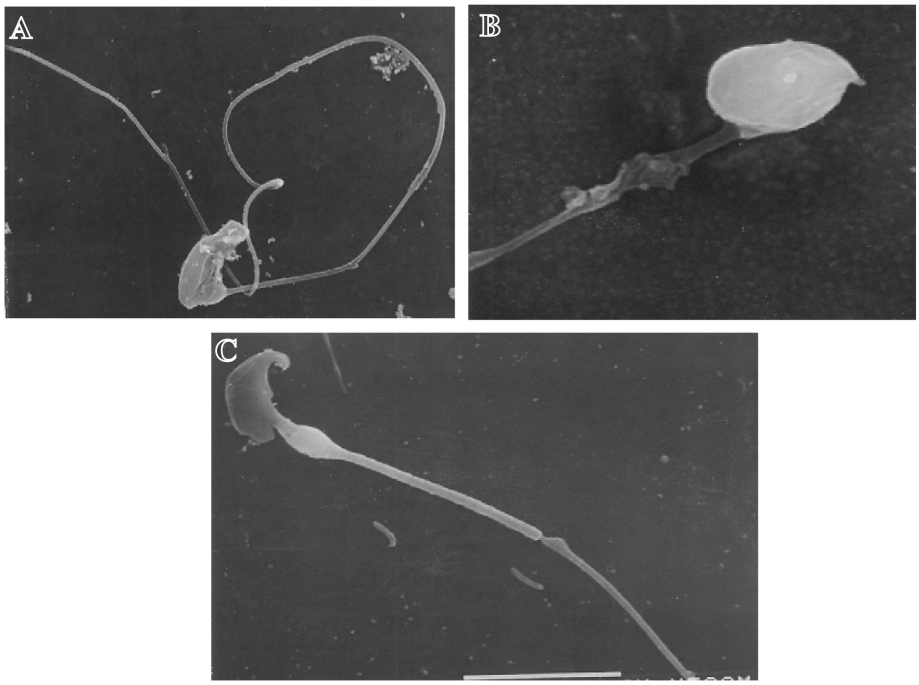

Figure 29. Scanning electron microscope (SEM) images of wild type and *Ppp1cc*-null testicular sperm. A: Shows absence of mitochondrial sheath in mutant sperm. **B:** Shows frayed mid-piece and misshaped testicular sperm head. Both A and B show abnormal head shape of mutant sperm. **C:** Wild type sperm with normal head shape and mid-piece.

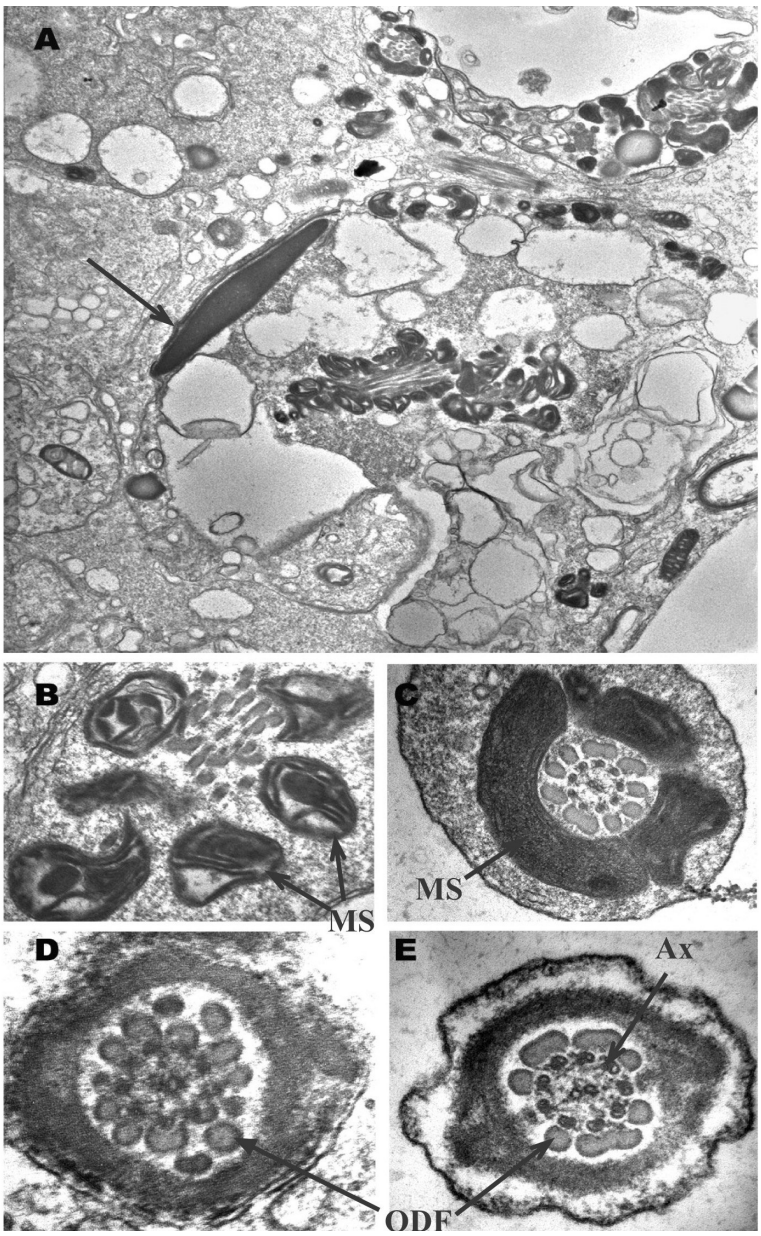

Figure 30. Transmission electron micrographs of testes from *Ppp1cc* -/- mutant and +/- control littermates. **A:** An example of degeneration of a condensing spermatid from a -/- male (arrow), indicated by fragmentation of tail structures and the presence of numerous vacuoles in the spermatid cytoplasm (X 30,000). **B:** Transverse section through

a mid-piece of -/- developing sperm tail. Note: Poor development of the mitochondrial sheath (MS) though individual mitochondria appear normal and many extra outer dense fibers (ODF) surrounding an apparently normal axoneme (X 60,000). **C:** Mid-piece from +/- littermate with normal ultrastructure (X 60,000). **D:** Transverse section through the principal piece of -/- developing sperm tail showing many extra ODFs (total of 13) and apparent developmental abnormality of the fibrous sheath, particularly the morphology of its longitudinal columns. (X 80,000). **E:** Principal piece from +/- littermate (X 80,000). ODF, outer dense fibers; MS, mitochondrial sheath; Ax, axoneme.

5. Altered expression of PP1α in testis of Ppp1cc-null mouse

Ppp1cc-null male mice are infertile due to impaired spermiogenesis (Varmuza *et al.*, 1999). Here, we examined if PP1α expression and localization is altered in testis of null mice. Levels of PP1α appeared to be higher in testis of adult *Ppp1cc*-null compared to wild-type mice testis (Fig. 20B). The localization pattern for PP1α was also altered in *Ppp1cc*-null (Fig. 31B) compared to wild-type testis sections (Fig. 16B). Unlike in wild-type testis sections (Fig. 16B), PP1α was present near the Sertoli cell borders and in early round spermatids in the testes of *Ppp1cc*-null mice (Fig. 31B). Fluorescence signal for PP1α was observed in spermatogonia, peritubular cells, pachytene spermatocytes, and interstitial cells which was similar in wild-type and *Ppp1cc*-null testes. No signal was observed when secondary antibody was used alone (data not shown).

In another parallel approach, E9 antibody (Santa Cruz Biotechnology) which detects all the isoforms of PP1 was used. Localization of PP1α was confirmed in *Ppp1cc*-null testes sections (Fig. 31D). Western blot also indicates an increase in expression of the PP1α in the null testes extracts in comparison to the wild type using E9 antibody (Fig. 31E).

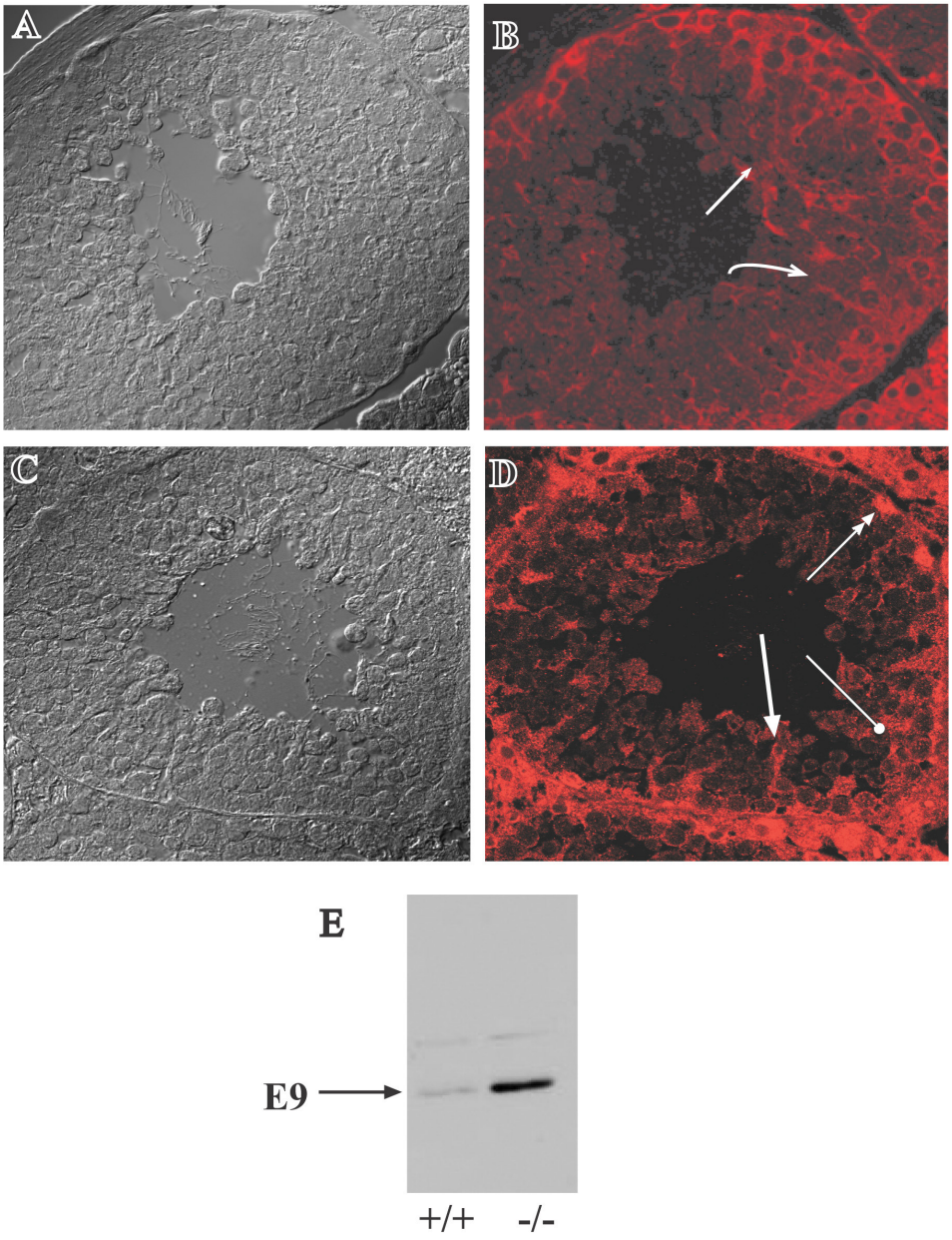

Figure 31. B: Distinct cellular localization of PP1α in mouse testis section lacking *Ppp1cc* gene. Expression of PP1α was observed in the Sertoli cell adjacent to the germ cells and early round spermatids besides being in interstitial cells, spermatogonia, peritubular cells and pachytene spermatocytes by PP1α antibody. **A, C:** The corresponding brightfield image

using DIC optics of confocal microscope. **D:** Expression of PP1α was observed in the Sertoli cell adjacent to the germ cells and early round spermatids besides being in interstitial cells, spermatogonia, peritubular cells and pachytene spermatocytes by E9 antibody. In **D**, arrow indicates sertoli cell-germ cell boundary. Double arrow head indicates spermatogonia nucleus staining. Bullet head arrow indicates staining in spermatids. These images are representation of observation on multiple sections and different testes preparations. Bar=40 μm. **E:** shows increased expression of PP1α using E9 antibody in wild type (+/+) and *Ppp1cc*-null testes (-/-).

6. Analysis of pre-meiotic and post meiotic protein expression in *Ppp1cc*-null testes in comparison with the wild type

a. Expression of pre-meiotic and post-meiotic protein expression in wild and null testes extracts.

The defects in the flagella of mutant sperm prompted us to examine whether expression of a number of proteins expressed in haploid cells was normal in null testis. Testis extracts from adult wild-type and *Ppp1cc*-null mice were subjected to Western blot analyses with a panel of antibodies. Testis-specific cytochrome c oxidase (Narisawa *et al.*, 2002), AKAP3/AKAP110 (Carr *et al.*, 2001) and SPNR (Schumacher *et al.*, 1995), known to be expressed in secondary spermatocytes and spermatids, showed comparable levels of protein expression in wild-type and mutant testis extracts (Fig. 32B). However, post-meiotically expressed genes such as fibrous sheath protein AKAP4/AKAP82 (Miki *et al.*, 2002), outer dense fiber protein odf2 (Schalles *et al.*, 1998), regulator of PP1 sds22 (Huang *et al.*, 2004), sperm surface protein SP17 (Carr *et al.*, 2001), and another fibrous sheath protein FSII (Carr *et al.,* 2001) were absent or markedly reduced in *Ppp1cc*-null compared to wild-type testis (Fig. 32A).

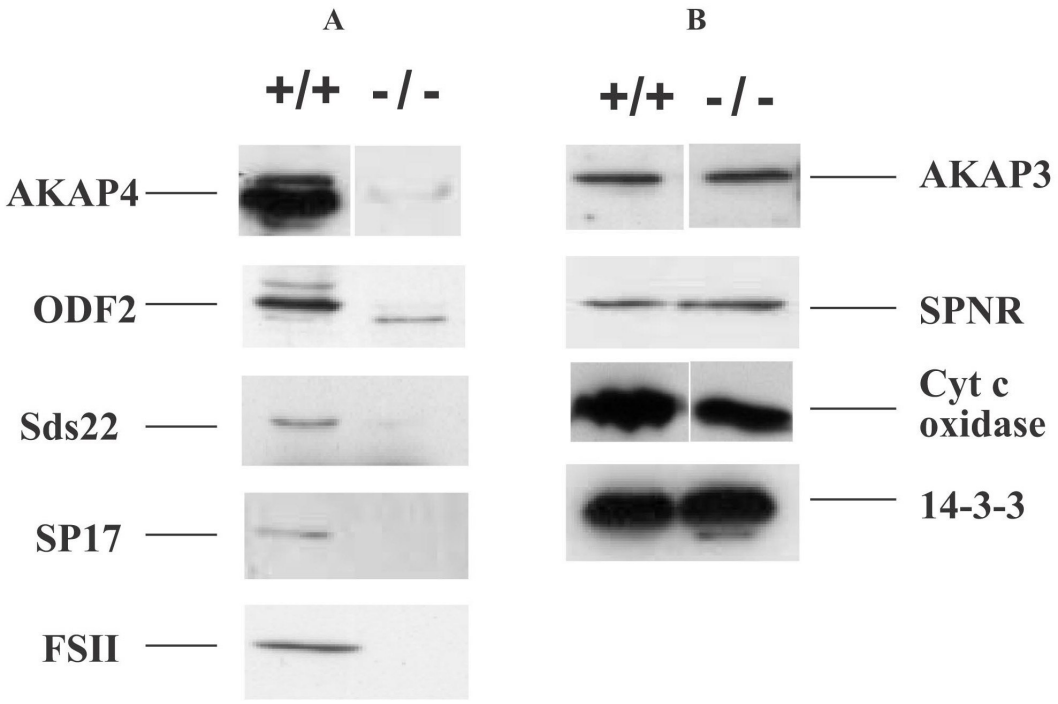

Figure 32 (A and B). Analyses of protein expression in *Ppp1cc*-null mice. Western blot analyses of testes-specific proteins are indicated. 14-3-3 was included to demonstrate repeatable equal loading. 20 µg of total testis protein from adult wild-type (+/+) and *Ppp1cc*-null (-/-) mice were used for each analysis.

b. Immunohistochemical analyses of postmeiotic protein expression show severely reduced or absence in protein expression in null vs. wild type.

Reduced levels of proteins in adult testis could reflect an insufficient number of cells where these proteins are produced. We used immunohistochemistry to determine if reduced cell number might be the cause of reduced protein levels. Immunofluorescence for AKAP4, ODF2 and SDS22 was observed in round spermatids and elongating spermatids in adult wild-type testis (Fig. 33A, E I). Immunofluorescence for FSII was observed in the condensing spermatids of the wild-type testis sections (Fig. 33M). In contrast, in adult *Ppp1cc*-null testis, although round and elongating spermatids were clearly present, albeit in lower number, there was a complete lack of fluorescence for these proteins (Fig. 33C, G, K, O) suggesting the possibility that PP1γ2 may have an effect on transcription or post-transcription/translation or post-translational stability of these proteins. SP-10 antibody (Reddi *et al.*, 1995) was used to show almost comparable staining in some of the round and elongating spermatids in wild and null testes sections (Fig. 34A and B).

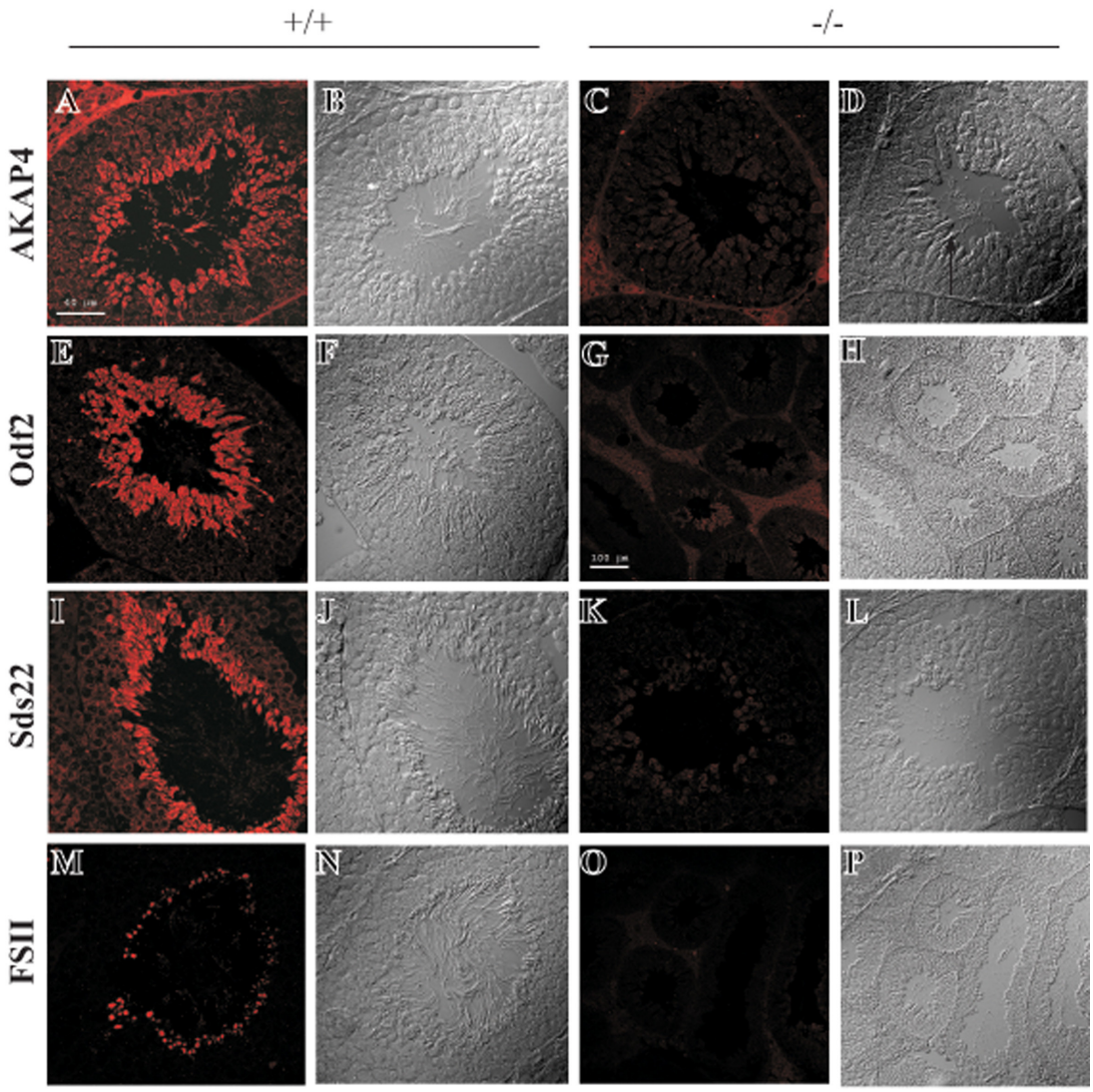

Figure. 33. Immunohistochemical staining for selected post-meiotic protein markers in wild-type (+/+) and null (-/-) mouse testes sections. A, E, I: show wild-type testes sections with AKAP4, odf2, and sds22 antibodies, respectively. AKAP4, odf2, and sds22 are prominently expressed in round spermatids and elongating spermatids of wild-type testes sections. Their expression is absent in other germ cells including spermatogonia and spermatocytes. **M:** FSII antibody against wild-type testis sections showing expression of FSII only in elongating spermatids of wild-type mice. **C, G, K, O:** show *Ppp1cc*-null testes

sections probed with AKAP4, odf2, sds22 and FSII antibodies, respectively. Reduced or absent immunoreactivity was detected in the *Ppp1cc*-null mouse testes sections with the antibodies mentioned above in round spermatids and elongating spermatids. Arrow indicates round and elongating spermatids in null testes sections. **B, F, J, N** show the corresponding brightfield image using DIC optics of confocal microscope of **A, E, I, M** respectively. **D, H, L, P** show the corresponding brightfield image using DIC optics of the confocal microscope of **C, G, K, O** respectively. These images are representative of observations of multiple sections and different testes preparations. Bar=40 μm (**A-F, I-N**), 100 μm (**G, H, O, P**)

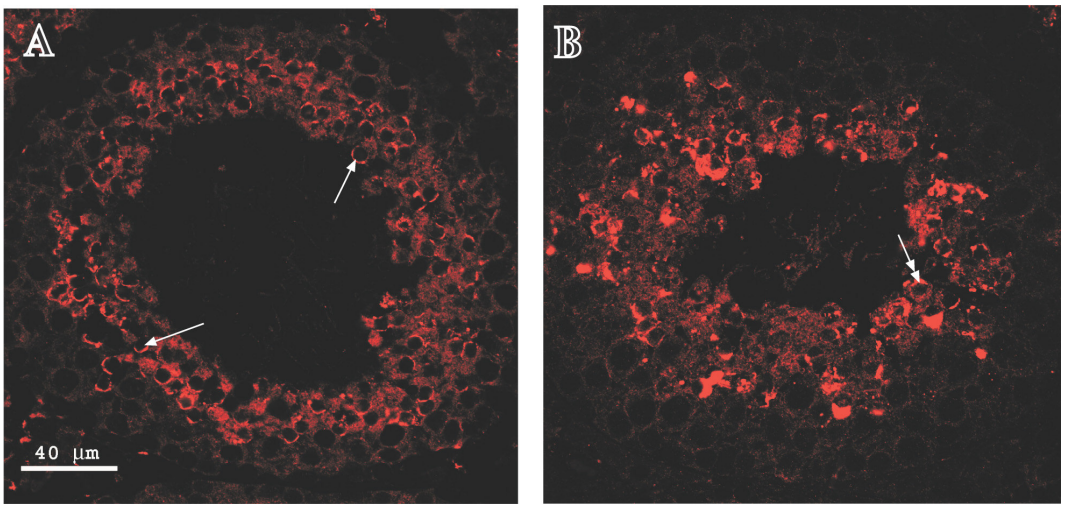

Figure 34. Sub-cellular distribution of SP-10 in wild type and *Ppp1cc*-null testes sections. A: Shows acrosome staining in condensing and elongating spermatids in wild type testes sections. Arrows show acrosome cap staining. **B:** Shows staining in null testes sections. Double headed arrow shows acrosome cap staining. Bar: 40 µm.

c. Comparable amounts of transcripts were detected in both wild and null testes for Akap4, ODF2 and sds22 using LCM

To determine if PP1γ2 is playing a transcriptional or post-transcriptional role in expression of the above mentioned genes, we performed LCM using isolated spermatids from both wild type and null testes sections. Around 2000 round spermatids were collected from both testes sections using Laser Capture Micro-dissection. After confirming RNA integrity and equal loading by β-actin primers, AKAP4, odf2, sds22 primers were used to observe the amount of expression of these genes in both wild type and *Ppp1cc*-null testes. Interestingly, abundant levels of transcripts for two of these proteins, AKAP4, odf2, sds22 were present in round spermatids in *Ppp1cc*-null testes (Fig. 35) suggesting the possibility that PP1γ2 has an effect on post-transcription/translation or post-translational stability of these proteins.

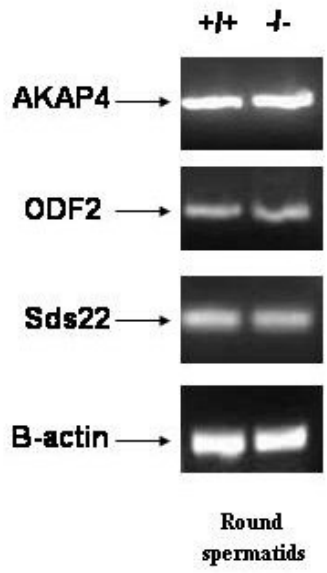

Figure 35. Expression of AKAP4, odf2 and sds22 mRNA in round spermatids from wild type and *Ppp1cc*-null testes sections. Round spermatids were collected using Laser Capture Micro-dissection and mRNA was isolated as described in *Materials and Methods*. Comparable amount of mRNA for the above mentioned proteins were present in wild type and *Ppp1cc* -null testes. β-actin was used to show equal loading.

d. Testicular sperm isolation and immunocytochemistry with AKAP4, odf2, sds22 and FSII

A sharp reduction of the proteins in testis sections suggested that may be PP1γ2 is playing a role in protein expression or mRNA stability of the above mentioned post-meiotic proteins. However, abundant transcripts of these proteins are present in null round spermatids in comparison with wild type indicating that may be reduced cell number could be the reason for lack of observance of immunofluroscence. To answer this question, testicular sperm was isolated and immunocytochemistry was performed with the following antibody after permeabilizing testcular cell suspension with Triton-X-100 in PBS. Interestingly we observed comparable staining in testicular sperm of both wild and *Ppp1cc*-null animals for AKAP4, odf2, FSII and sds22 (Fig. 36).

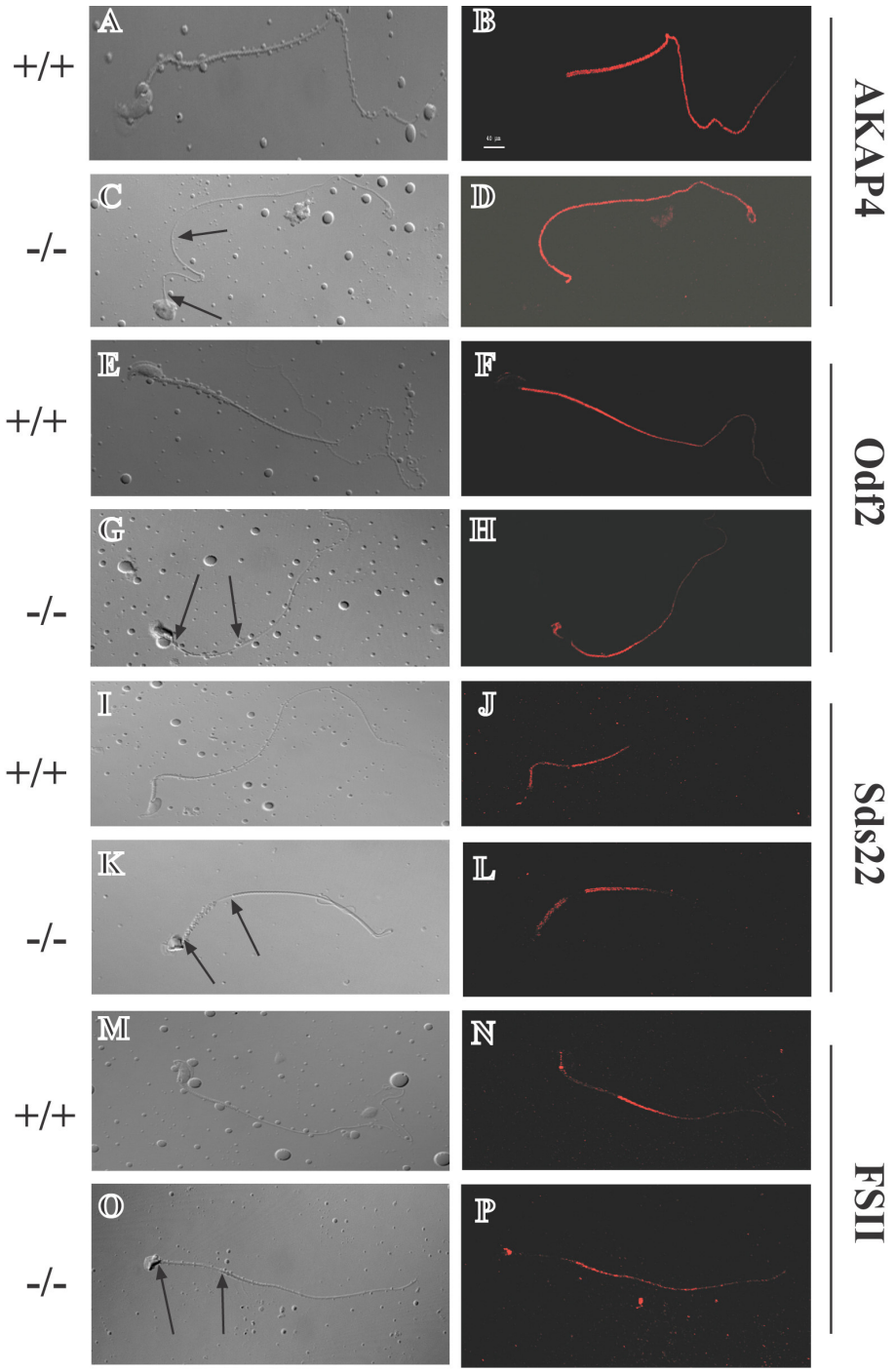

Figure 36. Immunocytochemical staining for AKAP4, odf2, FSII and sds22 in wild-type (+/+) and *Ppp1cc*-null (-/-) mouse testicular sperm. Images on the left are the corresponding brightfield DIC images of the confocal immunofluorescence images on the right. **F, J and N:** Show wild-type testicular sperm labeled with odf2, FSII and sds22

antibodies, respectively. Odf2, FSII and sds22 are prominently expressed in the mid-piece and principle piece of the testicular sperm. **B:** AKAP4 antibody shows expression of AKAP4 only in the principle piece of wild-type testicular sperm. **D, H, L and P:** Show *Ppp1cc*-null testicular sperm probed with AKAP4, odf2, sds22 and FSII antibodies, respectively. Comparable staining was observed in the wild type and the null testicular sperm with AKAP4, odf2, sds22 and FSII antibodies. These images are representative of observations on multiple testicular sperm. Arrows indicate the mid-piece region in testicular sperm in C, G, K, O. Bar 40 μm (**A- P**).

In summary, findings of this aim are:

1. *Ppp1cc*-null mice testes show reduced sperm number and epididymis from null mice show complete absence of sperm
2. *Ppp1cc-null* mice show a severe defect in spermiogenesis leading to an almost absence of elongating spermatids in mutant testes.
3. Various other morphological defects were observed in mutant testes in comparison to wild type which include smaller tubule size, presence of multiple vacuoles, presence of diploidy in spermatids, spermiation defects, sertoli cell defects.
4. Testicular sperm from *Ppp1cc*-null mice show abnormal head shape, defects in mitochondrial organization and outer dense fibers and subtle defect in the fibrous sheath suggesting role for PP1γ2 in sperm morphogenesis (as PP1γ1 is absent in sperm)
5. Altered expression of AKAP4, Odf2, FSII and Sds22 observed in *Ppp1cc*-null testis is most likely due to reduced cell type or decreased protein expression.

D. PP1γ2- Mammalian specific isoform

The requirement of the PP1γ2 isoform during spermiogenesis is intriguing considering that other isoforms of PP1 can substitute for PP1γ in all other cells and in the female; an exception is, thus, developing sperm. In this regard it may be noted that analysis of genome data bases and additional studies from our laboratory show that PP1γ2, with its unique C-terminus extension, is apparently present only in mammals. Studies for expression of PP1γ2 in spermatozoa from different species showed that PP1γ2

is present in spermatozoa of bull, mouse and hamster (Fig. 37A). However, PP1γ1 is present in only non-mammalian species (*Xenopus*) (Fig. 37B). PP1γ1 expression is absent in spermatozoa of bull, mouse and hamster (mammals) suggesting that PP1γ2 plays an important role in spermatogenesis and sperm development in mammalian system in a specific way.

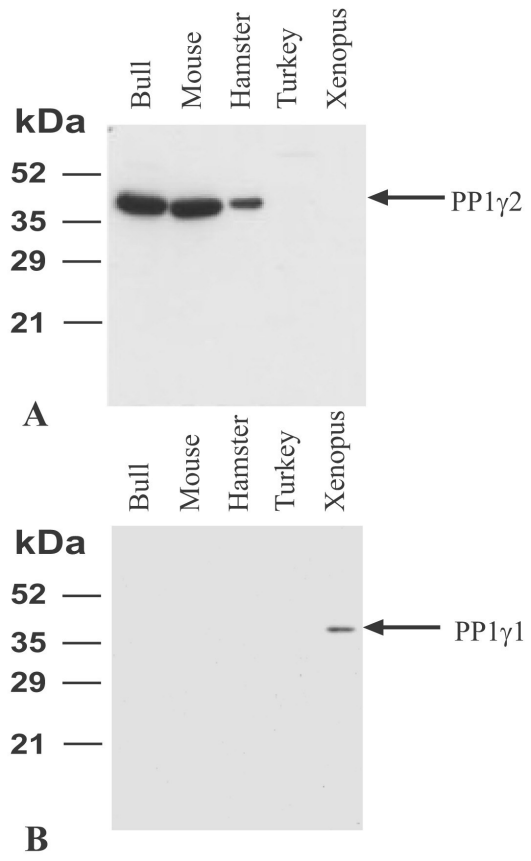

Figure 37. Presence of immunoreactive PP1γ2 and PP1γ1 from different species A and B: Sperm extracts (20 μg in each except for X*enopus* sperm was used) as indicated below were subjected to SDS-PAGE followed by Western blot analysis with PP1γ2 and PP1γ1 antibodies.

E. Presence of PP1γ2 in epididymis using Reverse transcriptase suggesting role of PP1γ2 in epididymal sperm transit after spermiation

To determine if caudal epididymis contain PP1γ2 transcripts, the expression of PP1γ2 mRNA was examined by Reverse Tarnscriptase analysis using RNA isolated from various mouse tissues (caudal epididymis, testes, ovary, liver, spleen and lung). PP1γ2 levels were highest in testes however other tissues including caudal epididymis showed the presence of the PP1γ2 transcript (Fig. 38A). Cyclophilin was used as loading control (Fig. 38B).

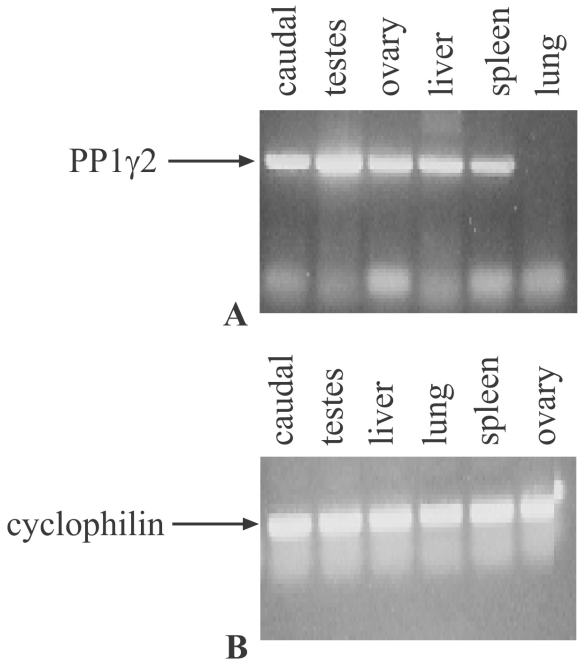

Figure 38. Tissue distribution of mouse PP1γ2 transcript (A): Total RNA was isolated from 90-day-old male mouse and analyzed by the cDNA signal amplification assay for PP1γ2 mRNA content. **(B):** Equal loading was demonstrated by cyclophilin.

Discussion

Sperm are the haploid germ cells that contribute genes to the egg to restore the dipoid chromosome number at fertilization. Haploid round spermatids, produced by meiosis, undergo dramatic morphological changes to become sperm. During this process of spermiogenesis, the nucleus of the haploid germ cell takes shape, the mitochondria are rearranged in a specific manner, the flagellum develops and the acrosome forms (Johnson and Everrit, 2002). There are also changes in chromatin structure with protamines replacing histone proteins. Although the regulatory mechanisms of cellular differentiation and morphogenesis during spermatogenesis are still unclear, protein phosphorylation are likely to be involved as an important molecular mechanism in the regulation of spermatogenesis because several protein kinases and phosphatases are expressed specifically in the testis. Several protein kinases have been reported to be expressed specifically before or during meiosis in the testes. They are known to play a role in spermatogenesis. These kinases include protein-tyrosine kinases (c-Abl, c-Kit, and FerT) (Iwaoki *et al.*, 1993; Manova et al, 1990; Sorrentino *et al.*, 1991; Yoshinaga *et al.*, 1991; Keshet et al, 1991), serine/threonine kinases (Mak, c-Mos, and TESK) (Matsushime *et al.*, 1990; Mutter *et al.*, 1987; Toshima *et al.*, 1995), a dual-specific kinase (Nek-1) (Letwin *et al.*, 1992), the catalytic subunit of casein kinase and CAMkinase 4 (Joy *et al.*, 2004; Xin *et al.*, 1999). Another well studied kinase, is PKA which plays a role in sperm progressive motility but does not appear to be involved in spermatogenesis (Burton, 2002).

Our knowledge of the role of protein phosphatases, in spermatogenesis is quite limited. Earlier reports on phosphatases include a protein tyrosine phosphatase (OST-PTP) (Mauro *et al.*, 1994), a serine/threonine phosphatase calcineurin B subunit isoform b (Muramatsu et. al, 1992), and Twine a dual specific phosphatase (Alphey *et al.*, 1992). A recent report by Varmuza and colleagues demonstrated that the lack of *Ppp1cc* gene leads to male infertility due to impaired spermiogenesis (Varmuza *et al.*, 1999; Hrabchak *et al.*, 2003). Interestingly, epididymis of *Ppp1cc* mutant mice contained no sperm. So far this was the first evidence showing a distinct role of phosphatases (PP1) in spermatogenesis and/or spermiogenesis. In contrast, the role of phosphatases including PP1 in somatic cells, have been studied in greater detail. The various isoforms of PP1 have diverse role in the biological system (Cohen, 2002). It is believed that these enzymes are organized both spatially and temporally and they can change their intracellular localization dynamically during cell cycle progression and during other cellular processes (Inagaki *et al.*, 1994). Dynamic relocalization of the PP1 isoforms occurs through interactions with targeting subunits (Lamond, 2001). The differential distribution of PP1 isoforms in cells within tissues have not been performed in any detail except some work in brain extracts and sections (Strack *et al.*, 1999; da Cruz e Silva *et al.*, 1995). In this study, we showed for the first time the detailed analysis of differential distribution of the PP1 isoforms (PP1γ1, PP1γ2, PP1α) in mouse testes. Though the *Ppp1c*-null mice were produced earlier, a detailed analysis of the testicular sperm was not performed at that time. These *Ppp1cc*-null mice lacked epididymal sperm. Thus, the roles of PP1γ1 and/or PP1γ2 in sperm morphogenesis and spermiogenesis could not be determined. Overall our results

indicate that PP1γ2 in testes may be playing a critical and isoform specific role in sperm morphogenesis.

A. Expression analysis, cellular distribution and sub-cellular localization of the three PP1 isoforms (PP1α, PP1γ1, PP1γ2)

In this study, we found that PP1γ1, PP1γ2 and PP1α are differentially expressed during postnatal testis development. Expression of PP1γ2, as measured by Western blot, increased from day 14 to later stages in testis. The expression of PP1γ2 at day 35 and later is comparable to that of in adult mouse (Fig. 12). This result is in agreement with PP1γ2 transcript levels detected by reverse-transcriptase-PCR (Fig. 13). Low levels of messenger RNA for PP1γ2 were first detected in the testis at day 8 mice. Expression increased at 14 day and 18 day, the period when haploid cells (round spermatids) start to appear in testis (Bellve, 1979). In comparison to PP1γ2, PP1γ1 expression appeared to decrease from day 8 and later. This obsevation by Western blots is also in agreement with RNA data - PP1γ1 transcripts progressively decreased in parallel with protein data. PP1α protein expression also appeared to decrease in postnatal testes development. However, RNA analysis showed that PP1α transcripts appear to remain at similar levels thoughout the developmental stages.

Celluar distribution of the PP1 isoforms in in testis sections of wild-type mice, showed that PP1γ2 is the only isoform abundant in the cytoplasm of secondary spermatocytes, round and elongating spermatids with weak expression in premeiotic germ cells and pachytene spermatocytes. For the most part, PP1γ1 and PP1α expression

is restricted to spermatogonia, pachytene spermatocytes and interstitial cells. Relatively weak expression of PP1α and PP1γ1 was observed in other germ cells. Our immunohistochemistry results for PP1γ1 and PP1γ2 in germ cells are in agreement with RNA data (Fig. 19). PP1γ1 expression is confined to spermatogonia and spermatocytes while PP1γ2 expression is present in all individual germ cells. This dramatic specificity of PP1 suggests isoform specific function for PP1γ2 in spermatogenesis.

Subcellular distribution of PP1γ2 protein was determined by transient transfection studies in HEK293 cells using two eukaryotic expression vectors-with and without myc tag. This heterologous expression study was conducted to test the hypothesis that PP1γ2 may be an isoform which is localized in the cytosol because of unique C-terminus sequence. The only unique feature of the PP1γ2 isoform compared to the PP1γ1 isoform is its 21 amino acid carboxy terminus segment (Cohen, 2002) which lacks a nuclear localization signal present in the C-terminus sequences of the other isoforms. All other PP1 isoforms are found in nucleus except when they are retained in the cytosol by targeting and tethering proteins (Bollen, 2004). Immunocytochemistry of transfected cells showed the PP1γ2-fusion protein was predominantly expressed in cytoplasm. Occasional nuclear stain was observed which could be due to different cell cycle stages. Earlier report with PP1γ1 antibody demonstrated dynamic localization of PP1γ1 in somatic cells in different cell cycle stages (Andreassen, 1998). Even though PP1γ1 immunoreactivity is observed in both cytosol and nucleus, it is predominantly expressed in the nucleus. An obvious interpretation of the difference in localization of the two closely related isoforms is that there are isoform specific regulatory subunits that retain PP1γ2 in the cytosol. A few isoform specific protein have been reported for PP1γ1, Spinophilin and Neurabin

(Carmody *et al.*, 2004) and for PP1γ2 binding protein, for example, Spz1 binding to PP1γ2 (Hrabchak *et al.*, 2004). We believe that regulatory proteins specific for PP1γ2 are expressed in testis.

In PP1γ2 transfected cells, there is a concomitant decrease in immunoreactive PP1γ1. This observation raises the intriguing possibility that PP1γ2 may regulate the expression of the other isoform PP1γ1. This regulation may occur at the transcriptional or post transcriptional level. It is possible that a similar mechanism may exist in developing germ cells in testes. Further studies are required to test this hypothesis and to determine the mechanism by which the overall switch from PP1γ1 to PP1γ2 expression occurs in germ cells.

In summary, our studies suggest that the contribution of the different isoforms of phosphatase 1 varies according to cell–specific physiological requirements. Distinct expression of PP1γ2 message and protein in postnatal testes and post-meiotic germ cells suggests a unique role for PP1γ2 in testes development, spermatogenesis and spermiogenesis.

B. Analysis and characterization of PP1γ2 and its potential role in spermatogenesis and sperm morphogenesis

The predominant spatio-temporal expression of PP1γ2 in round spermatid cells and elongated spermatids suggests that PP1γ2 might play an important role in the process of differentiation of the male germ cells to mature spermatozoa. To elucidate the function of PP1γ2 in greater detail, we obtained *Ppp1cc*-null mice from Dr. Susan Varmuza

(Toronto, Canada) (Varmuza *et al.*, 1999). Heterozygous animals appeared phenotypically normal and were fertile. This indicated that there was no haploinsufficiency of the PP1γ allele. Homozygous mice for PP1γ deleted allele were generated in CD1 animals. Western blot with testes extracts confirmed the absence of the PP1γ1 and PP1γ2 in testes of *Ppp1cc*-null animals. Testes of *Ppp1cc*-null mice appeared smaller than the testes of wild type (littermates) mice. Histopathology suggested a disruption in normal spermiogenesis. There was a significantly reduction in spermatids and testicular spermatozoa in *Ppp1cc*-null testes. Loss of spermatids occured at the round spermatid stage and increased in severity resulting in a marked reduction in condensing and elongating spermatids and an almost complete absence of mature sperm. Intriguingly, PKA knock out and casein kinase knock out mice model don't show this phenotype. Our results thus suggest that PP1γ2, along with an unknown protein kinase, may be involved in protein phosphorylation and dephosphorylation events during spermiogenesis.

Reduced number of sperm in testes is probably due to either increased cell death as reported earlier using tunnel assay (Varmuza *et al.*, 1999) or due to obvious spermiation defect (which is observed in the sections of both brightfield and electron microscope (Fig. 24) leading to phagocytotic activity of Sertoli cells (Russel *et al.*, 1990; Nakanishi, Shiratsuchi 2004). Yet another possible explanation is that the epididymis is unable to transport immotile sperm out of the lumen of testes. This could be due to absence of PP1γ2 in the epididymis itself. To test this hypothesis we performed RNA analysis on different mouse tissues including caudal epididymis with PP1γ2 primers and found that PP1γ2 mRNA is indeed present in epididymis. However expression of PP1γ2 protein is not yet confirmed in this tissue. Immunohistochemical analysis did not

conclusively confirm this observation since sperm debris present in the epididymis may prevent identification of stain in epithelial cells.

A detailed ultra-structural analyses using light and transmission electron microscopy showed numerous structural defects in elongating spermatids and testicular spermatozoa of the *Ppp1cc*-null male mice. Abnormal head shapes were also observed in agreement with a previous report (Davies *et al.*, 2003). Prominent were poorly developed or missing mitochondrial sheaths, and supernumerary, disorganized outer dense fiber florets throughout sperm tails. We also detected frequent degeneration of condensing spermatids, indicated by fragmentation of tail structures and the presence of numerous vacuoles in the cytoplasm of elongating spermatids. A subtle abnormality in the development of the fibrous sheath was observed, specifically in the formation of distinct, triangular-shaped longitudinal columns and inward projections that replace the ODFs associated with axonemal microtubule doublets 3 and 8 in wild-type sperm. These observations suggest that PP1γ2 is required for flagellar integrity and the development of flagellar structures. Western blot analysis and immunohistochemistry of *Ppp1cc*-null testes also showed increased expression and altered localization of PP1α to round spermatids and to Sertoli cells at the germ cell boundary. The reason for this change of PP1α expression and localization in the absence of PP1γ expression is not yet known.

Our studies using Western blot and immunohistochemistry showed the absence or a sharp reduction in the levels of post-meiotic proteins, (AKAP4/AKAP82, odf2, sds22, FSII), in *Ppp1cc*-null testes. Some of these proteins appear to be associated with sperm tail development and function (Vijayaraghavan *et al.*, 1996; Huang *et al.*, 2002; Huang *et al.*,

2004; Miki *et al.*, 2002; Schalles *et al.*, 1998; Carr *et al.*, 2001). This reduction of protein expression could be due to a lack of or reduced number of cell types expressing these proteins or due to reduced protein expression in spermatids. Though studies using selected antibodies and immumnofluorescence in testes sections suggested reduced protein expression in null testes, further examination using immunocytochemistry of testicular sperm showed that AKAP4, odf2, FSII and sds22 are present in mutant sperm. This suggests that the apparent reduction in intracellular protein levels seen in Western blots could be due to a reduced number of differentiating spermatids in null testis where these proteins are synthesized. It is not possible to rule out the possibility that defective tail development may be due to reduced levels of these flagellar proteins. Additional studies are required to distinguish between these possibilities.

Our studies in this proposal showed that in addition to its previously recognized role in sperm motility regulation (Vijayaraghavan *et al.*, 1996; Smith *et al.*,. 1996; 1999), PP1γ2 appears essential for tail morphogenesis during spermiogenesis. This requirement of the PP1γ2 isoform during spermiogenesis is surprising considering that other isoforms of PP1 substitute for PP1γ in all other cells and in the female; an exception is, thus, developing sperm. In this regard it may be noted that analysis of genome data bases and additional studies from our laboratory show that PP1γ2 with its unique C-terminus extension is mammalian-specific. Our experiments showed that PP1γ2 isoform is present in all mammalian spermatozoa studied - mouse, hamster, bovine, and absent in non-mammalian species like *xenopus* and sea urchin (Fig. 37). In contrast, PP1γ1 is present in *xenopus* sperm extracts. It is therefore tempting to speculate that PP1γ2 may have an isoform-specific function in the development of outer dense fibers and the fibrous sheath, structures found in

mammalian sperm. If this is true then PP1γ2, but not PP1γ1, should restore sperm formation and fertility in *Ppp1cc*-null mice. Moreover since sperm lack PP1γ1, it is more likely that lack of PP1γ2 is responsible for the morphological defects in sperm. To test this hypothesis we made transgenic mice expressing either PP1γ1 or PP1γ2 under the testis specific Pgk2 promoter. Studies to determine which of the two isoforms may rescue the phenotype in *Ppp1cc*-null mice are underway in our laboratory.

C. Is PP1γ2 indispensable to spermatogenesis?

The defect in spermatogenesis in PP1γ knockout males could be due to the lack of either PP1γ1 or PP1γ2 or due to the absence of both isoforms. Will mice lacking only one of the isoforms be normal? Can PP1γ2 alone is sufficient to restore the structural defects of sperm and fertility? Our previously mentioned isoform specific rescue experiments partially answer this question.

Preliminary observations from the experiments in which the PP1γ2 gene is introduced into the PP1γ knock out mouse are presented in appendix I. Briefly, morphological analysis of epididymal sperm showed structural defects involving head shape and mitochondrial sheath are restored in PP1γ2 rescue mice (see appendix I). Moreover examination of testes, in PP1γ2 rescue mice, indicated most of the structural integrity of testis was restored in these experimental mice. Sertoli cell defects, vacuoles, lack of germ cells from the basal layer of seminiferous tubule and mislocation of germ cells appeared to be mostly absent in the PP1γ2 rescue animals. Sperm number appeared

to increase in the PP1γ2 rescue animals compared to the *Ppp1cc*-null animals. Evidence for these statements are present in appendix I.

In summary, the major findings of this dissertation are:

- PP1γ2 is predominantly present in testis.
- PP1γ2 is the only isoform of PP1 in sperm.
- Postnatal mRNA and protein expression of PP1γ2 increases while PP1γ1 and PP1α mRNA and protein remains constant or decrease during testes development.
- PP1γ2 shows a distinct cellular and sub-cellular distribution in germ cells and somatic cells in comparison with PP1γ1 and PP1α.
- mRNA expression of PP1γ2 is detected in post-meiotic germ cells and developing spermatogonia (even though expression of protein is first observed in secondary spermatocytes) in contrast to PP1γ1 which is present only in spermatogonia and pachytene spermatocytes.
- *Ppp1cc*-null mice testes show reduced sperm number and epididymis from null mice show complete absence of sperm
- *Ppp1cc-null* mice show severe defect in spermiogenesis leading to almost absence of elongating spermatids in mutant testes.
- Various other morphological defects were observed in mutant testes in comparison to wild type which include smaller tubule size, presence of multiple vacuoles, presence of diploidy in spermatids, spermiation defects, sertoli cell defects.

- Testicular sperm from *Ppp1cc*-null mice show abnormal head shape, defect in mitochondrial organization and outer dense fibers and subtle defect in fibrous sheath suggesting role for PP1γ2 in sperm morphogenesis (as PP1γ1 is absent in sperm).
- Altered expression of AKAP4, Odf2, FSII and Sds22 observed in *Ppp1cc*-null testis is most likely due to reduced cell type or decreased protein expression.
- PP1γ2 could partially rescue the *Ppp1cc*-null phenotype.

Bibliography

Alphey L., Jimenez J., White C. H., Dawson I., Nurse P. and Glover D. M., Twine, a cdc25 homolog that functions in the male and female germline of Drosophila, *Cell,* 1992, (69): 977–988.

Amanda B and O'Donnell L., Characterization of Normal Spermiation and Spermiation Failure Induced by Hormone Suppression in Adult Rats Biol Reprod., 2003, (68): 1299-1307.

Andreassen PR, Lacroix FB, Villa-Moruzzi E and Margolis RL., Differential Subcellular Localization of Protein Phosphatase-1 α, γ1, and δ Isoforms during Both Interphase and Mitosis in Mammalian Cells, J. Cell Biol., 1998, 141(5): 1207-1215

Ashizawa K, Wishart GJ, Tomonaga H, Nishinakama K, Tsuzuki Y., Presence of protein phosphatase type 1 and its involvement in temperature-dependent flagellar movement of fowl spermatozoa. FEBS Lett., 1994, (350): 130-134.

Ashizawa K, Wishart GJ, Nishinakama K, Sakamoto T, Tsuzuki Y., Regulatory mechanisms of fowl sperm motility: possible role of endogenous myosin light chain kinase-like protein. J Reprod Fertil., 1995, (104): 141-148.

Austin CR., Observations on the penetration of the sperm into the mammalian egg Australian Journal of Scientific Research, 1951, (4): 581–596.

Baarends W.M., Hoogerbrugge J.W., Roest H.P., Ooms M., Vreeburg J., Hoeijmakers J.H.J. and Grootegoed J.A. Histone ubiquitination and chromatin remodeling in mouse spermatogenesis. Dev Biol., 1999, 207(2): 322-333.

Baltz JM., Williams PO. and Cone RA., Dense Fibers Protect Mammalian Sperm against Damage1biology of reproduction, 1990, (43): 485-491.

Barford D, Das AK, Egloff MP The structure and mechanism of protein phosphatases: insights into catalysis and regulation. Annu Rev Biophys Biomol Struct., 1998, (27):133–164.

Bedford, J.M. and Calvin, H.I., Changes in -S-S- linked structures of the sperm tail during epididymal maturation, with comparative observations in sub-mammalian species. J. Exp. Zool., 1974, (187): 181–204.

Bedford, J. M., Significance of the need for sperm capacitation before fertilization in eutherian mammals. Biol. Reprod., 1983, 28: 108-120

Bedford JM, Hoskins DD. The mammalian spermatozoon: morphology, biochemistry and physiology. In: Lamming GE (ed.), Marshall's Physiology of Reproduction. Edinburgh, London, Melbourne, New York: Churchill Livingstone; 1990: 379–568.

Bellve AR. Purification, culture and fractionation of spermatogenic cells. Methods in Enzymology, 1979; (225): 84-112.

Bonner RF, Emmert-Buck M, Cole K, Pohida T, Chuaqui R, Goldstein S, Liotta LA., Laser capture microdissection: molecular analysis of tissue. Science, 1997, (278): 1481–1483.

Bracho GE, Fritch JJ, Tash JS., Identification of Flagellar Proteins That Initiate the Activation of Sperm Motility in vivo. Biochem Biophys Res Commun., 1998, 242(1): 231-237.

Breitbart H., Signaling pathways in sperm capacitation and acrosome reaction. Cellular and Molecular Biology, 2003, (49): 321–327.

Bronson, R.A., Cooper, G.W. and Rosenfeld, D.L., Sperm-specific iso-and auto-antibodies inhibit binding of human sperm to the human zona pellucida. Fertil. Steril., 1982, (38): 724–729.

Browder L.W., Erickson C.A. and Jeffery W.R., Developmental Biology. Third edition., 1991, Saunders College Pub. Philadelphia.

Burgos, M.H., and Fawcett, D.W., Studies on the fine structure of the mammalian testis. J. Biophys. Biochem. Cytol., 1955, (1): 287–300.

Carmody LC, Bauman PA, Bass MA, Mavila N, DePaoli-Roach AA and Colbran RJ., A protein phosphatase-1γ1 isoform-selectivity determinant in dendritic spine-associated neurabin, JBC Papers in Press. Published on March 11, 2004.

Carr D W. and Acott T.S., Inhibition of bovine spermatozoa by cauda epidiymal fluid: I. Studies of a sperm motility quiescence factor. Biol Reprod., 1984, (30): 913-925.

Carr DW, Fujita A, Stentz CL, Liberty GL**,** Olson GE, and Narumiya S. Identification of Sperm-specific Proteins That Interact with A-kinase Anchoring Proteins in a manner Similar to the Type II Regulatory Subunit of PKA. J. Biol. Chem., 2001, (276): 17332-17338.

Ceulemans, H. and M. Bollen, Functional diversity of protein phosphatase 1, a cellular economizer and rest button. Physiological Reviews, 2004, (557): 1-8.

Chang MC (1951) Fertilizing capacity of spermatozoa deposited into the Fallopian tubes Nature 168 697–698.

Chakrabarti R., Douglas K., Jing L., Joanne O., Stephen P. and Vijayaraghavan Srinivasan, Analysis of *Ppp1cc*-Null Mice Suggests a Role for PP1γ2 in Sperm Morphogenesis, (published online, 2007)

Cohen PTW., Protein phosphatase 1 – targeted in many directions. *Journal of Cell Science,* 2002, (115): 241-256.

da Cruz e Silva EF, Fox CA, Ouimet CC, Gustafson E, Watson SJ, Greengard P., Differential expression of protein phosphatase 1 isoforms in mammalian brain. J Neurosci, 1995, (15): 3375–3389.

Davis BK., Interaction of lipids with the plasma membrane of sperm cells. I. The anti-fertilization action of cholesterol. Arch Androl., 1980, (5): 249-254.

Davis BK., Uterine fluid proteins bind sperm cholesterol during capacitation in the rabbit. Experientia (Basal), 1982, (38): 1063-1064.

Davies, T. and Varmuza S., Development to blastocyst is impaired when intracytoplasmic sperm injection is performed with abnormal sperm from infertile mice harboring a mutation in the protein phosphatase 1cgamma gene. Biol Reprod, 2003, 68(4): 1470-1476.

Eddy E.M., O'Brien D.A., Fenderson B.A., and Welch J.E., Intermediate filament-like proteins in the fibrous sheath of the mouse sperm flagellum. In Robaire, B. (ed.), The Male Germ Cell: Spermatogonium to Fertilization. New York Academy of Science. 1992, New York, 224–239.

Eddy EM., Male Germ Cell Gene Expression Recent Progress in Hormone Research, 2002, (57): 103-128.

Eddy E. M., Toshimori K, and O'Brien D. A., Fibrous sheath of mammalian spermatozoa. Micros. Res. Tech., 2004, (61): 103-115.

Eddy, M. The spermatozoon. Knobil and Neill's Physiology of Reproduction, 3rd edition, ed. Jimmy D Neill, Elsevier, 2006, 4-54.

Emmert-Buck MR, Bonner RF, Smith PD, et al. Laser capture microdissection. Science, 1997, (274): 998–1001.

Esposito G, Jaiswal BS, Xie F, Krajnc-Franken M, Robben TJ, Strik AM, Kuil C, Philipsen RLA, van Duin M, Conti M, Gossen JA., Mice deficient for soluble adenylyl cyclase are infertile because of a severe sperm-motility defect. Proc Natl Acad Sci U S A, 2004; 101: 2993-2998.

Farooqui AA., Biochemistry of sperm capacitation. J Biochem., 1983, (15): 463-468.

Fawcett, D.W., Ito, S., and Slautterback, D.L. The occurrence of intercellular bridges in groups of cells exhibiting synchronous differentiation. J. Biophys. Biochem. Cytol., 1959, (5): 453–460.

Fawcett D. W. A comparative view of sperm ultrastructure. Biol. Reprod. Suppl. 1970, (2): 90-126.

Fawcett, D.W. The mammalian spermatozoon. Dev. Biol., 1975, (11): 391–436.

Genuth S., The endocrine system. In:Berne RM, Levy, MN., editor. Physiology. 4th ed., 1998, St. Louis: Mosby., 779-1014.

Go KJ., Wolf DP., Albumin-mediated changes in sperm sterob content during capacitation. Biol Reprod, 1985, (32): 145-155.

Hamner, C. E. and Williams, W. L., Effect of the female reproductive tract on sperm metabolism in the rabbit and fowl. Reprod. Fert. 1963, (5): 143-15.

Helps, N. R., Luo, X., Barker, H. M. and Cohen, P. T., NIMA-related kinase 2 (Nek2), a cell-cycle-regulated protein kinase localized to centrosomes, is complexed to protein phosphatase 1. Biochem. J., 2000, (15): 509-518.

Hecht, N.B. Regulation of haploid expressed genes in male germ cells. J. Reprod. Fertil., 1990, (88): 679–693.

Hoskins, D.D., D. Munsterman, and M.L. Hall, The control of bovine sperm glycolysis during epidiymal tran sit. Biology of Reproduction, 1975, (12): p. 566.

Hoskins, D. D., Brandt, H. and Acott, T. S. Initiation of sperm motility in the mammalian epididymis. Fed. Proc., 1978, 37(11): 2534-2542.

Hrabchak C, Varmuza S., Identification of the spermatogenic zip protein Spz1 as a putative protein phosphatase-1 (PP1) regulatory protein that specifically binds the PP1cgamma2 splice variant in mouse testis. J Biol Chem., 2004 279(35): 37079-37086.

Huang Z, Khatra B, Bollen M, Carr DW, Vijayaraghavan S. Sperm PP1γ2 is regulated by a homologue of the yeast protein phosphatase binding protein sds22. Biol Reprod., 2002, (67): 1936-1942.

Inagaki, N., Ito, M., Nakano, T. and Inagaki, M., Spatiotemporal distribution of protein kinase and phosphatase activities. *Trends Biochem. Sci*., 1994, (19): 448-452.

Iwaoki, Y., Matsuda, H., Mutter, G. L., Watrin, F., and Wolgemuth, D. J., Differential expression of the proto-oncogenes c-abl and c-mos in developing mouse germ cells. *Exp. Cell Res.*, 1993, 206, 212–219.

Jassim, A., Gillott, D.J., AI-Zuhdi, Y. Gray, A., Foxon R., and Bottazzo R., Isolation and biochemical characterization of the human sperm tail fibrous sheath. Hum. Reprod., 1992, (7): 86–94.

Johnson MH. and Everitt BJ., Testicular function in the adult, Essential reproduction, 5th edition, 2002, Blackwell science Ptd limited, Australia.

Jones R. Plasma membrane structure and remodelling during sperm maturation in the epididymis. J Reprod Fertil Suppl 1998.

Joy Y. W., Thomas J. R., David E. C., Kimberly A. B., McKnight, G. S. and Means, A. R., Spermiogenesis and exchange of basic nuclear proteins are impaired in male germ cells lacking Camk4, Nature Genetics, 2000, (25): 448 – 452.

Kathryn M. J. and Bernard R., Dynamic Changes in Gene Expression along the Rat Epididymis, Biol of Reprod., 2001, (65): 696-703.

Keshet E., Itin A., Fischman K. and Nir U. The testis-specific transcript (ferT) of the tyrosine kinase FER is expressed during spermatogenesis in a stage-specific manner *Mol. Cell. Biol.,* 1990, (10): 5021–5025.

Kistler, M. K., Sassone, C. P., Identification of a functional cyclic adenosine 3',5'-monophosphate response element in the 5'-flanking region of the gene for transition protein 1 (TP1), a basic chromosomal protein of mammalian spermatids. Biol Reprod., 1994, 51(6): 1322-1329.

Kitagawa Y., Sasaki K, Shima H, Shibuya M, Sugimura T, Nagao M., Protein phosphatases possibly involved in rat spermatogenesis. Biochemical and Biophysical Research Communications, 1990, (171): 230-235.

Kotaja N, Kimmins S, Brancorsini S, Hentsch D, Vonesch JL, Davidson I, Parvinen M, Sassone-Corsi P. Preparation, isolation and characterization of stage-specific spermatogenic cells for cellular and molecular analysis. Nat Methods., 2004, (1): 249-254.

Laemmli UK. Cleavage of structural proteins during the assembly of the head of bacteriophage T4. Nature, 1970, (227): 680-685.

Langlais J, Roberts KD. A molecular membrane model of sperm capacitation and the acrosome reaction of mammalian spermatozoa. Gamete Res., 1985, (12): 183-224.

Leblond CP. Clermont Y., Definition of the stages of the cycle of the seminiferous epithelium in the rat. Ann N Y Acad Sci., 1952, 55 (4): 548-573.

Lesage B., Beullens M., Nuytten M., Van Eynde A., Keppens S., Himpens B., Bollen M. Interactor-mediated Nuclear Translocation and Retention of Protein Phosphatase-1. J. Biol. Chem., 2004, (279): 55978-55984.

Letwin K., Mizzen L., Motro B., Ben D. Y., Bernstein A., and Pawson T., A mammalian dual specificity protein kinase, Nek1, is related to the NIMA cell cycle regulator and highly expressed in meiotic germ cells, *EMBO J.*, 1992, (11): 3521–3531.

Lindemann, C. B., A cAMP-induced increase in the motility of demembranated bull sperm models, Cell, 1978, (13): 9-18.

Manova, K., Nocka, K., Besmer, P., and Bachvarova, R. F. Gonadal expression of c-kit encoded at the W locus of the mouse. *Development,* 1990, (110): 1057–1069.

Martin D., and Fawcett DW., Further Observations on the Numbers of Spermatogonia, Spermatocytes, and Spermatids Connected by Intercellular Bridges in the Mammalian Testis, 1971, Biology of Reproduction, (4): 195-215.

Matsushime, H., Jinno, A., Takagi, N., and Shibuya, M., A novel mammalian protein kinase gene (mak) is highly expressed in testicular germ cells at and after meiosis, *Mol. Cell. Biol.,* 1990, (10): 2261–2268.

Mauro, L. J., Olmsted, E. A., Skrobacz, B. M., Mourey, R. J., Davis, A. R., and Dixon, J. E., Identification of a hormonally regulated protein tyrosine phosphatase associated with bone and testicular differentiation, *J. Biol. Chem.,* 1994, (269): 30659-30667.

McCarrey JR, Berg WM, Paragioudakis SJ, Zhang PL, Dilworth DD, Arnold BL, Rossi JJ., Differential transcription of Pgk genes during spermatogenesis in the mouse. Dev Biol., 1992, 154(1): 160-168.

Miki K, Willis WD, Brown PR, Goulding EH, Fulcher KD, Eddy EM. Targeted disruption of the Akap4 gene causes defects in sperm flagellum and motility. Dev Biol., 2002; (248): 331-342.

Mortimer, D. Sperm recovery techniques to maximize fertilizing capacity.Reprod Fertil Dev. 1994, 6(1):25-31.

Mounib, M. S. and Ceang, M. C., Effect of in utero incubation on the metabolism of rabbit spermatozoa. Nature (London), 1964, (201): 943-944.

Mulcahy LT, Andrews PD, Wickramasinghe S, Sleeman J, Prescott A, Lam YW, Lyon C, Swedlow JR and Lamond AI., Time-lapse imaging reveals dynamic relocalization of PP1γ throughout the mammalian cell cycle, MBC in Press, published on 2002.

Muramatsu T., Giri P. R., Higuchi S., and Kincaid R. L., Molecular Cloning of a Calmodulin-Dependent Phosphatase from Murine Testis: Identification of a Developmentally Expressed Nonneural Isoenzyme, *Proc. Natl. Acad. Sci.*, *U. S. A.* 1992, (89): 529–533.

Murofushi HIshiguro K, Takahashi D, Ikeda J, Sakai H., Regulation of sperm flagellar movement by protein phosphorylation and dephosphorylation. Cell Motility and the Cytoskeleton, 1986, (6): 83-88.

Mutter G. L., and Wolgemuth D. J., Distinct Developmental Patterns of c-mos Protooncogene Expression in Female and Male Mouse Germ Cells, *Proc. Natl. Acad. Sci. U. S. A,* 1987, (84): 5301–5305.

Nakanishi Y, Shiratsuchi A., Phagocytic removal of apoptotic spermatogenic cells by Sertoli cells: mechanisms and consequences. Biol Pharm Bull, 2004, (27):13–16.

Narisawa S, Hecht NB, Goldberg E, Boatright KM, Reed JC, and Millán JL. Testis Specific Cytochrome c-Null Mice Produce Functional Sperm but Undergo Early Testicular Atrophy. Mol and Cell Biol, 2002, (22): 5554-5562.

Nolan MA, Babcock DF, Wennemuth G, Brown W, Burton KA, McKnight GS. Sperm-specific protein kinase A catalytic subunit C2 orchestrates cAMP signaling for male fertility. Proc Natl Acad Sci U S A, 2004; (101): 13483-13488.

Oakberg, E.F. Duration of spermatogenesis in the mouse and timing of stages of the cycle of the seminiferous epithelium. Am. J. Anat., 1956, (99): 391-409.

O'Brien D.A. and Bellve A.R., Protein constituents of the mouse spermatozoa II. Temporal syntheses during spermatogenesis. Dev. Biol., 1980, (75): 405–418.

Oliver CJ. and Shenolikar S., Physiologic Importance of Protein Phosphatase Inhibitors, Frontiers in Bioscience, 1998, (3): 961-972.

Okunade, G. W., Miller M. L., Pyne G. J., Sutliff R. L., O'Connor K. T., Neumann, J.C., Andringa A., Miller D. A., Prasad V., Doetschman T., Paul R. J., and Shull G. E., Targeted ablation of plasma membrane Ca^2-ATPase isoforms 1 and 4 Indicates a critical role in hyperactivated sperm motility and male fertility for PMCA4, Papers In Press, J. Biol. Chem, 2004.

Orgebin-Crist MC., Sperm maturation in rabbit epididymis. Nature, 1967, (216): 816-818.

Orth J, Christensen K. Localization of ^{125}I-labeled FSH in the Testes of Hypophysectomized Rats by Autoradiography at the Light and Electron microscope Levels. Endocrinology, 1977, (101): 262-278.

Prabhakara PR, Naaby-Hansen S, Aguolnik I, Tsai JY, Silver LM, Flickinger CJ, and Herr JC., Complementary Deoxyribonucleic Acid Cloning and Characterization of mSP-10:The Mouse Homologue of Human Acrosomal Protein SP-10 Biology Of Reproduction, 1995, (53): 873-881.

Quill TA., Sugden SA., Rossi KL., Doolittle LK., Hammer RE. and Garbers DL., Hyperactivated sperm motility driven by CatSper2 is required for fertilization Proc Natl Acad Sci U S A., 2003, 100(25): 14869–14874.

Rambourg A, Clermont Y., Three-dimensional electron microscopy: structure of the Golgi apparatus. Eur J Cell Biol ., 1990, 51: 189–200.

Ren D., Navarro B., Perez G., Jackson A. C., Hsu S., Shi Q., Tilly J. L., Clapham D. E., A sperm ion channel required for sperm motility and male fertility. Nature, 2001, (413): 603-609.

Robaire B, Hermo L. Efferent ducts, epididymis, and vas deferens: structure, functions, and their regulation. In: Knobil E, Neill J (eds.), The Physiology of Reproduction. New York: Raven Press; 1988.

Rossi P, Sette C, Dolci S, Geremia R., Role of c-kit in mammalian spermatogenesis. Endocrinol Invest., 2000, 23(9): 609-615.

Russell, L. D., Ettlin, R. A., Sinha Hikim, A. P. and Clegg, E. D., Histological and Histopathological Evaluation of the Testis, ed. L. D. Russell, R. A. Ettlin, A. P. Sinha Hikim and E. D. Clegg, pp. 1-40. Clearwater, FL: Cache River Press.

Russell LD, Hikim APS, Ettlin RA, Clegg ED., Histological and histopathological evaluation of the testis. Clearwater, FL: Cache River Press, 1990.

Sakata Y, Saegusa H, Zong S, Osanai M, Murakoshi T, Shimizu Y, Noda T, Aso T, Tanabe T., Ca(v)2.3 (alpha1E) Ca2+ channel participates in the control of sperm Function, FEBS Lett., 2002, 516(1-3): 229-233.

San Agustin JT, Witman GB. Role of cAMP in the reactivation of demembranated ram spermatozoa. Cell Motil Cytoskeleton, 1994, (27): 206–218.

Sasaki K, Shima H, Kitagawa Y, Irino S, Sugimura T, Nagao M. Identification of members of the protein phosphatase 1 gene family in the rat and enhanced expression of protein phosphatase1a gene in rat hepatocellular carcinomas. Jpn J Cancer Res., 1990; (81): 1272-1280.

Schalles U, Shao X, van der Hoorn FA, Oko R. Developmental expression of the 84 kDa ODF sperm protein: localization to both the cortex and medullar outer dense fibers and to the connecting piece. Dev Biol., 1998; (199): 250-260.

Schumacher JM, Lee K, Edelhoff S, Braun RE. Spnr, a murine RNA-binding protein that is localized to cytoplasmic microtubules. J Cell Biol., 1995, (129):1023-1032.

Sharpe RM., Regulation of spermatogenesis. In: KnobilE, Neill JD, ed. The physiology of reproduction. 2nd ed., 1994, New York: Raven Press. 1363-1434.

Si, Y., Hyperactivation of hamster sperm motility by temperature-dependent tyrosine phosphorylation of an 80-kDa protein. Biol Reprod, 1999, 61(1): 247-252.

Si, Y. and M. Okuno, Role of tyrosine phosphorylation of flagellar proteins in hamster sperm hyperactivation. Biol Reprod, 1999, 61(1): 240-246.

Simone NL, Bonner RF, Gillespie JW, Emmert-Buck MR, Liotta LA., Laser-capture microdissection: opening the microscopic frontier to molecular analysis. Trends Genet, 1998, (7): 272–276.

Skålhegg BS, Huang Y, Su T, Idzerda RL, Mcknight GS and Burton KA**.,** Mutation of the C Subunit of PKA Leads to Growth Retardation and Sperm Dysfunction. Molecular Endocrinology, 2002, 16(3): 630–639.

Smith GD, Wolf DP, Trautman KC, Silva EF da Cruz e, Greengard P and Vijayaraghavan S., Primate sperm contain protein phosphatase 1, a biochemical mediator of motility., Biol Reprod., 1996, 54(3): 719-727.

Smith, G.D., Wolf D. P., Trautman K. C. and Vijayaraghavan S., Motility potential of macaque epididymal sperm: the role of protein phosphatase and glycogen synthase kinase-3 activities. J Androl, 1999, 20(1): 47-53.

Sorrentino V., Giorgi M., Geremia R., Besmer P. and Rossi P., Expression of the c-kit proto-oncogene in the murine male germ cells. Oncogene 1991, 6(1): 149- 151.

Strack S, Kini S, Ebner FF, Wadzinski BE, Colbran RJ., Differential cellular and subcellular localization of protein phosphatase 1 isoforms in brain. J Comp Neurol., 1999, (413): 373-384.

Takahashi, D., Murofushi H, Ishiguro K, Ikeda J, Sakai H., Phosphoprotein phosphatase inhibits flagellar movement of triton models of sea urchin spermatozoa. Cell Struct Funct, 1985, (10): 327-337.

Toshima, J., Ohashi, K., Okano, I., Nunoue, K., Kishioka, M., Kuma, K., Miyata, T., Hirai, M., Baba, T., and Mizuno, K., Identification and Characterization of a Novel

Protein Kinase, TESK1, Specifically Expressed in Testicular Germ Cells, *J. Biol. Chem.*,1995, (270): 31331–31337.

Turner TT. and Giles R. D., A sperm motility inhibiting factor in the rat epididymis. Am J Physiol, 1982, (242): R199-R203.

Turner TT., Spermatozoa are exposed to a complex microenvironment as they traverse the epididymis. Ann N Y Acad Sci 1991; (637): 364-384.

Varmuza, S., Jurisicova A., Okano K., Hudson J., Boekelheide K., and Shipp EB., Spermiogenesis is impaired in mice bearing a targeted mutation in the protein phosphatase 1c gamma gene. Dev Biol, 1999, 205: 98-110.

Vijayaraghavan S, Stephens DT, Trautman V, Smith GD, Khatra B, Silva EF da Cruze and Greengard P., Sperm Motility Development in the Epididymis is Associated with Decreased Glycogen Synthase Kinase-3 and Protein Phosphatase 1 Activity. Biology of Reproduction, 1996, (54): 709-718.

Vijayaraghavan S., Chakrabarti R. and Myers K., Regulation of sperm function by protein phosphatase PP1γ2, Proceedings of Gamete Biology: Emerging frontiers in fertility and contraceptive development, (in press), 2006.

Wang PJ, Chien MS, Wu FJ, Chou HN, Lee SJ., Inhibition of embryonic development by microcystin-LR in zebrafish, Danio rerio. Toxicon., 2005, (45): 303-308.

Wera, S. and B.A. Hemmings, Serine/threonine protein phosphatases. Biochemical Journal, 1995, (311):17-29.

Wolfes H., Kogawa K**.,** Millette CF., and Cooper GM., Specific expression of nuclear protooncogenes before entry into meiotic prophase of spermatogenesis. Science, 1989, 245(4919): 740-743.

Xin X., Toselli P. A., Russell L.D., and Seldin D. C., Globozospermia in mice lacking the casein kinase II α' catalytic subunit, Nature Genetics, 1999, (23): 118 -121.

Yanagimachi, R., Mechanisms of fertilizationin mammals. In: Fertilization and embryonic development in vitro (L. Mastroianni and J. D.Biggers, eds.). Plenum Publ., New York, 1981, 81-182.

Yanagimachi, R., Mammalian fertilization. In Knobil, E. and Neill, J.D. (eds), The Physiology of Reproduction. Raven Press, New York, USA, 1988, 135–185.

Yanagimachi R., Mammalian fertilization. In The Physiology of Reproduction, Eds E Knobil & J Neill. New York: Raven Press, 1994, 189–317.

Yoshinaga K., Nishikawa S., Ogawa M., Hayashi S., Kunisada T., F., Role of c-kit in mouse spermatogenesis: identification of spermatogonia as a specific site of c-kit expression and function. *Development,* 1991, (113): 689–699.

Appendix I

To confirm our hypothesis that PP1γ2 is playing the critical role in sperm morphology, we made transgenic mice with either PP1γ1 or PP1γ2 construct under the sperm specific Pgk2 promoter. The PP1γ2 construct was made by Kimberley Myers and PP1γ1 construct was made by David Soler. Microinjection was performed by Case Western Reserve University, Cleveland, Ohio. Analysis of testes extracts of founders of either PP1γ2 or PP1γ1 showed no overexpression (Fig. 39). This suggests that since these are signaling molecules there may be a feed back inhibitory loop of these enzymes which prevents over-expression. To determine if the transgene is being expressed as protein we mated these founders with *Ppp1cc*-null mice. After 2 subsequent generations, we obtained mice which lacks an endogenous copy for both PP1γ1 and PP1γ2 and with either of the transgenes (PP1γ1 or PP1γ2). Analysis of testes extracts of one of the experimental founder lines of PP1γ2 transgene shows an almost comparable level of expression of the protein to the wild type (Fig. 40). The transgene was designed to be expressed only in the testes. However, because ectopic expression of transgenes is frequently encountered in transgenic mice, we examined tissue specificity of expression of the PP1γ2 transgene. No immunoreactive band against PP1γ2 was observed in other somatic tissues (data not shown). Immunohistochemical analysis showed comparable staining of PP1γ2 in both wild type and experimental mice testes sections (Fig. 42). The expression pattern indicated the localization of the transgenic protein to the seminiferous tubules where sperm maturation occurs. However so far we have not obtained a PP1γ1 rescue animal

with comparable expression of the transgene with the wild type. Efforts are underway. Interestingly, PP1γ2 rescue animal showed partial rescue of testes structure and sperm morphology. Testes sections of the experimental mice show an intermediate phenotype between wild type and *Ppp1cc*-null mice (Fig. 41). Vacuoles, mislocated germ cells, absence of basal layer of germ cells were much reduced compared to the null type. Sperm number of experimental mice also appeared to increase compared to the null animals. In the *Ppp1cc*-null animals, testes contain reduced sperm and epididymis contains no sperm. However in the PP1γ2 rescue animals we observed sperm in the epididymis which looked normal. Detailed analysis using bright field microscope demonstrated restoration of the head shape and the mitochondrial sheath structure defect in these animals. Further morphological analysis using electron microscope to determine the defects of the ODF and FS in these animals is awaited. Thus these preliminary data suggests that introducing PP1γ2 in the *Ppp1cc*-null mice lacking both isoforms (PP1γ1 and PP1γ2) are capable of partial rescue of the morphological defects in sperm. Our observation was on an outbred strain of CD1 animals and genetic background of the transgenic animals was on partially B6 background. Experiments with transgenic mice with a restricted expression of either PP1γ1 or PP1γ2 in testis using the Pgk2 promoter in inbred B6 background are currently underway. Further analysis is required to confirm this data.

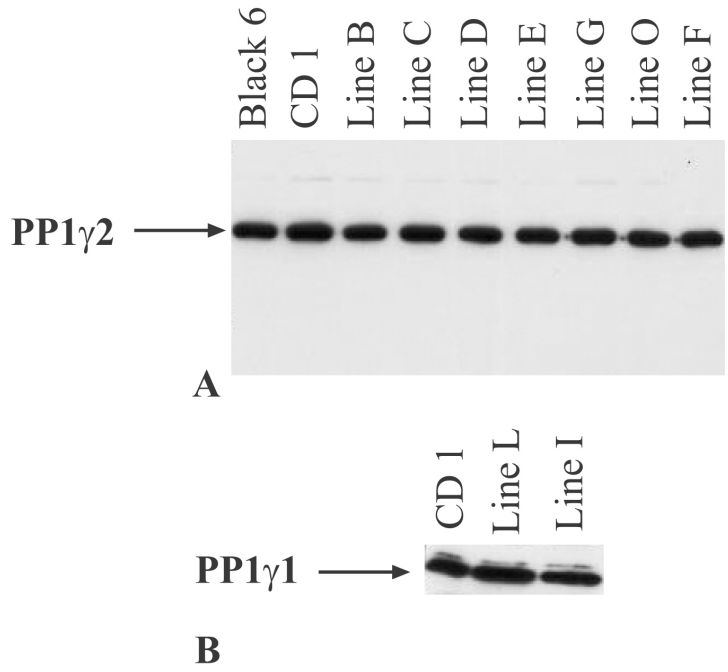

Figure 39. Determination of over-expression of PP1γ2 and PP1γ1 in transgenic mouse testes. A: Expression of the PP1γ2 transgene in seven transgenic lines. Western blot of testes extracts. A rabbit anti-PP1γ2 antibody was used. Lane 1 and 2, wild type black 6 and CD1 mouse; lane 3, transgenic line No. B; lane 4, transgenic line No. C; lane 5, transgenic line No. D; lane 6, transgenic line No. E; lane 7, transgenic line No. G; lane 8, transgenic line No. O; lane 9, transgenic line No. F. Equal protein amount was loaded in all the lanes. **B:** Expression of the PP1γ1 transgene in two transgenic lines. A rabbit anti-PP1γ1 antibody was used. Lane 1, wild type CD1 mouse; lane 2, transgenic line No. L; lane 3, transgenic line No. I. Equal protein amount was loaded in all the lanes.

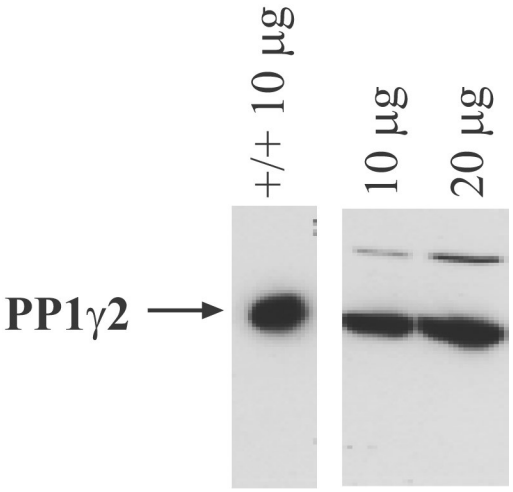

A.

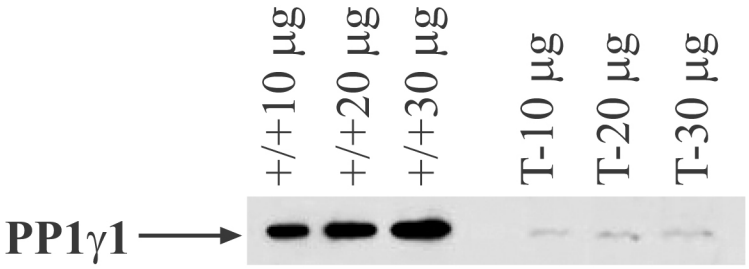

B.

Figure 40. Western blot analysis for transgene expression (PP1γ2 and PP1γ1) in the testes lacking endogenous PP1γ gene expression. A: Lane 1, testis of wild-type mouse; lane 2 and 3, testis of the experimental mouse testes (PP1γ2 rescue animal) **B:** Lane 1-3, testis of wild-type mouse, different concentration; lane 5-7, testis of the experimental mouse testes (PP1γ1 rescue animal).

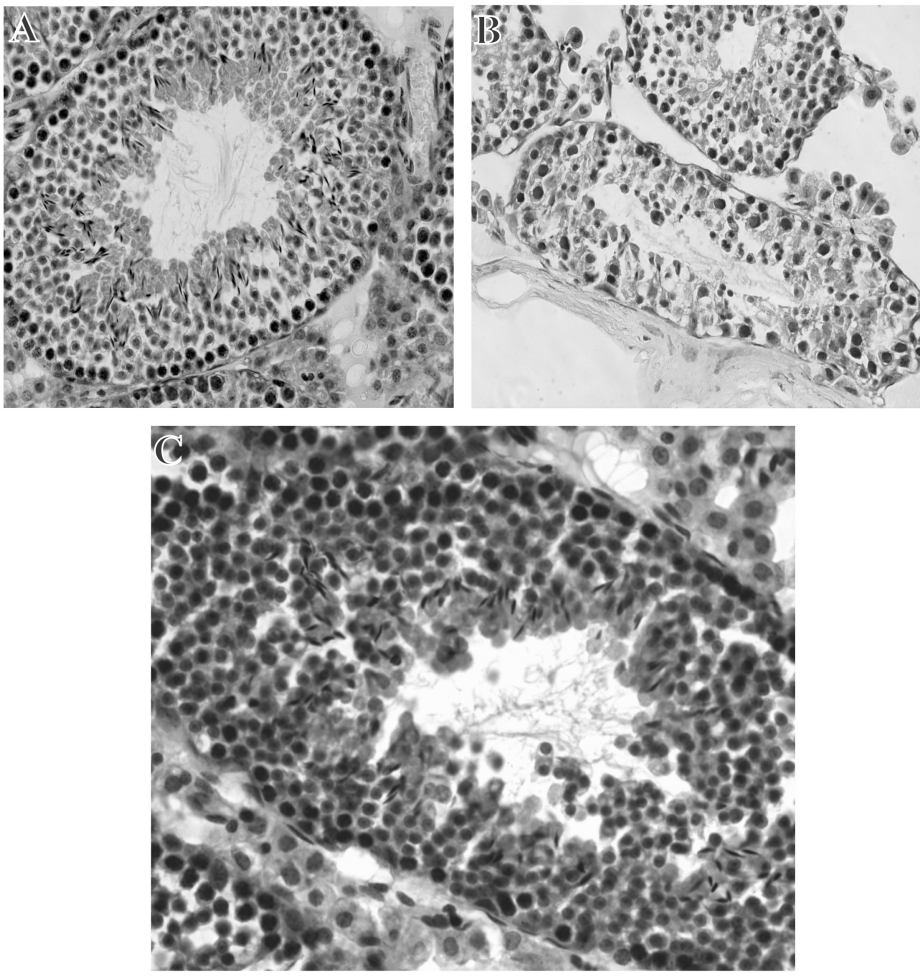

Figure 41. **Morphological analysis of testes sections of wild type (A), null (B) and PP1γ2-rescue experimental (C) mice. C:** Basic organization of the testes appeared to be partially rescued in the PP1γ2 rescue animal. Vacuoles, mislocation of germ cells, absence of germ cells from the basal layer of testes were much reduced in the experimental testes section (rescue) in comparison to the *Ppp1cc*-null testes section **(B)**. **A:** Wild type mouse testes section.

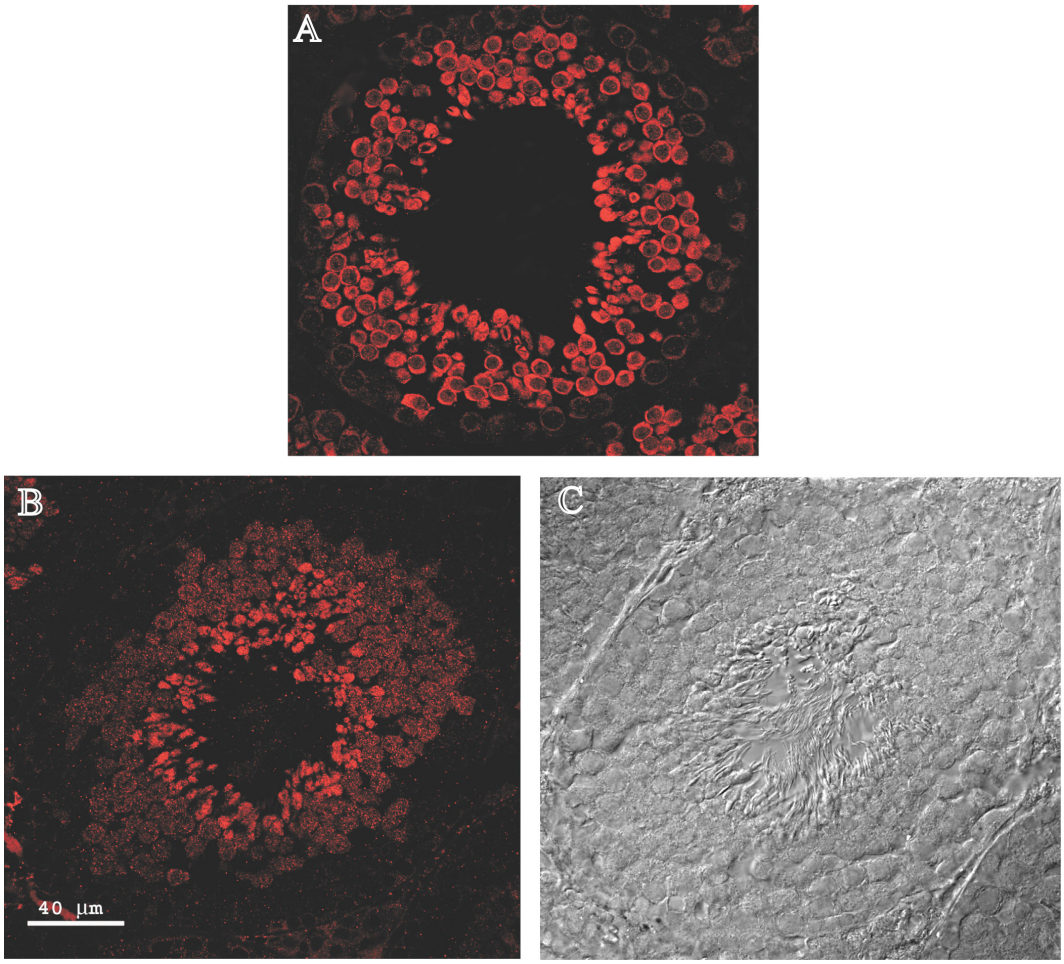

Figure 42. Expression of transgene in the testes section of PP1γ2 rescue experimental mice. A: Wild type testes section with anti-PP1γ2 antibody. **B:** Experimental mouse testes section showing comparable staining with wild type **(A)**. **C:** Corresponding bright field image of B. Note: number of sperm appears to be increased in the experimental mice **(C)** in comparison with the *Ppp1cc*-null type (Fig. 41 B) Bar: A-C is 40 µm

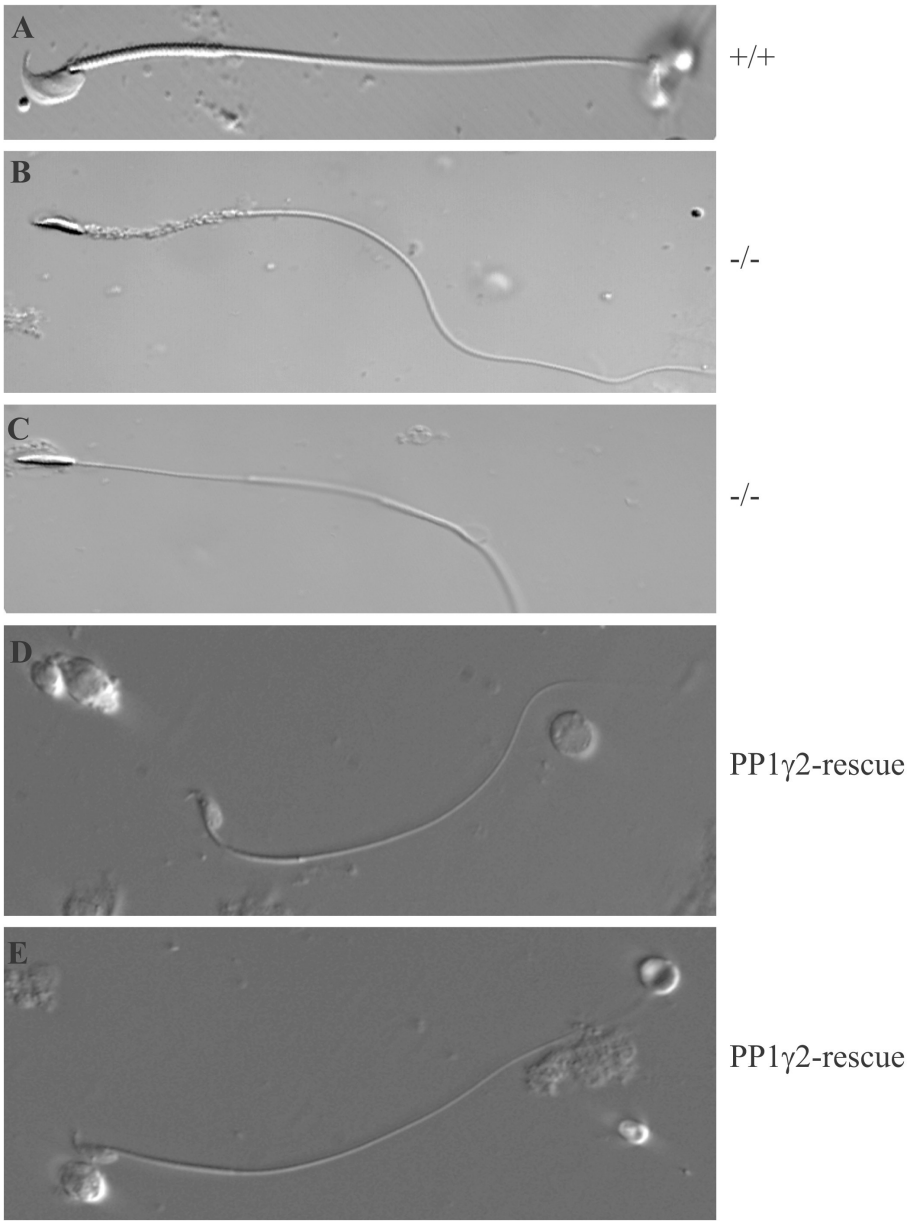

Figure 43. Morphology of testicular and epididymal spermatozoa of wild type, *Ppp1cc*-null and experimental mouse (PP1γ2 rescue) shown with DIC optics. A: Normal hooked shape head and tightly wrapped mitochondrial sheath of epididymal spermatozoa of wild

type mouse. **B, C:** *Ppp1cc*-null testicular sperm display malformed heads and mid-pieces. **B:** shows frayed mid-piece and **C:** shows complete absence of mid-piece. **D and E:** Tightly wrapped mitochondrial sheath with normal hook shape head of experimental mouse epididymal sperm. Bar= 40 μm